

https://dspace.org/

A comparison of the limit equilibrium and numerical modelling approaches to risk analysis for open pit mine slopes

Chiwaye, Henry Tonderai

2010-08-10
http://hdl.handle.net/10539/8376

Downloaded from a DSpace repository. https://dspace.org/

A COMPARISON OF THE LIMIT EQUILIBRIUM AND NUMERICAL MODELLING APPROACHES TO RISK ANALYSIS FOR OPEN PIT MINE SLOPES

Henry Tonderai Chiwaye

A dissertation submitted to the Faculty of Engineering and the Built Environment, University of the Witwatersrand, Johannesburg, in fulfillment of the requirements for the degree of Master of Science in Engineering

Johannesburg 2010

DECLARATION

I declare that this dissertation is my own, unaided work. It is being submitted for the Degree of Master of Science in the University of the Witwatersrand, Johannesburg. It has not been submitted before for any degree or examination in any other University.

……

(Signature of candidate)

…… day of …… (year) ……

at ……

ABSTRACT

Risk analysis is an important step in the design of rock slopes in open pit mining. Risk is defined as the product of the probability of slope failure and the consequences of the failure, and is generally evaluated in terms of safety and economic risk. Most of the risk analysis carried out at present is based on the use of Limit equilibrium (LE) techniques in evaluating the probability of failure (POF) of the slopes. The approach typically makes use of full Monte Carlo simulations of the Limit Equilibrium models, with all uncertain variables randomly varied. The number of required simulations is generally over a thousand, at times as high as 20000, in order to produce statistically valid results of the POF. Such an approach is clearly not amenable to the use of numerical modelling programs due to the high computational effort required, hence the major use of LE methods.

This project explores the impact of using numerical modelling (with the program PHASE 2) instead of the traditional LE techniques (using the program SLIDE) in evaluating the probability of slope failure. The difference in the overall assessed risk, in terms of economic impact, for the mining operation was then evaluated. Instead of full Monte Carlo simulations within the numerical analysis stability model, an alternative method called the Response Surface Methodology was used for the probabilistic analysis. The use of numerical modelling in the assessment of risk results in a significant difference in the assessed risk. LE models tend to be conservative in terms of stability and POF results. However, they give lower estimates of failure volumes than the numerical models. As a result, the assessed risk from LE models can be lower or higher than that from numerical analyses. A case study of an open pit mine was used to validate these findings.

The effect of using 2D plane strain models instead of 3D analysis was also investigated. Numerical models built with FLAC were compared with FLAC3D models. Circular and elliptical pits were considered, with varying radii of curvature. The results showed that for circular pits 2D assumptions are adequate if the radius of curvature is sufficiently large or, for an elliptical pit, if the distance from the small radius ends is sufficiently large. In situations other than these the 2D models give conservative estimates of stability and probability of failure. A detailed comparison of failure volumes was difficult due to the fact that the 2D models do not give the out of plane extent of the failure. However, using simplistic assumptions, the overall assessed risk from FLAC and FLAC3D is shown to be different.

ACKNOWLEDGEMENTS

Firstly I thank SRK Consulting Engineers (Johannesburg) for providing me with all the software used in the research and access to their well stocked library. Additionally they allowed me to work on a number of open pit slope design projects, including the case study documented in this project, which increased my appreciation of the slope design process.

Luis Fernando Contreras taught me a great deal concerning the design of rock slopes. Many thanks for his willingness to share with me some of his earlier work on risk analysis for open pit mine slopes. Additionally, he introduced me to the concept of Response Surface Methods, the method which became the sole tool used to compute probabilities of failure in the numerical analyses described in this work.

Finally I acknowledge the immense assistance I got from my supervisor, Professor T.R. Stacey, in the form of his expert supervision and guidance.

DEDICATION

To Dick Stacey: for successfully changing my career path from Industrial Engineering to Rock Mechanics. Hope this project correlates well with the degree of faith you have always had in me.

TABLE OF CONTENTS

DECLARATION ..... **ii**
ABSTRACT ..... **iii**
ACKNOWLEDGEMENTS ..... **iv**
DEDICATION ..... **v**
TABLE OF CONTENTS ..... **vi**
LIST OF TABLES ..... **ix**
LIST OF FIGURES ..... **xii**
LIST OF SYMBOLS ..... **xvii**
CHAPTER 1 ..... **1**
1 INTRODUCTION **1**
1.1 Problem Definition 3
1.2 Objectives and Scope of Research 4
1.3 Research Methodology 5
1.4 Content of the Dissertation 6
CHAPTER 2 ..... **7**
2 LITERATURE REVIEW **7**
2.1 Open Pit Mining and Slope Stability 7
2.1.1 Stability in Open Pit Mining 8
2.1.2 Economics and Safety 8
2.2 The Rock Mechanics of Rock Slopes 9
2.2.1 Rock Mass Strength 9
2.2.2 Discontinuities in Rock Masses 10
2.2.3 Role of Groundwater in Slope Stability 12
2.2.4 In-situ Rock Stresses 13
2.2.5 Failure Mechanisms 14
2.3 Slope stability Analysis Methods 18
2.3.1 Introduction 18
2.3.2 Limit Equilibrium (LE) Methods 20
2.3.3 Numerical Modelling 23
2.3.4 Comparison of Numerical and Limit Equilibrium Methods 30
2.3.5 Probabilistic Methods 32
2.3.6 Risk Approach 38
2.3.7 Summary 43
CHAPTER 3 ..... **44**
3 SLOPE STABILITY MODELS **44**
3.1 Limit Equilibrium Analysis (SLIDE) 44

3.1.1 Analysis Methods 44
3.1.2 Surface Options 45
3.1.3 Probabilistic analysis 45
3.2 Numerical modelling 46
3.2.1 PHASE 2 (Finite Element Analysis) 46
3.2.2 FLAC (Finite Difference) 48
3.2.3 FLAC3D (Finite Difference) 48
3.3 Conducted Analyses 49
3.3.1 Rock Mass Properties 49
3.3.2 Response Surface Methodology Verification 51
3.3.3 Deterministic FOS calculations 56
3.3.4 Probabilistic Analysis 62
3.3.5 Risk Analysis 64
CHAPTER 4 69
4 RESULTS AND DISCUSSION 69
4.1 Response Surface Methodology Verification 69
4.1.1 Homogeneous slope (Assuming Normal Distributions for c and Φ) 69
4.1.2 Homogeneous slope (Assuming Lognormal Distributions for c and Φ) 71
4.1.3 Heterogeneous slope (Assuming Normal Distributions for c and Φ) 72
4.1.4 Summary 73
4.2 Deterministic Analysis 74
4.2.1 Slope Angle 74
4.2.2 Pit Depth 76
4.2.3 k ratio 78
4.2.4 Locked-in Horizontal Stresses 80
4.2.5 Dilation Angle 82
4.2.6 Tensile Strength 84
4.2.7 Sequential Mining 86
4.2.8 Strain Softening 88
4.2.9 Concave Geometry 89
4.2.10 Bathtub Geometry 92
4.3 Probabilistic Analysis 94
4.3.1 LE vs. Numerical Models 94
4.3.2 2D vs. 3D Models 101
4.4 Risk Analysis 103
4.4.1 LE vs. Numerical Models 103
4.4.2 2D vs. 3D Models 106
4.5 Summary of results 109
4.5.1 Response Surface Methodology 109
4.5.2 Deterministic Analysis 109
4.5.3 Probabilistic Analysis 110

4.5.4 Risk Analysis 111
CHAPTER 5 112
5 CASE STUDY (MINE X) 112
5.1 Introduction 112
5.2 Geology and Hydrogeology 112
5.3 Rock Mass and Structural Properties 113
5.3.1 Rock mass characterisation 113
5.3.2 Rock mass strength parameters 114
5.3.3 Joint (Foliation) strength parameters 116
5.3.4 Rock Mass Elastic parameters 118
5.4 Analysed Section 119
5.5 FOS, POF and Risk models 120
5.5.1 Variable input parameters 120
5.5.2 SLIDE models 121
5.5.3 FLAC models 121
5.5.4 Consequence analysis 122
5.6 Results 123
5.6.1 FOS 123
5.6.2 Probability of failure 125
5.6.3 Risk analysis 127
5.6.4 Summary of results 128
CHAPTER 6 129
6 CONCLUSIONS AND RECOMMENDATIONS 129
REFERENCES 132
APPENDIX A 144
Appendix B 145

LIST OF TABLES

Table 1.1 Sources of uncertainty in pit slopes (after Steffen et al, 2007) 2

Table 3.1 Hoek Brown strength parameters for the rock units used in the stability models 50

Table 3.2 Mohr Coulomb and deformation properties derived from the Hoek Brown parameters 50

Table 3.3 Strength parameters used for the SLIDE RSM verification models..... 55

Table 3.4 Summary of conducted analyses for deterministic FOS comparisons 57

Table 3.5 Peak and residual strength parameters for the strain softening model 60

Table 3.6 Material properties for the Bathtub models 61

Table 3.7 Uncertain Input parameters for models used to compare POF values computed with LE models and POF values computed with Numerical models. 63

Table 3.8 Probability values used in the event tree used to determine probabilities of occurrence of various economic consequences. 66

Table 3.9 Costs involved with actions performed after a slope failure 67

Table 4.1 Summary of POF results for models run to compare Monte Carlo simulation in SLIDE and the Response Surface Methodology. 70

Table 4.2 Summary of POF results for models run to compare Monte Carlo simulation in SLIDE and the Response Surface Methodology. 71

Table 4.3 Summary of POF results for heterogeneous models run to compare Monte Carlo simulation in SLIDE and the Response Surface Methodology. 72

Table 4.4 Sensitivity of FOS to variations in slope angle with all other parameters kept constant..... 74

Table 4.5 Sensitivity of FOS to variations in pit depth. All other parameters were kept constant..... 76

Table 4.6 Sensitivity of FOS to variations in k ratio. All other parameters were kept constant 78

Table 4.7 Sensitivity of FOS to variations in locked-in stresses. All other parameters were kept constant 80

Table 4.8 Sensitivity of FOS to variations in dilation angle. All other parameters were kept constant 82

Table 4.9 Sensitivity of FOS to variations in tensile strength. All other parameters were kept constant 84

Table 4.10 Comparison of mining in one step and mining in seven steps 86

Table 4.11 Comparison of FOS / failure volumes obtained with a perfectly plastic vs. strain softening model 88

Table 4.12 Sensitivity of FOS to variations in radius of curvature. All other parameters were kept constant 90

Table 4.13 Sensitivity of FOS to variations in the distance from curved end of elliptical pit. All other parameters were kept constant 92

Table 4.14 Probabilities of failure from SLIDE and Phase2 for the scenario with 2 variables. 94

Table 4.15 New strength parameters for the calibrated SLIDE models. 98

Table 4.16 POF results when using calibrated SLIDE models 98

Table 4.17 Comparison of the POF and failure volumes from FLAC and FLAC3D models 101

Table 4.18 Adjustment of the probability of overall slope failure from Phase2 and SLIDE to give the probability of loss of profits. 104

Table 4.19 Calculation of the expected loss of profit (risk) for the various models analysed using Phase2 and SLIDE. 105

Table 4.20 Adjustment of the probability of overall slope failure from FLAC and FLAC3D to give the probability of loss of profits. 107

Table 4.21 Calculation of the expected loss of profit (risk) for the various models analysed using FLAC and FLAC3D. 108

Table 5.1 Summary of lithological units 114

Table 5.2 Summary of rock mass strength parameters 116

Table 5.3 Summary of joint strength parameter estimates 117

Table 5.4 Summary of elastic parameters 119

Table 5.5 Rock mass and foliation dilation angles 122

Table 5.6 Results of the risk analysis for SLIDE and FLAC models..... 127

LIST OF FIGURES

Figure 1.1 Definition of POF and its relationship with FOS according to uncertainty magnitude (after Tappia et al, 2007) 3

Figure 2.1 Discontinuity pattern for a slope with a slope height of, in clockwise order, (a) 30m (b) 90m (c) 50m. All slopes have a slope angle of 50° and the same pre-existing joint set patterns, after Sjoberg (1999)..... 11

Figure 2.2 The shape of typical sliding surfaces: (a) large radius circular surface in homogeneous, weak material, with the detail of forces on slice; (b) non-circular surface in weak, surficial material with stronger rock at base. (after Willie and Mah ,2004) 15

Figure 2.3 Images showing the common failure mechanisms in rock slopes (after Hoek 2009) 17

Figure 2.4 Typical open pit geometry showing relationship between overall slope angle, inter-ramp angle, and bench geometry..... 18

Figure 2.5 Block on an inclined plane. The weight has been resolved into components parallel and perpendicular to the sliding surface..... 21

Figure 2.6 The forces acting on the sides of a typical slice. 22

Figure 2.7 a) Finite difference model showing large-strain failure of a rock slope (after Stead et al. 2000), (b) Finite Element mesh of a rock slope..... 25

Figure 2.8 Generic Flow-chart of the open pit slope design process (after SRK, 2006)40

Figure 2.9 Benchmark criteria for safety impact of slope failure; acceptability criteria defined by different organisations (after Health and Safety Executive, 2001)..... 42

Figure 3.1 Recommended dimensions for numerical analysis to ensure boundaries do not influence analysis results, after Lorig and Varona (2004). 46

Figure 3.2 3 noded and 6 noded triangular elements for Finite Element Analysis 47

Figure 3.3 Displacement boundary conditions used in all 2D numerical models..... 48

Figure 3.4 Sensitivity of FOS to friction angle showing the locations of the “-”case, the “+” case, and the base case..... 52

Figure 3.5 Graph showing the distribution of FOS from Monte Carlo simulations and definition of the probability of failure. 53

Figure 3.6 The Slope geometries used for validating the RSM approach to probabilistic slope design; (a) homogeneous slope (b) heterogeneous slope 54

Figure 3.7 Phase2 result image showing (left) maximum shear strain contours with polyline drawn to approximate the surface and (right) deformation vectors58

Figure 3.8 Heterogeneous slope used for the models to test the effect of locked-in stress, tensile strength, and dilation angle on slope stability..... 58

Figure 3.9 3D image of the pit used to analyse the effects of concave curvature on slope stability. The image was generated in FLAC3D but analysis done with Phase2. 61

Figure 3.10 Elliptical pit in FLAC3D showing positions of sections considered, at various distances from the curved ends. 62

Figure 3.11 Phase2 model showing geometry used for the comparison of SLIDE and Phase2 POF computations. 63

Figure 3.12 The event tree developed for the evaluation of economic impact of slope failures. The risk evaluation considered 3 different consequences; Normal operating conditions, Loss of Profit, and Force Majeure. (after Steffen et al, 2006) 65

Figure 4.1 Comparison of POF values (for normally distributed variables) calculated using Monte Carlo Simulation in SLIDE (MC) and the RSM formulation for different levels of correlation between c and Φ. 70

Figure 4.2 Comparison of POF values (for lognormally distributed variables) calculated using Monte Carlo Simulation in SLIDE (MC) and the RSM formulation for different levels of correlation between c and Φ. 71

Figure 4.3 Comparison of POF values (for normally distributed variables) calculated using Monte Carlo Simulation in SLIDE (MC) and the RSM formulation for different levels of correlation between c and Φ. 72

Figure 4.4 (top) Predicted FOS values with SLIDE and Phase2 for varying slope angles, (bottom) predicted failure volumes 75

Figure 4.5 (top) Predicted FOS values with SLIDE and Phase2 varying pit depths, (bottom) predicted failure volumes 77

Figure 4.6 (top) Predicted FOS values with SLIDE and Phase2 for varying k ratio values, (bottom) predicted failure volumes 79

Figure 4.7 (top) Predicted FOS values with SLIDE and Phase2 for varying Locked-in horizontal stress values, (bottom) predicted failure volumes 81

Figure 4.8 (top) Predicted FOS values with SLIDE and Phase2 for varying Dilation angle values, (bottom) predicted failure volumes 83

Figure 4.9 (a) Predicted FOS values with SLIDE and Phase2 for varying Dilation angle values, (b) predicted failure volumes 85

Figure 4.10 (top) Predicted FOS values with SLIDE and Phase2 for varying Pit depths simulating the mining in 1 step and in seven steps, (bottom) predicted failure volumes 87

Figure 4.11 Predicted FOS values Phase2 for varying Pit depths using a perfectly plastic and strain softening model 88

Figure 4.12 Predicted Phase2 failure volumes for varying Pit depths using a perfectly plastic and strain softening model 89

Figure 4.13 (top) Predicted FOS values with Plane strain and axisymmetric models in Phase2 for varying radii of curvature, (bottom) predicted failure volumes 91

Figure 4.14 (a) Predicted FOS values with FLAC and FLAC3D at varying distances from the concave ends of an elliptical pit, (b) predicted failure volumes .. 93

Figure 4.15 A comparison of the POF determined from SLIDE and three Phase2 models for different levels of correlation between the cohesion and friction angle. 95

Figure 4.16 The effect on POF of increasing the number of uncertain variables from two to four. 96

Figure 4.17 Results from sensitivity analysis for model 3 showing the relative contribution to variance of the various input parameters. 97

Figure 4.18 POF curves for calibrated SLIDE models (dotted lines) compared to the POF from Phase2 models. 99

Figure 4.19 SLIDE and Phase2 POF results for models with 2 independent input variables..... 100

Figure 4.20 Failure volumes from SLIDE and Phase2 for scenarios where all inputs are at their mean values..... 101

Figure 4.21 POF curves from FLAC and FLAC3D for three different sections along the pit slope..... 102

Figure 4.22 Failure volumes from FLAC and FLAC3D for the base case scenarios at 3 cross sections along the pit wall..... 103

Figure 4.23 Adjustment of the probability of overall slope failure to the probability of loss of profit, P (LOP), for the SLIDE and Phase2 models..... 104

Figure 4.24 Overall risk associated with the slope determined using SLIDE and Phase2 stability models. 105

Figure 4.25 Plot of how the risk determined from calibrated SLIDE models (dotted curve) compares with that from the un-calibrated SLIDE models and Phase2 models. 106

Figure 4.26 Adjustment of the probability of overall slope failure to the probability of loss of profit, P (LOP), for the FLAC and FLAC3D models. 107

Figure 4.27 Overall risk associated with the slope as determined using FLAC and FLAC3D. 108

Figure 4.28 Phase2 result image showing contours of maximum shear strain which depict the failure surface. The SLIDE failure surface has been superimposed onto the image..... 110

Figure 5.1 Methodology for the estimation of rock mass strength parameters..... 114

Figure 5.2 Conversion from rock structure in Laubscher 1990 to GSI (Contreras, 2009)..... 115

Figure 5.3 Rock mass strength parameters used for the design of slopes at Mine-X116

Figure 5.4 Methodology for the estimation of Joint (foliation) strength parameters. 117

Figure 5.5 Joint strength parameters for the rock units. Also shown are the Base friction angle (BFA) and residual friction angle (RFA) values for the various rock types. 118

Figure 5.6 Section used for the stability analysis for Mine X showing the rock units, slope height, overall slope angle, and the water table (blue line). 119

Figure 5.7 Slope showing the apparent dip of the foliation planes in each domain. 120

Figure 5.8 Predicted failure surfaces from the SLIDE (left) and FLAC model. 123

Figure 5.9 FLAC plots of plasticity indicators showing the mode of failure of the slope. 124

Figure 5.10 FLAC plots of velocity vectors at failure 125

Figure 5.11 Results of Monte Carlo simulations in Crystal Ball for the: a) SLIDE (left) and b) FLAC models. 125

Figure 5.12 Contribution to variance of the different variables for the: a) SLIDE (left) and b) FLAC models. 126

Figure 5.13 Plot showing the POF and the assessed risk from the SLIDE and FLAC models. The blue curve is the POF and the red is the risk curve. 128

LIST OF SYMBOLS

γ	Unit weight
c	Cohesion
FDM	Finite Difference Method
FEM	Finite Element Method
FFr	Fracture Frequency
FOS	Factor of Safety
GSI	Geological Strength Index
IRS	Intact Rock Strength
JCr	Joint Condition Rating
LE	Limit Equilibrium
LOP	Loss of profits
mi	Hoek Brown m parameter for intact rock
MZAR	Million South African Rand
PDE	Partial Differential Equation
P(LOP)	Probability of Loss of Profits
POF	Probability of Failure
RMR	Rock Mass Rating
RSM	Response Surface Methodology
SSR	Shear Strength Reduction
UCS	Uniaxial Compression Strength
UTB	Indirect Uniaxial Tensile Strength test (Brazilian test)
TCS	Triaxial Compression Strength
Φ	Friction angle

CHAPTER 1

1 INTRODUCTION

The determination of the acceptable slope angle for open pit mines is a key aspect of the mineral business. It implies seeking the optimum balance between the additional economic benefits gained from having steeper slopes (as in this way the excavation of waste is minimized), and the additional risks resulting from the consequent reduced stability of the pit slopes (Steffen et al, 2008; SRK 2006). In general, as the slope angle becomes steeper, the stripping ratio (waste to ore ratio) is reduced and the mining economics improve. However, these benefits are counteracted by reduced stability of the slopes and the consequent increased risk to the operation. Since the slope angle is a key design parameter that determines the stability of a slope, the determination of the acceptable slope angle is a key aspect of the mine business. The difficulty in determining the acceptable slope angle stems from the existence of uncertainties associated with the stability of the slopes. Table 1.1 summarizes the main sources of uncertainty in pit slopes.

The oldest approach to slope design is that based on the calculation of the factor of safety (FOS). The FOS can be defined as the ratio between the resisting forces (strength) and the driving forces (loading) along a potential failure surface. If the FOS has a value of one, the slope is said to be in a limit equilibrium condition, whereas values larger than one correspond to stable slopes. In this approach each parameter used in the design of the slope is assumed to be known with certainty. The uncertainties are accounted for through the selection of a FOS for design larger than 1.0. The main disadvantage of the FOS approach for slope design is that the acceptability criterion is based on case studies and combines the effect of many factors that makes it difficult to judge its applicability in a specific geomechanical environment. In other words, the acceptability criterion is empirical

and might not be applicable to a geomechanical setting that is different from the ones used as case studies to come up with the criterion (Tappia et al, 2007).

Table 1.1 Sources of uncertainty in pit slopes (after Steffen et al, 2007)

Slope Aspect	**Source of Uncertainty**
Geometry	Topography Geology/Structures Groundwater surface
Rock mass Properties	Strength Deformation Hydraulic conductivity
Loading	In situ stresses Blasting Earthquakes
Failure Prediction	Model reliability

An alternative to the FOS approach to slope design is the probabilistic method. This method is based on the calculation of the probability of failure (POF) of the slope. In this case the input parameters are described as probability distributions rather than point estimates of the values. By combining these distributions within the deterministic model used to calculate the FOS, the probability of failure of the slope can be estimated. Figure 1.1 shows the definition of POF and its relationship with FOS according to uncertainty magnitude. A drawback of the FOS methodology that persists in the POF approach is the difficulty to define an adequate acceptability criterion for design.

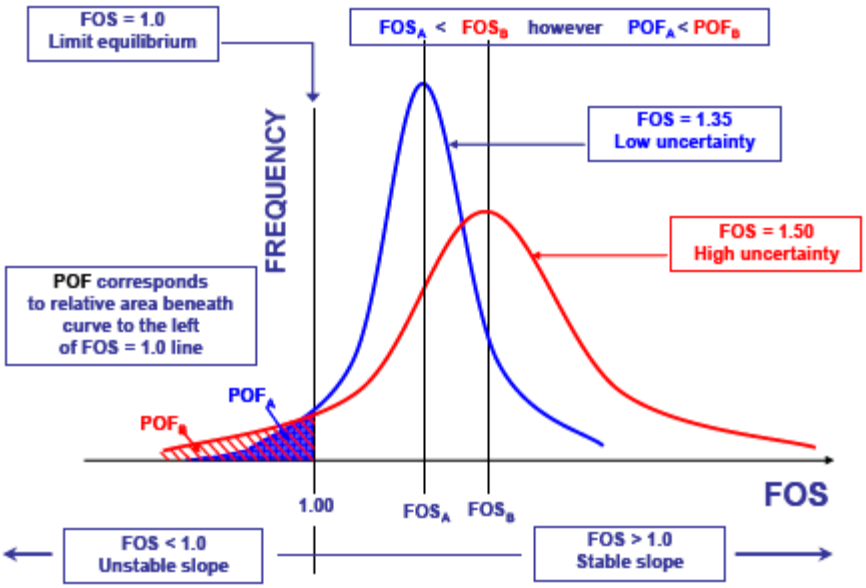

Figure 1.1 Definition of POF and its relationship with FOS according to uncertainty magnitude (after Tappia et al, 2007)

The risk approach is an extension of the probabilistic approach in which the consequences of the failure are taken into consideration. The risks associated with a major slope failure can be categorized by the following consequences: Injury to personnel, damage to equipment, economic impact on production, force majeure (a major economic impact), industrial action, and public relations (such as stakeholder resistance). Commercial risks quantified must be acceptable to the mine owners, and are related to the probability of failure. Hence the acceptability criterion for economic risk is set by management. Safety risks are usually regarded as outside management discretion with most companies seeking compliance with industry norms or other indicators of societal tolerance.

1.1 Problem Definition

In order to carry out a risk analysis a thorough evaluation of the probability of failure (POF) of the slope is required, Steffen et al (2008). Ideally, the factor of safety distribution (and hence the POF) would be computed by the Monte Carlo simulation method, which allows direct representation of the various uncertainties. In this technique, many simulations are done using randomly chosen values from the parent distributions of the various

uncertainties represented in the analysis, with the results given in the form of a probability distribution of the computed factor of safety. Typically, several thousand simulations will be made to determine ("forecast") the probability of performance modeled. Realistically, the Monte Carlo approach cannot be used directly with models based on numerical analyses, as each simulation in these codes takes a relatively long time. As a result, this requirement of large numbers of runs for the Monte Carlo simulations has resulted in the simplistic limit equilibrium (LE) methods being used in evaluating the POF and risk associated with open pit mine slopes. This is despite the fact that most slope stability problems involve complex geometries and loading conditions which can only be adequately modelled using numerical methods. It would therefore be desirable to directly incorporate numerical models into probabilistic and risk analyses. To achieve this, an approximate probabilistic approach recently developed, the Response Surface Methodology (RSM), which requires fewer runs than Monte Carlo simulation to calculate the POF, can be used with numerical models in probabilistic analysis. However, the validity of this RSM approach to slope stability analysis still needs to be ascertained. Moreover, the effect of directly incorporating numerical models into risk analyses needs to be investigated by comparing the assessed risk with that from LE models.

1.2 Objectives and Scope of Research

The objectives of this research are:

- To verify the accuracy of the Response Surface Methodology for probabilistic slope stability analysis.
- To assess whether the parameters not accounted for in a LE analysis have any significant effect on the stability of slopes.
- To compare the POF results obtained using LE methods with those using numerical methods.

- To compare the different failure surfaces (and failure volumes) predicted by both methods and the effects any differences have on the consequences of failure, and hence the eventual assessed risk.
- To assess the impact on stability / risk of using 2D plane strain models instead of 3D models.

1.3 Research Methodology

The research carried out mainly involved the analysis of typical slope models using LE and numerical methods. A risk analysis for an open pit diamond mine in Africa was carried out as a case study to validate the findings from the hypothetical slope models. The methodology adopted can be summarized as follows:

- Validation of the accuracy of the Response Surface Methodology in probabilistic slope stability analysis.
- Investigation of the influence on slope stability of parameters, such as dilation angle and field stresses, not accounted for in LE analyses.
- Comparison of the probability of failure values obtained from LE stability models and those from numerical models.
- Comparison of failure volumes predicted by LE and numerical models.
- Comparison of the assessed risk on selected hypothetical geometries, assuming hypothetical financial information.
- Comparison of the assessed FOS, POF, and risk on selected hypothetical geometries, using 2D vs. using 3D models.
- Diamond open pit mine risk analysis (Case study)

1.4 Content of the Dissertation

A survey of the concepts and literature relevant to this research is presented in the next chapter. Chapter 3 contains a description of all the hypothetical stability models used in this research. The descriptions include the geometries used, the material properties, the modeling tools, and the modeling assumptions. In chapter 4 the results of the analyses described in chapter 3 are presented. The results of the verification of the Response Surface Methodology are also included in this chapter. A discussion of the results is also included in the chapter. Chapter 5 contains a description of the diamond mine case study and the results from the analysis. The conclusions and recommendations from the research are found in chapter 6. Finally the appendices include some detailed information on various items covered during the research.

CHAPTER 2

2 LITERATURE REVIEW

This chapter gives a survey of the literature relevant to the issues being investigated in this project. The rock mechanics concepts relevant to slope stability analysis are briefly described. After that, various slope stability analysis methods are then described. A summary of the literature survey is given at the end of the chapter.

2.1 Open Pit Mining and Slope Stability

In mining, open pits account for the major portion of the world's mineral production, (Wyllie and Mah, 2004). The dimensions of open pits range from areas of a few hectares and depths of less than 100 m for some high grade mineral deposits and quarries in urban areas, to areas of hundreds of hectares and depths as great as 800 m, for low grade ore deposits. In general, mine rock slopes are transient and short to medium term structures which derive their right of existence from economic considerations. Any unnecessary conservatism is, therefore, wasteful and unacceptable in terms of its primary purpose (SRK, 2006). The slopes therefore must be designed to be as stable as necessary, but no more than that. In open pit mining the only design parameters that can be varied are the shape of the slope, the slope angle and, to some extent, the slope height, (Sjoberg, 1999). The task of deciding whether a design satisfies the stability requirements constitutes one of the goals of slope design (SRK, 2006). Due to the high risk nature of the mining business some instabilities are often accepted in open pits (Ross-Brown, 1973). In the following section, the concept of stability in open pit mining and basic economics of open pit mining are described.

2.1.1 Stability in Open Pit Mining

The required stability conditions of rock slopes depend on various issues including the consequences of the failure and life span of the excavation (Hoek and Bray, 1974). For example, for cuts above a busy highway it will be important that the overall slope be stable, and that few, if any, rock falls reach the traffic lanes, (Wyllie and Mah, 2004). Such requirements will dictate that more careful blasting be used to excavate the slope, and probably the use of support elements to stabilise the slope. Because the useful life of such stabilization measures may only be 10–30 years, depending on the climate and rate of rock degradation, periodic maintenance may be required for long-term safety. In contrast, slopes for open pit mines are usually designed with factors of safety in the range of 1.2–1.4, and it is accepted that movement of the slope, and possibly some partial slope failures, will occur during the life of the mine. In fact, an optimum open pit slope design is one that fails soon after the end of operations.

2.1.2 Economics and Safety

The determination of the acceptable slope angle for open pits is a key aspect of the mineral business. The design process is a trade-off between stability and economics. Steep cuts are usually less expensive to construct than flat cuts because there is less volume of excavated rock, less acquisition of right-of-way and smaller cut face areas (Wyllie and Mah, 2004). On the other hand, the flatter a slope is, the better the stability. The goal then is to seek the optimum balance between the additional economic benefits gained from having steeper slopes, and the additional risks resulting from the consequent reduced stability of the pit slopes (Steffen et al, 2008). Failure of slopes poses a risk in terms of both safety and economics. This risk can be evaluated by understanding the probability of failure and the consequences of the failure.

2.2 The Rock Mechanics of Rock Slopes

Certain fundamental principles of rock mechanics are crucial to the design of rock slopes in any application, whether civil or mining. The effect of discontinuities on the strength of the rock mass, the role of groundwater in slope stability, and the role of the prevailing stress regime before any excavation of the rock takes place will be discussed in this section. Some typical failure mechanisms of rock slopes will also be described.

2.2.1 Rock Mass Strength

The first task in any form of analysis used for the design of rock slopes is to determine reliable estimates of the strength and deformation characteristics of the rock mass. Because rock is a natural geological material, the physical or engineering properties have to be established, rather than defined through a manufacturing process, (Jing, 2003). The strengths of intact rock and single discontinuities have received much attention in the rock mechanics literature, and can be considered fairly well understood (Sjoberg, 1999). The strength of planar discontinuities can be fairly well described by the Coulomb shear strength criterion (Byerlee, 1978). The presence of discontinuities like joints and fractures in rocks results in the actual strength of the in-situ rock mass being less than the strength of intact rock. Because in-situ rock strength measurements are usually not practically and economically feasible, various methods are used to downgrade the intact rock strength, (Sjoberg, 1997). One popular method of estimating this “downgraded” rock mass strength from intact rock properties is the Hoek Brown strength criterion, (Hoek et al, 2002).

The Hoek-Brown criterion uses a parameter called the geological strength index (GSI) and the effects of blasting to downgrade the strength of the rock mass, (Hoek et al, 1992; Hoek et al 1994; Hoek et al 1998). Due to the difficulty associated with explicitly describing rock mass strength based on the actual mechanisms of failure, most strength criteria, including the Hoek-Brown criterion, treat the rock mass as an equivalent continuum, (Sjoberg, 1999). The criterion was first presented by Hoek and Brown (1980), with subsequent revisions and updates by Priest and Brown (1983), Hoek and Brown (1988), Hoek et al. (1995), Hoek and

Brown (1997), and Hoek, Carranza-Torres, and Corkum (2002). Sjoberg (1999) noted that the Hoek-Brown criterion appears to work fairly well for first estimates of rock mass strength, but actual verifications of the criterion are still lacking, particularly for application to large scale rock slopes. A substantial number of slope stability analysis programs use the Mohr Coulomb strength criterion, which describes the strength of the rock using the cohesion and friction angle. As a result Hoek et al (2002) derived equations to convert Hoek-Brown parameters into equivalent Mohr-Coulomb parameters. An associated Windows program called "RocLab" (Rocscience Inc.) has been developed to provide a convenient means of solving and plotting these equations.

2.2.2 Discontinuities in Rock Masses

A rock mass may consist of intact rock only, but is more commonly formed from an array of intact rock blocks with boundaries formed by discontinuities (Hack, 1996). The geological structure is obviously one of the most important factors governing slope stability. Examples of different types of discontinuities are shown in Figure 2.1. The low-stress conditions in shallow slopes imply that structurally controlled failures, such as plane shear and wedge failures, dominate in such rock slopes. Hoek et al (2000) pointed out that the role of second order structures (for example, joints), is more of a problem from a practical standpoint, than first order structures like faults. They go on to state; "An assumption commonly made is that these second order structural features are randomly or chaotically distributed and that the rock mass strength can be defined by a simple failure criterion in which 'smeared' or 'average' non-directional strength properties are assigned to the rock mass" (Hoek et al, 2000, pp 645).

Sjoberg (1999) concurred with the previous statement when he noted that when the slope is large relative to the discontinuity size, the rock mass will appear to be significantly fractured. He went on to illustrate this difference in scale as shown in Figure 2.1 for (1) a 30-metre high bench slope with a 70° bench face angle, (2) an inter-ramp slope of 90-metre height and 50° inter-ramp angle, and (3) an overall slope with a height of 500m and

a 50° overall slope angle, respectively. In these figures, a two-dimensional cross-section of the slope is shown with two hypothetical joint sets.

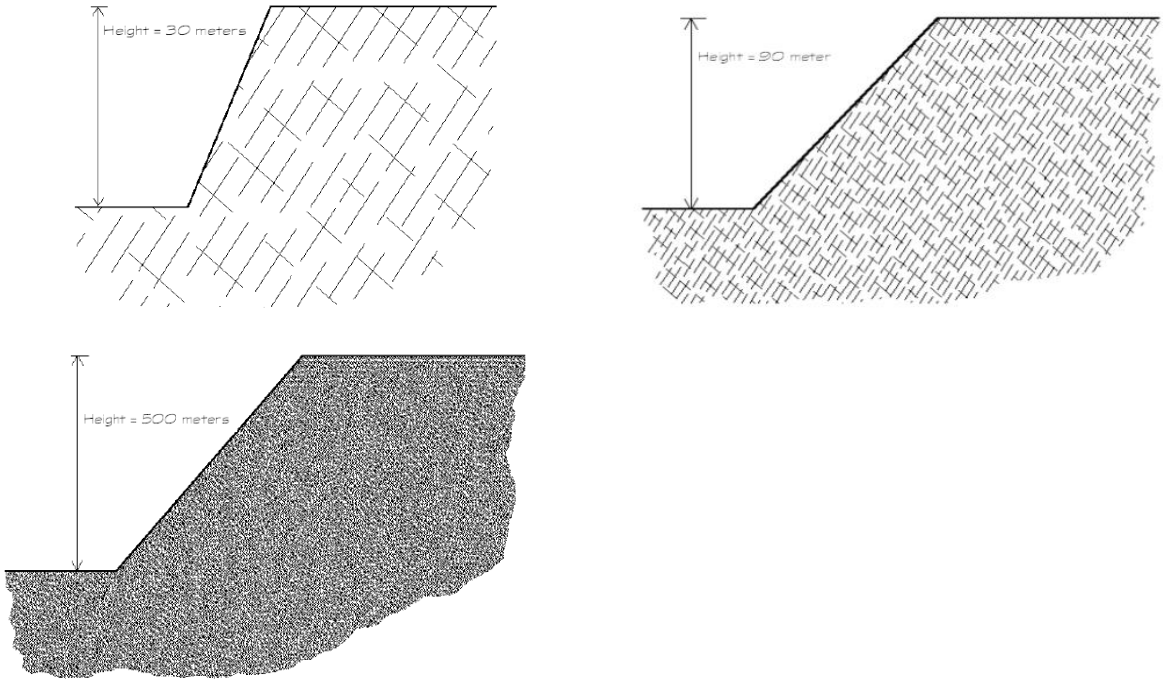

Figure 2.1 Discontinuity pattern for a slope with a slope height of, in clockwise order, (a) 30m (b) 90m (c) 500m. All slopes have a slope angle of 50° and the same pre-existing joint set patterns, after Sjoberg (1999)

On the use of the Hoek-Brown criterion described earlier, Hoek (2006) recommends that when the block size is of the same order as that of the structure being analysed or when one of the discontinuity sets is significantly weaker than the others, the Hoek-Brown criterion should not be used. In the case of the bench slope in Figure 2.1a, the stability of the structure should be analysed by considering failure mechanisms involving the sliding or rotation of blocks and wedges defined by intersecting structural features, in other words a discontinuum approach. This implies that bench scale slope design must treat the discontinuities explicitly since stability is structurally controlled. However, in the case of the 500m slope, the rock mass can be treated as a continuum material with properties downgraded to account for the existence of the discontinuities, Hoek (2002).

2.2.3 Role of Groundwater in Slope Stability

The presence of ground water in a rock slope can have a detrimental effect upon stability. Wyllie and Mah (2004) summarised the effects of groundwater on slope stability as follows:

- Water pressure reduces the stability of the slopes by diminishing the shear strength of potential failure surfaces. Water pressure in tension cracks or similar near vertical fissures reduces stability by increasing the forces that induce sliding.
- Changes in moisture content of some rocks can cause accelerated weathering and a decrease in shear strength.
- Freezing of ground water can cause wedging in water-filled fissures due to temperature dependent volume changes in the ice. Also, freezing of surface water on slopes can block drainage paths resulting in a build-up of water pressure in the slope with a consequent decrease in stability.
- Erosion of weathered rock by surface water and of low strength infillings by ground water can result in local instability where the toe of a slope is undermined, or a block of rock is loosened.
- Excavation costs can be increased when working below the water table. For example, wet blast holes require the use of water resistant explosives that are more expensive than non-water-resistant explosives. Also, flow of ground water into the excavation or pit will require pumping and possibly treatment of the discharge water, and equipment trafficability may be poor on wet haul roads.

Sjoberg (1999) adds that existing groundwater pressures can act as additional driving forces on failure surfaces for certain failure modes. It is water pressure, and not rate of flow, which is responsible for instability in slopes, and it is essential that measurement or calculation of this water pressure forms part of site investigations for stability studies. Atkinson (2000), stated that fully depressurised slopes can usually be excavated more steeply by 10 or more degrees. He further noted, pp 89, “Although flattening of a wet

slope is sometimes an option, dewatering of the slope is usually a more desirable and economic alternative".

Today, numerical analyses are commonly used to assist in assessing groundwater pressure. Groundwater flow modelling may be done independently of the usual mechanical calculations of the numerical model, or it may be done in parallel with the mechanical modelling, so as to capture the effects of fluid/solid interaction, (Itasca, 2005). The latter types of models are termed coupled hydro-mechanical numerical models. Codes like Phase2 (Rocscience Inc.), FLAC/FLAC3D/UDEC (Itasca Inc.), are capable of performing coupled hydro-mechanical analyses. Galera et al (2009) used FLAC3D to carry out coupled hydro-mechanical analyses to predict the pore pressure drop due to the volumetric expansion associated with the excavation of a pit. However, when using numerical models, coupled analyses (in particular, three-dimensional ones) are cumbersome and seldom used. In normal engineering practice, two-dimensional approximations are commonly used, and the coupled effects neglected, Sjoberg (1999). Hoek et al (2000), pp 649, concluded, "The technology and tools for groundwater pressure and flow evaluation and control are well developed and it is considered that no further research into this area is required."

2.2.4 In-situ Rock Stresses

It is well known that rock 'noses' or slopes that are convex in plan are less stable than concave slopes. This is generally because of the lack of confinement in convex slopes and the beneficial effects of confinement in concave slopes. These observations provide practical evidence that lateral stresses, in the rock in which slopes are excavated, can have an important influence on slope stability, Hoek et al (2000). These stresses can be beneficial in that they provide confinement to the rock mass or they may be high enough to cause fracturing and failure of the rock mass (Stacey and Wesseloo, 1998). Stacey (2007) mentioned a number of slopes where stress conditions appear to have played a major part in the development of instability. He also noted that stress can play an important role in

determining the behaviour of slopes with low heights and provides a summary of several such failures.

Hoek et al (2000) lamented the fact that measurement of the in situ stress field in the vicinity of large slopes is seldom carried out. This is because the in situ stress field is generally considered to be of minor significance. This assumption may be adequate for small slopes but it needs to be questioned for the design of very large slopes. Lorig (1999), based on the results of numerical analysis, suggests that in situ stresses have no significant effect on the safety factor. However, as noted by Hoek et al (2000), they do have an influence on deformations, and if the slope is composed of materials that weaken as a result of deformation then the in situ stress can have a very important effect in reducing strength and thereby affecting slope stability. Rock failure in slopes is generally associated with low stress drops (Dight and Baczynski, 2009).

Hoek et al (2000) recommended that before embarking on a programme of in situ stress measurement for any specific site, it is probably worth carrying out a parametric study using a three-dimensional model, such as FLAC3D, to determine whether variations in horizontal in situ stresses have a significant impact upon the stresses induced in the near-surface rock in which slope failures could occur.

2.2.5 Failure Mechanisms

The analyses in this work focus entirely on slopes in which the rock mass can be treated as a continuum material with properties downgraded to account for the existence of the discontinuities (Hoek et al, 2002). For such cases, failure is generally “rotational” in nature.

2.2.5.1. Rotational Failure

For very weak rock, where the intact material strength is of the same magnitude as the induced stresses, the structural geology may not control stability and failure modes such as those observed in soils may occur, (Eberhardt, 2003). Such types of failure are generally referred to as circular failures or rotational failures. Observations of slope failures in these materials suggest that this slide surface generally takes the form of a circle, and most stability theories are based upon this observation, (Hoek and Bray, 1974). The actual shape of the "circular" failure surface is influenced by the geological conditions in the slope, (Wyllie and Mah, 2004). For example, in a homogeneous weak, or weathered rock mass, or a rock fill, the failure is likely to form as a shallow, large radius surface extending to the toe of the slope from a tension crack close behind the slope crest (Figure 2.2 (a)). This contrasts with failures in high cohesion, low friction materials where the failure surface may be deeper, with a smaller radius, and may exit beyond the toe of the slope. Figure 2.2(b) shows an example of conditions in which the shape of the slide surface is modified by the slope geology. Here the circular surface in the upper, weathered rock is truncated by the shallow dipping, stronger rock near the base.

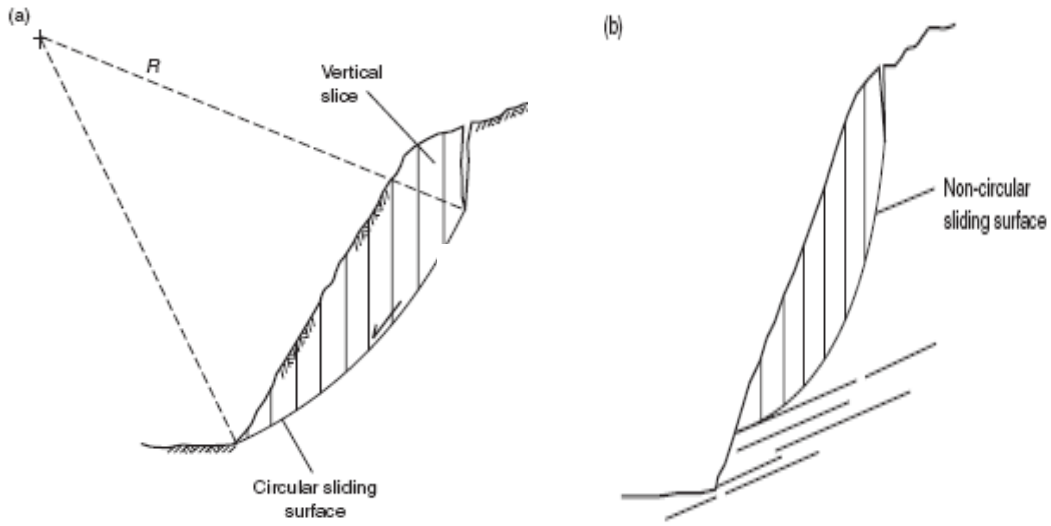

Figure 2.2 The shape of typical sliding surfaces: (a) large radius circular surface in homogeneous, weak material, with the detail of forces on slice; (b) non-circular surface in weak, surficial material with stronger rock at base. (after Willie and Mah ,2004)

Stability analyses of both types of surface can be carried out using "circular" failure methods, although for the latter case it is necessary to use an investigation procedure that allows the shape of the surface to be defined, (Wyllie and Mah, 2004). For each combination of slope parameters there will be a sliding surface for which the factor of safety is a minimum—this is usually termed the critical surface. Limit Equilibrium codes such as SLIDE (Rocscience) and continuum numerical modelling packages such as Phase2 (Rocscience Inc.), FLAC and FLAC3D (Itasca inc.) can be used to evaluate the stability of slopes failing in the rotational failure mode.

2.2.5.2. Other Failure Mechanisms

Other mechanisms of failure are common in slope stability analyses. Plane failure in a rock slope is where a block of rock has slid on a single plane dipping out of the face, (Rocscience, 2001). Wedge failures take place when rock mass slides along the line of intersection of two discontinuities which strike obliquely to the slope (Wyllie and Mah, 2004). LE programs such as Rocscience's SWEDGE, and numerical modelling codes such as Itasca's 3DEC can be used to assess the stability of such wedges. Toppling failure is different from the other failure modes in that, instead of having a sliding rock mass, toppling involves rotation of columns or blocks of rock about a fixed base. Goodman and Bray (1976) produced a formal mathematical solution to a simple toppling problem. This solution represents a basis for designing rock slopes in which toppling is present, and has been further developed into a more general design tool (Zanbak, 1983; Adhikary et al., 1997; Bobet, 1999; Sageseta et al., 2001). Figure 2.3 shows the common failure mechanisms observed in rock slopes.

2D and 3D physical models were used by Stacey (2006) to study failure mechanisms associated with rock slopes. The conclusion from the study was mainly that failure in rock is progressive, with deformations taking place throughout the slope. He also observed from the models that slope failure involved a combination of two or three mechanisms, making the failure process a complex phenomenon (Franz et al, 2007; Simmonds and Simpson, 2006). Another important failure mechanism is where failure initiates and

progresses both along existing weakness planes and in intact rock (called rock bridges). These rock bridges have a significant impact on rock slope stability as they limit the continuity/persistence of geological discontinuities (Dight and Baczynski, 2009).This mode of failure is referred to as a step-path failure mechanism (Eberhardt et al, 2004; Elmo et al, 2009; Elmo et al, 2007). Apart from the common failure mechanisms described here, there are many other currently unknown possible failure mechanisms (Sjoberg, 2000).

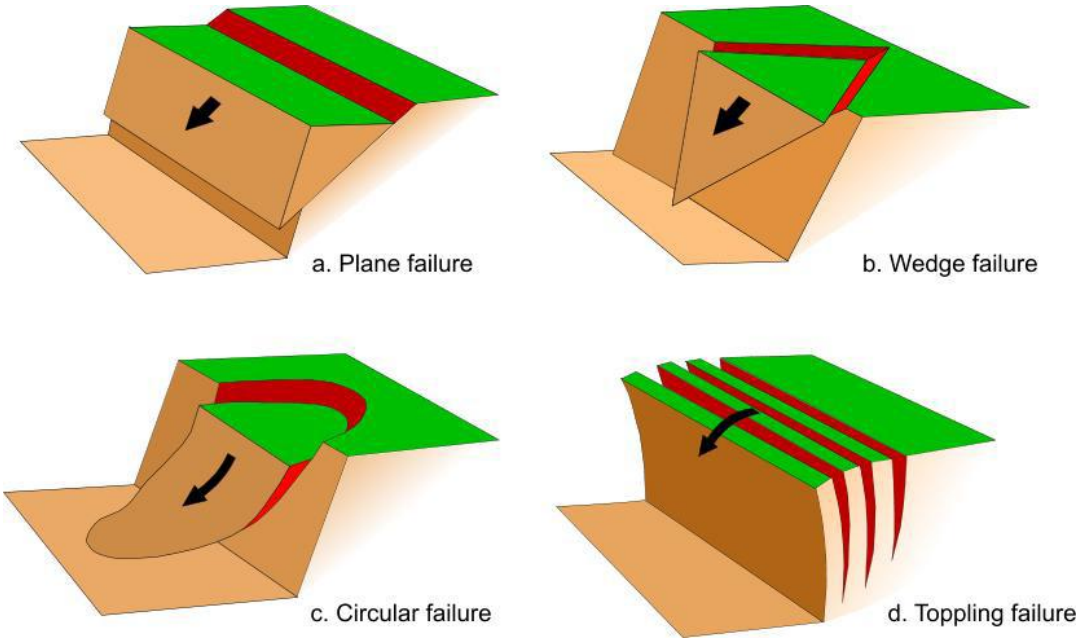

Figure 2.3 Images showing the common failure mechanisms in rock slopes (after Hoek 2009)

Different methods of how to model failure of brittle and hard rock masses have been proposed. An elastic-brittle material model is often used to model brittle failure in hard rock masses (Hoek et al., 1995). The use of strain dependent models is more appropriate to the modelling of such brittle rocks (Hajiabdolmajid et al., 2002). An example of one such model is the cohesion softening friction hardening (CSFH) failure model (Edelbro, 2009; Hajiabdolmajid et al., 2002). According to Schmertmann and Osterberg (1960), the friction term is active only if movement between particles exists. Cohesion loss between particles implies the occurrence of such movement (Edelbro, 2009). For small plastic strains the frictional term has almost no influence but as the strains accumulate, the cohesion drops

and the significance of the friction angle increases. Edelbro (2008), using finite element analysis, showed that the CSFH model best captured the observed rock behaviour than the other conventional failure models.

2.3 Slope stability Analysis Methods

This section describes the various slope stability analysis methods available to the rock engineer. A more detailed description of LE methods and numerical modelling methods, and a comparison of the two approaches, is given. Probabilistic methods are then described together with the risk approach to the design of rock slopes.

2.3.1 Introduction

The three main components of an open pit slope design are as shown in Figure 2.4. Since different failure modes will prevail at different scales and thus affect different portions of the pit, each of the slope units must be designed separately, (Sjoberg, 1999).

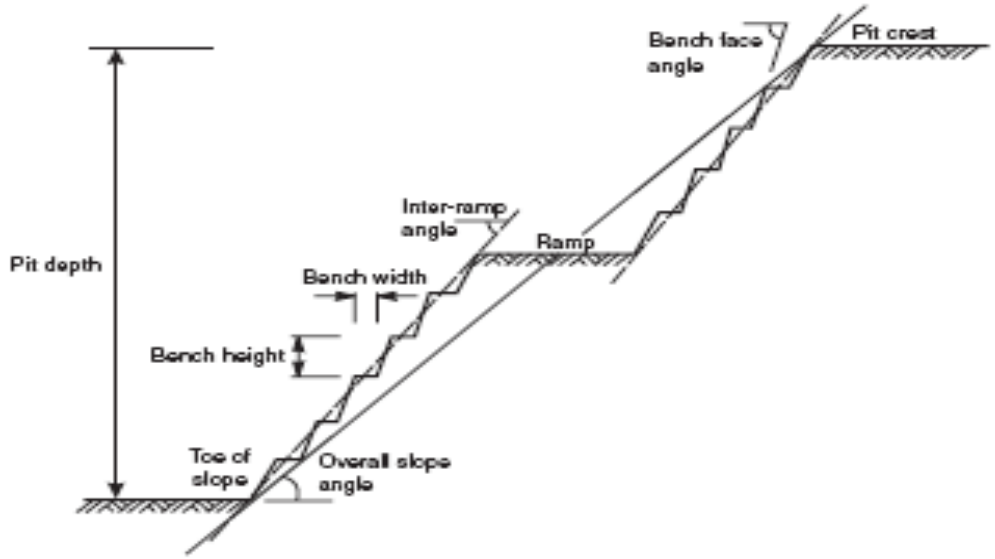

Figure 2.4 Typical open pit geometry showing relationship between overall slope angle, inter-ramp angle, and bench geometry

The stability of a slope can be expressed in one or more of the following terms (Wyllie and Mah, 2004):

- *Factor of safety*—Stability quantified by limit equilibrium of the slope, which is stable if FOS > 1.
- *Probability of failure*—Stability quantified by probability distribution of the difference between resisting and disturbing forces, which are each expressed as probability distributions.
- *Strain*—Failure defined by onset of strains great enough to prevent safe operation of the slope, or that the rate of movement exceeds the rate of mining in an open pit.
- *LRFD (load and resistance factor design)* — Stability defined by the factored resistance being greater than or equal to the sum of the factored loads.

Currently the factor of safety is the most common criterion for slope design, and there is wide experience in its application to all types of geological conditions, for both rock and soil. Furthermore, there are generally accepted factor of safety values for slopes excavated for different purposes, which promotes the preparation of reasonably consistent designs.

The calculation of strain in slopes is the most recent advance in slope design. The technique has resulted from the development of numerical analysis methods, and particularly those that can incorporate discontinuities (Starfield and Cundall, 1988). It is most widely used in the mining field where movement is tolerated, and the slope contains a variety of geological conditions. An important development concerning the calculation of strains in rock is the extension strain criterion (Stacey, 1981). The extension strain criterion states that failure takes place when the extension strain exceeds a critical value (Stacey et al, 2003). This extension strain can exist even in triaxially compressive stress fields. Dight et al (2009) used microseismic monitoring in an open pit mine and the results showed that the predominant rock failure around the pit was extensional.

The load and resistance factor design method (LRFD) has been developed for structural design, and is now being extended to geotechnical systems such as foundations and retaining structures (Wyllie and Mah, 2004).

2.3.2 Limit Equilibrium (LE) Methods

The LE procedure for calculating the factor of safety involves comparing the available shear strength along the sliding surface with the force required to maintain the slope in equilibrium. For all shear type failures, the rock can be assumed to be a Mohr–Coulomb material in which the shear strength is expressed in terms of the cohesion *c* and friction angle *φ, (*Wyllie and Mah, 2004). Given the diagram of Figure 2.5 calculation of the factor of safety involves the resolution of the force acting on the sliding surface (the weight of the block) into components acting perpendicular and parallel to this surface. The expression for the factor of safety is given by Equation 2.1. The block is at a condition of "limiting equilibrium" when the driving forces are exactly equal to the resisting forces and the factor of safety is equal to 1.0.

$$FOS = \frac{Resisting\ \ Forces}{Driving\ \ Forces} \qquad (2\text{-}1)$$

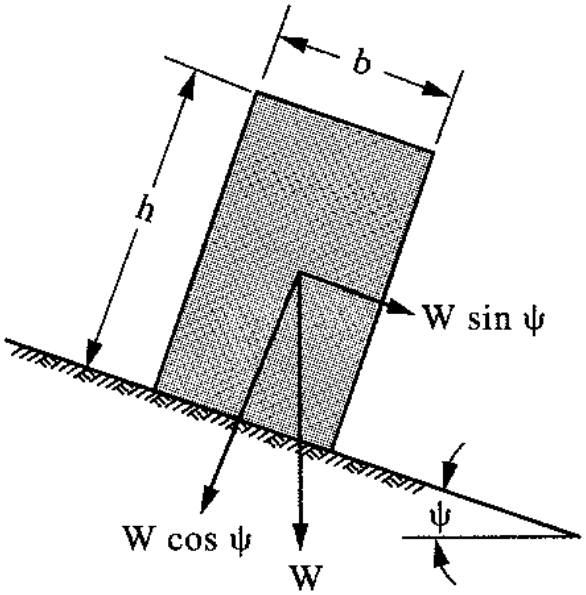

Figure 2.5 Block on an inclined plane. The weight has been resolved into components parallel and perpendicular to the sliding surface.

A FOS of less than 1.0 essentially indicates that the sum of the driving forces is greater than the sum of the resisting forces. Hoek et al (2000) pointed out that many of the LE models have been available for more than 25 years and can be considered reliable slope design tools. LE programs are generally very fast and as a result Hoek (2009) concluded that a well designed limit equilibrium program is probably the best tool for "what if" type analyses at a conceptual slope design stage or to investigate failures and possible remedial actions.

2.3.2.1. Method of Slices

When a slope does not have uniform properties throughout the slope, and failure occurs along a circular slide path that does not pass through the toe of the slope, it becomes impossible to use circular failure charts. In such cases it is necessary to use one of the methods of slices published by Bishop (1955), Janbu (1954), Nonveiller (1965), Spencer (1967), Morgenstern and Price (1965) or Sarma (1979). These methods involve division of the sliding mass into a series of slices that are usually vertical, but may be inclined to

coincide with certain geological features. Figure 2.6 shows a typical slice with the forces on the slice.

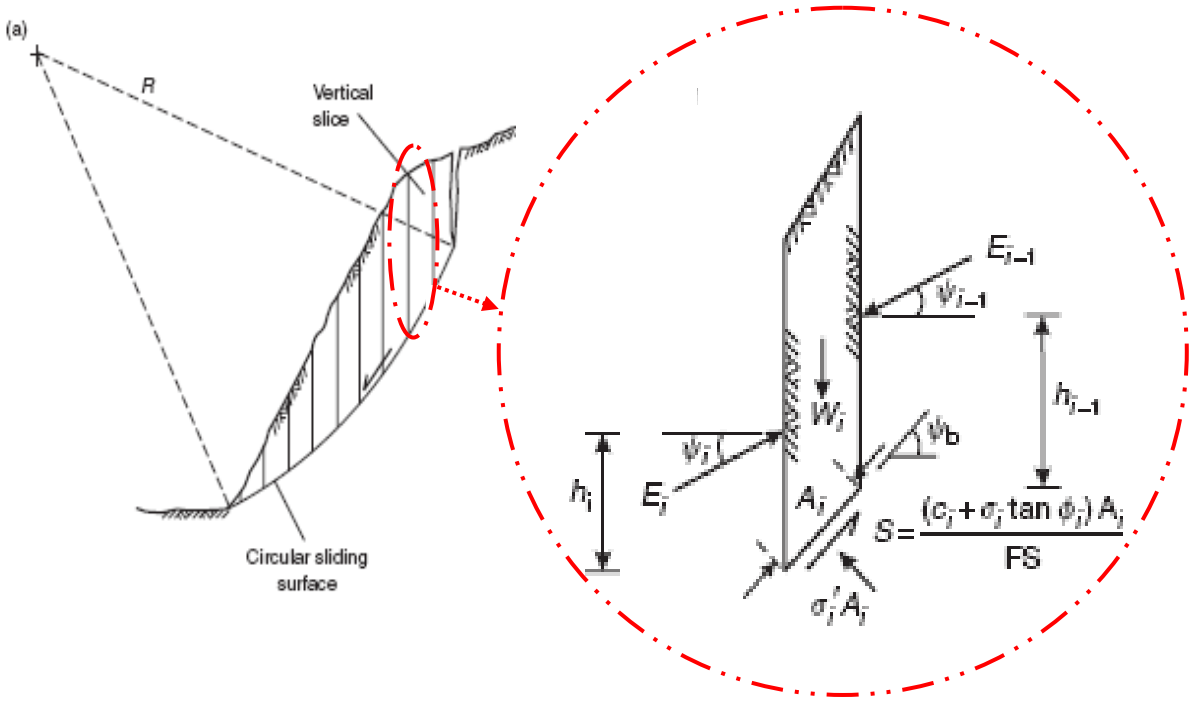

Figure 2.6 The forces acting on the sides of a typical slice.

Limit Equilibrium analyses are statically indeterminate and assumptions are required to make up the imbalance between equations and unknowns (Duncan, 1996). Bishop's method assumes a circular sliding surface and that the side forces on the slices are horizontal; the analysis satisfies vertical force equilibrium and overall moment equilibrium, (Bishop 1955). The Janbu method allows a sliding surface of any shape, and assumes that the side forces on the slices are horizontal and equal on all slices; the analysis satisfies force equilibrium, (Janbu, 1954). The more rigorous LE methods consider both force and moment equilibrium conditions. These methods consider both inter-slice forces (tangential and normal) and are applicable for any type of failure surfaces. Among these methods, the Morgenstern-Price (M-P) method and Janbu's generalized method (also known as the generalized procedure of slices, GPS method), are most common, (Aryal, 2008).

As pointed out by Nonveiller (1965), Janbu's method gives reasonable factors of safety when applied to shallow slide surfaces (which are typical in rock with an angle of friction in

excess of 30°, and in rockfill), but it is seriously in error and should not be used for deep slide surfaces in materials with low friction angles. More recently, Aryl (2008) noted that Bishop's method computes better solutions for circular failure surface analysis whereas Janbu's method is particularly useful in composite failure surfaces. Han and Leshchinsky (2004), pp 1, state that, "Although Bishop's method is not rigorous in a sense that it does not satisfy horizontal force limit equilibrium, it is simple to apply and, in many practical problems, it yields results close to the rigorous limit equilibrium methods."

Another common method of slices called the Janbu corrected method attempts to compensate for the fact that the Janbu method described earlier satisfies only force equilibrium, and assumes zero inter-slice shear forces. For a given slip surface, the Janbu Corrected safety factor is obtained by multiplying the Janbu safety factor for the surface, by a modification factor. The modification factor is a function of the slope geometry, and the strength parameters of the soil or rock, (Rocscience, 2008).

2.3.3 Numerical Modelling

LE methods, such as the method of slices, assess stability based on statics with no provision for directly linking stability with displacements. Hence when movement is detected in a slope, limit equilibrium methods are not suitable for evaluating the impact of such movements on the overall stability, (Corkum and Martin, 2004). Moreover they are limited to simplistic problems in their scope of application, encompassing simple slope geometries and basic loading conditions, and as such, provide little insight into slope failure mechanisms, (Eberhardt, 2003; Desai and Christian, 1977). However, many rock slope stability problems involve complexities relating to geometry, material anisotropy, non-linear behaviour, *in situ* stresses and the presence of several coupled processes (pore pressures, seismic loading, and etcetera). To deal with these complexities, numerical methods are used for slope stability analyses. These methods are more recent developments than limit equilibrium methods.

Numerical modelling starts by dividing the slope into a finite number of zones or elements. Forces and strains are then calculated for each element using the appropriate constitutive laws for the materials in the slope. The most common numerical analysis methods available are Finite Difference methods (FDM), Finite Element Methods (FEM), Discrete Element methods (DEM), Boundary Element methods (BEM), and Discrete Fracture Network methods (DFN). These numerical methods may be divided into three approaches: continuum and discontinuum modelling, (Eberhardt, 2003). Continuum codes assume the material is continuous throughout the body. FDM, FEM, and BEM are all continuum methods, (Jing, 2003). Discontinuities are treated as special cases by introducing interfaces between continuum bodies. Continuum modelling is best suited for the analysis of slopes that are comprised of massive, intact rock, weak rocks, and soil-like or heavily jointed rock masses (Itasca, 2005). Discontinuum modelling is appropriate for slopes controlled by discontinuity behaviour. Examples of discontinuum methods are DEM, for example UDEC (Itasca, 2004), and DFN. Eberhardt et al (2003) used hybrid finite-/discrete element models to study the progressive failure of massive rock slopes. More recently, Cundall and Damjanac (2009) presented a 3D numerical approach, called the synthetic rock mass (SRM), based on the distinct element method, which allows fractures to initiate and grow dynamically according to the imposed stress and strain level. The FEM and FDM are the most common numerical methods in slope stability analyses.

2.3.3.1. Finite Element and Finite Difference Schemes

In both the FDM and FEM the problem domain is divided (discretized) into a set of sub-domains or elements as shown in Figure 2.7 (Ryder and Jager, 2002). The FDM is a direct approximation of the governing partial differential equations (PDE) by replacing partial derivatives with differences at regular or irregular grids imposed over problem domains, thus transferring the original PDEs into a system of algebraic equations in terms of unknowns at grid points (Itasca, 2005; Desai and Christian, 1977). The solution of the system equation is obtained after imposing the necessary initial and boundary conditions. In the FEM usually polynomial functions are used to approximate the behaviour of PDEs at the element level and generate the local algebraic equations representing the behaviour of the elements (Zienkiewicz *et al.,* 1975). The local elemental equations are then assembled

into a global system of algebraic equations whose solution then produces the required information in the solution domain, after imposing the properly defined initial and boundary conditions, (Jing, 2003).

An important thing to note is that both the FDM and FEM produce a set of algebraic equations. While the methods used to derive the equations are different, the resulting equations are the same, (Itasca Consulting Group, 2005, Lorig and Varona, 2004). The salient advantages and limitations of the FDM and FEM are discussed by Hoek et al. (1993), and both have found widespread use in slope stability analysis. Two examples of programs using the FEM and FDM are Phase 2 and FLAC respectively.

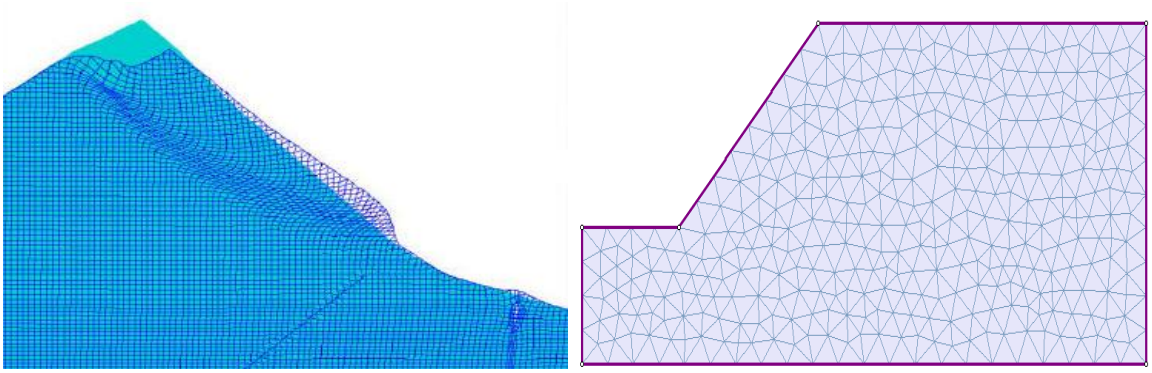

Figure 2.7 a) Finite difference model showing large-strain failure of a rock, (b) Finite Element mesh of a rock slope

For slopes, the factor of safety often is defined as the ratio of the actual shear strength to the minimum shear strength required to prevent failure, (Dawson et al, 1999). A logical way to compute the factor of safety with a finite element or finite difference program is to reduce the shear strength until “collapse” occurs in the model. The factor of safety is then the ratio of the rock’s actual strength to the reduced shear strength at failure. This method is called the shear strength reduction method, (Dawson et al, 1999, Griffith and Lane, 1999, Hammah et al, 2004).

2.3.3.2. Shear Strength Reduction Method

The shear-strength reduction technique was used first with finite elements by Zienkiewicz *et al.* (1975) to compute the safety factor of a slope composed of multiple materials. To perform slope stability analysis with the shear strength reduction technique actual shear strength properties, cohesion *(c)* and friction angle *(φ)*, are reduced for each trial according to equations 2-2 and 2-3. In these equations, *f* is known as the trial factor of safety.

$$c_{trial} = \left(\frac{1}{f}\right) c \qquad \textbf{(2-2)}$$

$$\varphi_{trial} = arctan\left(\frac{1}{f}\right) \tan \varphi \qquad \textbf{(2-3)}$$

The trial factor of safety is increased gradually until the slope fails .The value of *f* at which the slope starts to fail is known as the shear strength reduction factor, and is equal to the factor of safety. If multiple materials and/or joints are present, the reduction is made simultaneously for all materials. Dawson *et al*. (1999) show that the shear strength reduction factors of safety are generally within a few percent of limit analysis solutions when an associated flow rule, in which the friction angle and dilation angle are equal, is used. Hoek (2009) pointed out that the shear strength reduction method is now widely used in open pit slope stability studies because it includes all the benefits of limit equilibrium analyses and it allows the user to study slope displacements that are critical in the evaluation of open pit stability.

2.3.3.3. 2D vs. 3D Modelling

Real life problems are always 3 dimensional (Ryder and Jager, 2002). However, in some situations simplifying assumptions can be used that allow the problem to be modelled as a 2D problem. In fact 2D analyses are widely used, (Cala et al, 2006). These simplifications are usually either plane stress or plane strain assumptions, with the latter having more applicability to slope stability analyses. Plane strain conditions assume a two-dimensional geometry comprising a unit slice through an infinitely long slope (Rocscience, 2009).

However, this is not the condition encountered in practice—particularly in open pit mining where the radii of curvature can have an important effect on safe slope angles (Diering and Stacey, 1987). Strictly speaking, for slope stability analyses, three-dimensional analyses are recommended in the following, (Lorig and Varona, 2004):

- The direction of principal geologic structures does not strike within 20–30° of the strike of the slope.
- The axis of material anisotropy does not strike within 20–30° of the slope.
- The directions of principal stresses are neither parallel nor perpendicular to the slope.
- The distribution of geo-mechanical units varies along the strike of the slope.

Wesseloo and Dight (2009) noted that the influence of the intermediate principal stress is important under bi-axial loading conditions and it is therefore important to develop some appreciation of the true three dimensional stress field around an open pit. This can only be achieved by full three dimensional analyses. Wyllie and Mah (2004) noted that concave slopes are more stable than plane strain slopes due to the lateral restraint provided by material on either side of a potential failure in a concave slope. Rocscience Inc. (2009) mentioned that as the out-of-plane excavation dimension becomes less than approximately five times the largest cross-sectional dimension, the stress changes calculated assuming plane strain conditions begin to show some exaggeration because the stress flow around the "ends" of the excavation is not taken into account. Axisymmetric analyses can be used to simulate 3D effects, if the model is rotationally symmetric about an axis. Although the input is 2-dimensional, the analysis results apply to the 3-dimensional problem.

Piteau and Jennings (1970) studied the influence of curvature in plan on the stability of slopes in four diamond mines in South Africa. They found that the average slope angle for slopes with radius of curvature of 60m was 39.5° as compared to 27.3° for slopes with a radius of curvature of 300 m. Hoek and Bray (1981) summarized their experience with the

stabilizing effects of slope curvature by suggesting that when the radius of curvature of a concave slope is less than the height of the slope, the slope angle can be 10° steeper than the angle suggested by conventional stability analysis. As the radius of curvature increases to a value greater than the slope height, the correction should be decreased. For radii of curvature in excess of twice the slope height, the slope angle given by a conventional stability analysis should be used. Stacey (2006), using 3D physical models, concluded that in general it is not appropriate to use 2D cross sections to represent slopes, except in slopes with a radius of curvature tending to infinity. Cala et al (2006), pp 4, in their comparison of FLAC 2D and 3D modelling, concluded, "The effect of 3D is often considered as an additional safety reserve. But on the other hand, one must find a reasonable equilibrium between safety and economy ... It seems that there is a widespread opinion that considering problems in 2D is always conservative and that engineering design doesn't need the third dimension. Do we really have to be that conservative?" Lorig and Varona (2004) suggested that one reason that designers are reluctant to take advantage of the beneficial effects of concave slope curvature is that the presence of discontinuities can often negate the effects. However, for massive rock slopes, or slopes with relatively short joint trace lengths, the beneficial effects of slope curvature should not be ignored, particularly in open pit mines, where the economic benefits of steepening slopes can be significant.

Cala et al (2006) suggested that using several 2D cross-sections may sometimes provide a reasonable assessment of the 3D effect. Further they note that the application of LE methods to solve 3D problems is rather limited due to several simplifying assumptions (Hungr 1987, Chen et al. 2001 and Casamichele et al. 2004). Prior to 2003 three-dimensional analyses were uncommon, but advances in personal computers have permitted three-dimensional analyses to be performed routinely, (Lorig and Varona, 2004). Cala et al (2006) add; "It must be noted that an increasing number of investigators use 3D numerical calculations for estimating slope stability (Dawson and Roth 1999, Zettler et al. 1999, Hürlimann et al. 2002, Koniecky et al. 2004 and Yuz-hen et al. 2005)." FLAC3D and 3DEC are 3D numerical modelling programs widely used for slope stability analysis in Chilean open-pit mining (Karzulovic 2004). The stability and stresses resulting from underground mining beneath an open pit mine were evaluated using the 3D code FLAC3D

by de Bruyn et al (2009). Zhu and Zhou (2009) used 3DEC to study the dominating mechanisms of displacement for a dam abutment. Guo et al (2009) have proposed a new approach to 3D slope stability modelling in which the stability analysis is done on the basis of the current stress state of the slope and its whole potential sliding direction. This approach, though still lacking verification, appears to have a good future since the safety factor is obtained through the current stress state without excessive assumptions unlike that of LEM and Strength Reduction Method (SRM).

2.3.3.4. Excavation Sequence

For many slopes, according to Lorig and Varona (2004), stability seems to depend mostly on slope conditions, such as geometry and pore-pressure distribution at the time of analysis, and very little on the load path taken to get there. Jeyapalan and Jayawickrama (1983) gave a contrary opinion stating that one major shortcoming of the conventional approach is its inability to take account of the appropriate excavation sequence and this results in un-conservative slope angles for cut-down embankments. A reasonable approach regarding the number of excavation stages has evolved over the years. Using this approach, only one, two or three excavation stages are modelled. For each stage, two calculation steps are taken. In the first step, the model is run elastically to remove any inertial effects caused by sudden removal of a large amount of material. Second, the model is run allowing plastic behaviour to develop, Lorig and Varona (2004). Following this approach, reasonable solutions to a large number of slope stability problems have been obtained. However it must be noted that this approach is relevant to problems in which there are no time dependent mechanisms at play in the rock mass. For models involving visco-plastic behaviour, like creep behaviour, mining has to be modelled in small incremental steps to allow the fracture zone adequate time to evolve. Examples of visco-plastic modelling are found in Malan et al (1997) and Bosman et al (2000) who studied creep behaviour in underground mines.

2.3.4 Comparison of Numerical and Limit Equilibrium Methods

In numerical analysis, the failure surface can evolve during the calculation in a way that is representative of the natural evolution of the physical failure plane in the slope, (Wyllie and Mah, 2004). Cundall (2002) compared the characteristics of numerical solutions and limit equilibrium methods in solving for the factor of safety of slopes and concluded that continuum mechanics-based numerical methods have the following advantages: (1) No pre-defined slip surface is needed; (2) The slip surface can be of any shape; (3) Multiple failure surfaces are possible; (4) No statical assumptions are needed; (5)Structures (such as footings, tunnels, etc.) and/or structural elements (such as beams, cables, etc.) and interfaces can be included without concern about compatibility; and (6) Kinematics is satisfied. LE methods just give an estimate of the FOS with no information on deformation of the slope, something which numerical models can do. It is important to recognize that the limit equilibrium solution only identifies the onset of failure, whereas the numerical solution includes the effect of stress redistribution and progressive failure after failure has been initiated. The resulting factor of safety allows for this weakening effect, (Itasca Consulting Group, 2005). Hoek et al (2000) stated that numerical models can also be used to determine the factor of safety of a slope in which a number of failure mechanisms can exist simultaneously or where the mechanism of failure may change as progressive failure occurs.

However, numerical models take much longer times to compute compared to LE models. Valdivia and Lorig (2000) noted that LE methods can make thousands of safety factor calculations almost instantaneously but numerical methods require longer times to make just one safety factor calculation. Another drawback with numerical methods is that they are generally not easy to use. According to Hoek et al (2000), pp 657; “Using these codes correctly is not a trivial process and mines embarking on a numerical modelling programme should anticipate a learning process of one to two years, even with expert help from consultants.” Obtaining realistic input information for these models and interpreting the results produced are the most difficult aspects of numerical modelling in the context of large scale slopes, (Hoek et al, 2000). Han and Leshchinsky (2004), pp 3, stated that, “The inclusion of structural elements and interfaces may create numerical instability leading to

questionable solutions. Some specific searches are difficult to perform (for example, surficial slope instability needs to be prevented in order to study the deep-seated slope stability). Localized and inconsequential failures, which may not be of interest to the study (for example, locally overstressed soil), may mislead the investigation. In short, while continuum mechanics-based methods rigorously satisfy equilibrium and boundary conditions, it generally requires an experienced analyst in order to properly use it.

Valdivia and Lorig (2000) observed that for simple homogeneous slopes, the factors of safety calculated by LE and numerical methods are not very different. Hoek et al (2000) noted that factors of safety calculated with numerical models have been found to coincide very closely with those determined by limit equilibrium analyses in cases where limit equilibrium analyses are known to give reliable results. Cala and Flisiak (2001) observed that although the elastic properties have a significant influence on the computed deformations prior to failure, they negligibly influence the factor of safety. They also observed that the factor of safety and predicted failure surfaces were different for the LE and Numerical methods when it came to heterogeneous soil slopes. Han and Leshchinsky (2004) did an investigation and concluded that there is a difference in the location of the critical slip surface predicted by the LE method and the numerical method. Lorig and Varona (2004) noted that the shear strength reduction technique usually will determine a safety factor equal to or slightly less than limit equilibrium methods. Itasca Consulting Group (2002) gives a detailed comparison of four limit equilibrium methods and one numerical method for six different slope stability cases and concluded that the LE and numerical solutions can be different in complex loading situations. Dight and Baczynski (2009), pp 12, concluded thus, “It remains that numerical techniques are the only way to evaluate deformation in slopes and hence satisfy the serviceability criterion implicit in the definition of failure and hence will always offer the best way forward – if we can do enough simulations and verify the results.”

2.3.5 Probabilistic Methods

Due to rock masses being formed over large time periods under wide-ranging, complex physical conditions, their properties can vary significantly from place to place, even over short distances. As a result the engineering of excavations in rock involves large uncertainties (Hammah and Yacoub, 2009). Read (2009) grouped the uncertainties involved in slope design into three categories: geological uncertainty; parameter uncertainty; and model uncertainty. Christian (2004) summed up the importance of probabilistic analysis by stating that uncertainty and risk are central features of geotechnical and geological engineering. Narendranathan (2009) noted that probabilistic slope design potentially enables the slope engineer to design slopes with Factors of Safety (FOS) less than the usual 1.2 or even 1.0, providing the 'consequences' or risk can be catered for. In the introduction to Read and Stacey (2009), pp 3, it is stated, "It is often no longer sufficient to present slope design in deterministic (factor of safety) terms…."

Stacey (2001) noted that the significance of the probability of slope failure is not commonly understood. He presented a table, based on Kirsten (1982), which indicates the probabilities of failure for which open pit mine slopes should be designed. The ultimate goal of probabilistic stability analysis is to obtain the complete distribution of factors of safety or any other suitable performance function, given a set of random (uncertain) input variables with specified statistical properties. From this distribution, probability of failure can be determined. Various methods have been adopted in determining the probability of failure in geotechnical engineering. Some of the available methods are Monte Carlo Simulation, Point Estimate Methods, First Order Reliability Methods (FORM), First Order Second Moment Methods (FOSM), Response Surface Methods (RSM) etc. These methods can be considered generally well known, (Christian, 2004).

2.3.5.1 Monte Carlo Simulation

Monte Carlo Analysis is a computer-based method of analysis developed in the 1940's that uses statistical sampling techniques to obtain a probabilistic approximation to the solution

of a mathematical equation or model. Baecher and Christian (2003) described the Monte Carlo method as a method in which the analyst creates a large number of sets of randomly generated values for the uncertain parameters and computes the performance function (FOS for instance) for each set. The analyst must determine how many trials are necessary to ensure a desired level of accuracy in the results, Baecher and Christian (2003). A simulation can typically involve over 10,000 evaluations of the model. By using random inputs, the deterministic model is essentially turned into a stochastic model.

This method is often used when the model is complex, nonlinear, or involves more than just a few uncertain parameters. Monte Carlo simulation has the advantage that it is relatively easy to implement on a computer and can deal with a wide range of functions, including those that cannot be expressed conveniently in an explicit form, such as in the form of design charts. Morgan and Henrion (1990) pointed out that another advantage of Monte Carlo methods is that the precision of the output distribution may be estimated from the sample of output values using standard statistical techniques. Other important advantages of the Monte Carlo method are: flexibility in incorporating a wide variety of probability distributions without much approximation, and ability to readily model correlations among variables (Hammah and Yacoub, 2009).

However, although straightforward, Monte Carlo simulation can be very expensive computationally, especially when multiple runs are required to calculate sensitivities and/or when low probabilities are needed (Baker and Cornell, 2003; Baecher and Christian, 2003). Several techniques are available to accelerate convergence or, equivalently, to reduce variance. Latin Hypercube Sampling is the most common variance reduction scheme for Monte Carlo simulation.

2.3.5.2 Latin Hypercube vs. Random Sampling

In Monte Carlo analysis, one of two sampling schemes is generally employed: simple random sampling or Latin Hypercube sampling. Simple random sampling draws random values from the standard normal cumulative distribution function for each individual

variable by generating a random number from a uniform distribution on [0, 1]. However, as Chonggang Xu et al (2004) noted, there is no assurance that a sample element will be generated from any particular subset of the sample space. In view of this, Latin hypercube sampling was introduced into the Monte Carlo method by McKay et al. (1979).

Latin hypercube sampling is considered to be more efficient than simple random sampling, that is, it requires fewer simulations to produce the same level of precision. According t0 Diederichs and Kaiser (1996), the Latin Hypercube technique bears similarities to Monte Carlo but is more efficient and stratifies the sampling domain to reduce 'clumping' of input, which can invalidate the outcome (McKay et al 1979, Hoek et al 1995, Palisade Corporation 1994). Latin hypercube sampling is generally recommended over simple random sampling when the model is complex or when time and resource constraints are an issue. Morgan and Henrion (1990) stated, "Latin Hypercube sampling seems to be particularly helpful. Although it can introduce slight bias in the estimate of moments, in practice this seems negligible."

2.3.5.3 First Order Second Moment Method (FOSM)

The FOSM is an approximate probabilistic method that is based on a Taylor series expansion of the performance function. All terms in the Taylor series that are of a higher order than one are assumed negligibly small and then discarded (Baecher and Christian, 2003). From the remaining first order terms, the probability that the performance function is less than any given value can be calculated. One of the great advantages of the FOSM method is that it reveals the relative contribution of each variable in a clear and easily tabulated manner (Morgan and Henrion, 1990; Baecher and Christian, 2003). This is very useful in deciding what factors need more investigation and even in revealing some factor whose contribution cannot be reduced by any realistic procedure. Many of the other reliability analysis methods do not provide this information. Kinzelbach and Siegfried (2002) used the FOSM method to quantify the uncertainty in groundwater modelling and the results compared well with Monte Carlo simulation results.

Since FOSM is based on a Taylor series expansion, the evaluation of partial derivatives or their numerical approximations is critical to the use of the method (Harr, 1987). The attainment of these partial derivates is impossible in some cases such as when the performance function is given implicitly in the form of design charts. This is the greatest limitation of the FOSM method. Another shortcoming of the FOSM approach is that the results depend on the particular values of the variables at which the partial derivatives are calculated (Christian, 2004).

In order to improve the accuracy of the FOSM method, second order terms in the Taylor series are preserved giving rise to the second order second moment method (SOSM). However, Christian (2004) pointed out that while this method has found some applications in structural reliability studies, it has not found much application in geotechnical work. Morgan and Henrion (1990) pointed out that when higher order approximations, like SOSM, are used the model rapidly becomes algebraically complicated as the complexity of the model increases. The improvement in accuracy in SOSM is not always worth the extra computational effort (Baecher and Christian, 2003).

2.3.5.4 Point Estimate Method (PEM)

The point estimate method (PEM) was developed by Rosenblueth (Rosenblueth, 1975; Rosenblueth, 1981). The PEM uses a series of point-by-point evaluations (called point estimates) of the performance function at selected values (known as weighting points) of the input random variables to compute the moments of the response variable. The method applies appropriate weights to each of the point estimates of the response variable to compute moments. The weights can differ for different points. According to Christian (2004), the PEM method is a form of Gaussian quadrature.

Hoek (2006) noted that, while the PEM technique does not provide a full distribution of the output variable, as do the Monte Carlo and Latin Hypercube methods, it is very simple to use for problems with relatively few random variables and is useful when general trends are being investigated. When the probability distribution function for the output variable is known, for example, from previous Monte Carlo analyses, the mean and standard

deviation values can be used to calculate the complete output distribution. Hammah and Yacoub (2009), pp 2, stated that, “Although the method is very simple, it can be very accurate”. Harr (1987) agreed with the preceding statement and added that the method is easy to use and requires little knowledge of probability theory.

A great limitation of the original PEM for multiple variables is that it requires calculations at 2^n points, where n is the number of uncertain variables. When n is greater than 5 or 6, the number of evaluations becomes too large for practical purposes, (Baecher and Christian, 2003). Two relatively simple methods for reducing the number of points in the general case to 2n or 2n + 1 have been proposed (Hong 1996, 1998). However, Hammah and Yacoub (2009) pointed out that these methods for reducing the number of points move weighing points farther from mean values as the number of variables increases, and can lead to input values that extend beyond valid domains.

2.3.5.5 First Order Reliability Method (FORM)

While the FOSM method and its extension by the Rosenblueth PEM are powerful tools that usually give excellent results they do involve approximations that may not be acceptable. One approximation is that the moments of the failure criterion can be estimated accurately enough by starting with the mean values of the variables and extrapolating linearly (Baecher and Christian, 2003). In other words, there is an implicit assumption that it does not matter where the partial derivates are evaluated. A second is that the form of the distribution of the performance function is known and can be used to compute the probability of failure. But, according to Baecher and Christian (2003), in practice these assumptions are seldom valid. Hasofer and Lind (1974) addressed these concerns by proposing a different definition of the reliability index that leads to a geometric interpretation. The approach is named “The Hasofer-Lind Approach” or First Order Reliability Method (FORM). FORM was initially derived for use with non correlated variables. However Low and Tang (1997a) proposed a method of using the FORM method with correlated variables. The FORM method can also be adapted to be used on variables that are not normally distributed.

Low and Phoon (2002) used the FORM method with correlated non-normal variables for two geotechnical problems with complicated performance functions, namely the bearing capacity of a rectangular foundation with eccentric and inclined loadings, and the stability of an anchored retaining wall. They concluded that the probabilities of failure inferred from reliability indices are in good agreement with Monte Carlo simulations using the commercial package @RISK. In Low (2003), the FORM method is used to compute the reliability index involving spatially correlated normally and lognormally distributed random variables for an embankment on soft ground. The results compared well with Monte Carlo simulation results.

Novak (2005), in an overview of the state of art in reliability analyses noted that crude Monte Carlo simulation cannot be applied for time-consuming problems, as it requires a large number of simulations (repetitive calculation of structural response). Historically, this obstacle was successfully solved by approximate techniques FORM, SORM, (Hasofer and Lind, 1974; Madsen et al., 1986). In spite of some problems concerning the accuracy, these techniques are widely accepted nowadays and they became in some cases standard tools in codes calibration. The errors made when using FORM/SORM are acceptable in view of the large uncertainty in selecting the appropriate stochastic model and its parameters. As a result FORM/SORM is still much better than crude Monte Carlo methods that have been the yardstick to compare with or in some cases the only way to obtain results, Rackwitz (2001). However, as in FOSM, the requirement to evaluate partial derivates makes the FORM approach impossible to use in some cases where the performance function is not explicitly given.

2.3.5.6 Response Surface Methods (RSM)

The Response Surface Method (RSM) is a collection of statistical and mathematical techniques useful for developing, improving, and optimizing processes. The method was introduced by Box and Wilson (1951). The RSM computes the performance function at various combinations of the input variables and then uses regression techniques to create

a curve (surface in multi-dimensional space) that gives the response of the performance function to changes in the inputs. This curve is what is called the response surface. A number of methods of selecting the small sample of scenarios to run to create the response surface are in use. The most common method involves perturbing one input at a time, keeping the rest at their nominal values. Though this sampling approach is not very efficient computationally (Morgan and Henrion, 1990), it enjoys the benefit that it is simple and easy to implement in practice.

The most extensive applications of RSM are in the particular situations where several input variables potentially influence some performance measure (Factor of Safety, for instance) or quality characteristic of the process (Carley et al, 2004). Morgan and Henrion (1990) recommend the use of RSM for large computationally expensive models. One advantage of RSM is their flexibility in that they can handle any probability distribution as well as performance functions that are not given in explicit forms (design charts, for example). Due to their flexibility, RSM are used in different ways. Tapia et al (2007) described an approach which uses Monte Carlo simulation together with the RSM to carry out a risk analysis for an open pit mine. The same approach was also used by Contreras et al (2006) in a risk analysis for Cerrejon mine. Mollon et al (2009) used a different approach when they used the RSM with the FORM to carry out probabilistic analysis of a circular tunnel using the numerical modelling code FLAC3D. In other fields, the Response surface approach has been used for uncertainty analysis of some very large computer codes for simulation of the liquid metal fast breeder reactor (Vaurio 1982). Another example involves a regional photochemical air pollution model (Milford et al, 1988). However, the use of response surface methods has been relatively rare in Geotechnical Engineering.

2.3.6 Risk Approach

Risk can be defined as the probability of occurrence of an event combined with the consequence or potential loss associated with that event, (Whitman, 1983; Wilson and Crouch, 1987):

$$\textbf{Risk} = \textbf{P}(\textbf{event}) \times \textbf{Consequence of the event} \qquad \textbf{(2-4)}$$

Diederichs and Kaiser (1996) stated that the calculated probability of undesirable occurrence is meaningless unless the consequences of the occurrence are understood. Lilly (2000) summarised the consequences of slope failure as clean up costs, slope re-formation, haul road repair, un-recoverable ore, and damage to equipment, personnel and infrastructure. These consequences can be grouped into two broad classes, economic impact and safety impact (Steffen, 1997). The risk approach to slope design solves the main drawback of the Factor of safety approach and the probabilistic approach with regard to the selection of the appropriate acceptability criteria (SRK, 2006; Tapia et al, 2007). Steffen et al (2008) noted that adopting a risk approach to slope design for open pit mining operations effectively allows the owners to define their risk criteria, taking account of the specific consequences of potential failures and the benefits of steeper slopes at higher risk, and tasking the designers accordingly. Read and Stacey (2009), pp 3, echoed these sentiments when they stated, "A measure is required so that mine executives have sufficient information and understanding to be able to establish acceptable levels of risk." Bawden (2008) acknowledged the use of risk based design in slope stability when he stated, that in open pit slope stability, formal risk analysis procedures are commonly applied as part of the slope design process.

2.3.6.1 Methodology

There are many methods available for developing a risk-consequence process. However, they all contain some common steps, as described in the guidelines given by the Australian Geomechanics Society (2000). These are:

- Identify the event generating hazards;
- Assess the likelihood or probability of occurrence of these events;
- Assess the impact of the hazard;
- Combine the probability and impact to produce an assessment of risk;

- Compare the calculated risk with benchmark criteria to produce an assessment of risk,
- Use the assessment of risk as an aid to decision making.

Figure 2.8 is an illustration of the entire risk approach to design (SRK, 2006; Steffen et al, 2008).

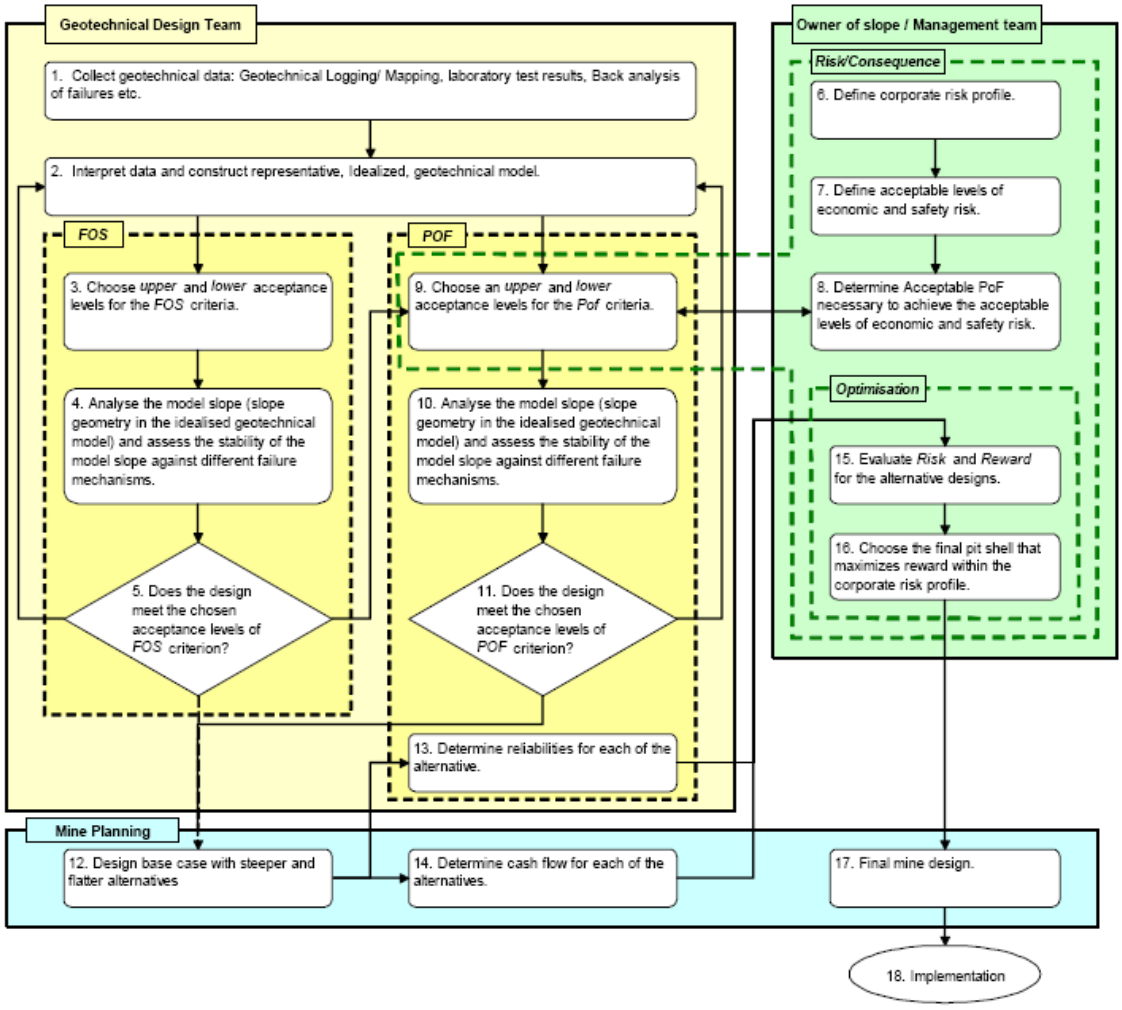

Figure 2.8 Generic Flow-chart of the open pit slope design process (after SRK, 2006)

As explained before, one of the objectives of risk analysis is the assessment of the consequences of slope failure on safety of personnel (SRK, 2006). This is done through the estimation of the probability of fatality caused by slope failures and the comparison of this result with acceptability criteria (Steffen et al, 2006; Tapia et al, 2007).

2.3.6.2 Acceptability Criteria for Safety Risk

In order to assess the meaning of the calculated probability of fatality values, these values need to be compared with benchmark criteria. A typical graph used for this purpose is indicated in Figure 2.9 which presents acceptability criteria for fatality defined by different sources (HSE, 2001; SRK, 2006; Tapia et al, 2007). The areas in the graph related with tolerability of risk are derived from risk guidelines developed in the United Kingdom (HSE, 2001), and correspond to risk thresholds in terms of local acceptability of deaths from industrial and other accidents. The graph is plotted as the number of fatalities from accidents versus the annual probability of exceeding that number. According to Tapia et al (2007), the annual probability identified as "The proposed BC Hydro individual risk" in Figure 2.9 can be accepted as the criterion for slope design. This number represents the risk exposure to 'natural death' by the safest population group in North America aged between 10 to 14 years within a person's life cycle. The interpretation is that 1 in 10 000 persons between the ages of 10 and 14 years will die every year from natural causes (HSE, 2001). Using this criterion for open pit slope design implies that a person subjected to the open pit working environment is not exposed to greater death risk resulting from a slope failure than he is of dying due to natural causes (SRK, 2006).

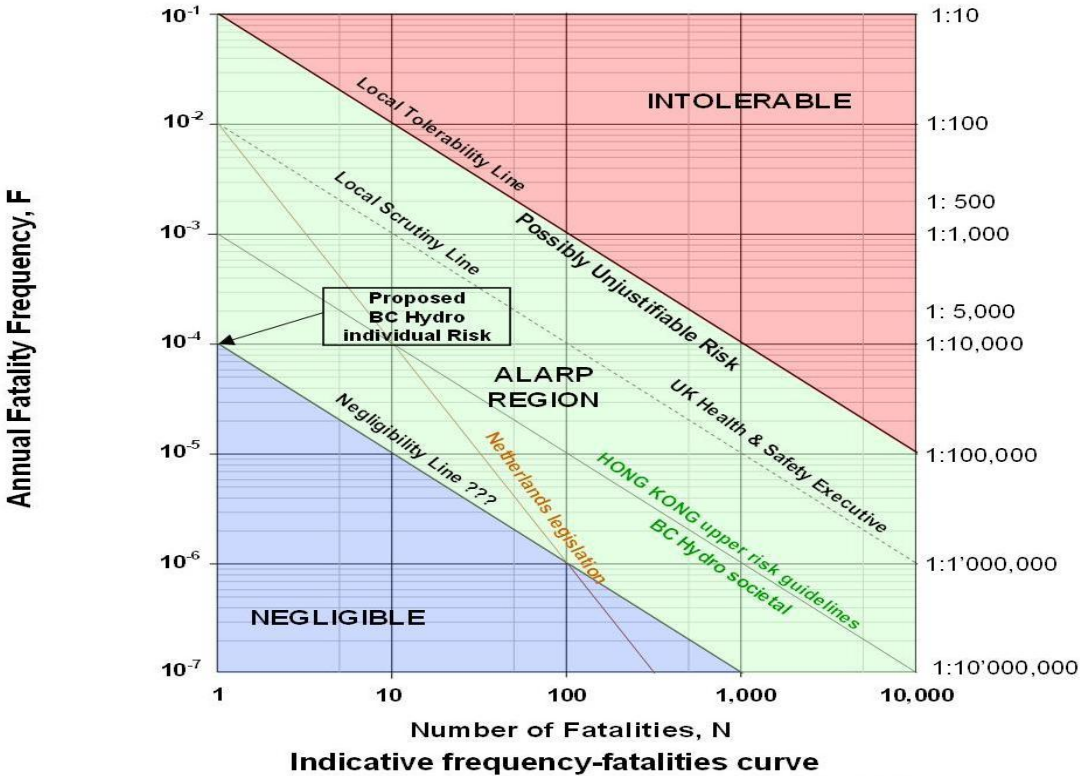

Figure 2.9 Benchmark criteria for safety impact of slope failure; acceptability criteria defined by different organisations (after Health and Safety Executive, 2001)

2.3.6.3 Challenges in Adopting the Risk Approach

Incorporating risk analysis into the design has its own challenges, especially to do with the requirement for more input information. Steffen et al (2008), pp 3, stated; “Because the risk analysis sets the acceptability criteria on the consequences rather than on the likelihood of the event, a thorough evaluation of the POF of the slope is required, incorporating other sources of uncertainty not accounted for with the slope stability model. For this purpose and for the analysis of consequences of slope failure, non formal sources of information (engineering judgment, expert knowledge) are incorporated into the process with the aid of methods such as development of logic diagrams and event tree analysis.” Consequently, risk analysis requires a lot more input data/information than the conventional FOS approach.

Davies (1997), writing on risk analysis in the mining industry, concluded; 'Most often the largest difficulties come from the manner in which estimates of probability, or likelihood, of event occurrence are developed. Ideally statistically significant sample numbers based upon an appropriate statistical model are required. However in mining, where the sheer extent of systems usually makes spatial variability a key parameter, statistically significant sampling is not feasible on either a mass or volumetric basis. The question then becomes, "What kind of risk assessment, if any, is practical and valid for most mining applications?"' It is important to note the risk analyses that are being carried out at present are based on simplified models, where issues like spatial variability are not explicitly modelled.

2.3.7 Summary

This chapter has given a brief survey of the literature relevant to this project. Most of the issues discussed can be considered well researched and understood at present. The next chapter contains the descriptions of the LE and numerical slope stability models that were used in this dissertation.

CHAPTER 3

3 SLOPE STABILITY MODELS

The previous chapter gave an overview of the relevant literature pertaining to the stability analysis of rock slopes. This chapter contains a description of all the LE and numerical models analysed in this project. The model geometries, material properties, loading conditions and modelling assumptions are all included. Also covered in this chapter is a description of the event trees used for the risk analyses. The results that were obtained from these models will be covered in Chapter 4.

3.1 Limit Equilibrium Analysis (SLIDE)

All LE modelling was carried out using the program SLIDE from Rocscience Inc. SLIDE is a 2D limit equilibrium slope stability program for evaluating the safety factor or probability of failure, of circular or non-circular failure surfaces in soil or rock slopes. SLIDE analyzes the stability of slip surfaces using vertical slice limit equilibrium methods. The Slide models used in the analyses all used the same generic settings. No water surfaces, external loads, or support elements were used. The following sections give brief descriptions of the settings/assumptions adopted in all analyses.

3.1.1 Analysis Methods

The Bishop simplified and Janbu's corrected methods of slices were used for all analyses. Bishop's method is more suited to circular failure mechanisms which can occur in homogeneous rock masses. For inhomogeneous rock masses, Janbu's corrected method is more appropriate, since it can handle non circular failure surfaces. Hence for all the models two values of Factor of Safety were reported, according to Bishop's method and Janbu's corrected method. The default number of 25 slices was used since this is sufficient to obtain an accurate solution for most problems (Rocscience, 2008).

3.1.2 Surface Options

A non-circular slip surface search method was used, namely path search. The *Path Search* in SLIDE generates random non-circular (piece-wise linear) slip surfaces. The number of surfaces used was 5000. All SLIDE models analysed had the Surface Optimisation feature enabled. The Optimize Surfaces feature is a very powerful search technique, based on a Monte Carlo technique, often referred to as "random walking" (Greco, 1996). This technique allows the user to search for lower safety factor slip surfaces, using the surfaces generated by Path Search or specific user-defined slip surfaces, as a starting point. After the FOS has been determined using the path search method, the location of one vertex on the slip surface is randomly modified and a new FOS calculated for the new surface. If the factor of safety for the modified surface is lower than the factor of safety for the initial surface, the new surface replaces the original surface, and the location of another vertex is modified. The process is repeated and until the factor of safety for the modified surface is higher than the factor of safety for the initial surface (or the change in the factor of safety is lower than some tolerance).

3.1.3 Probabilistic analysis

For the probabilistic analyses, five thousand values of each random variable (for example, Cohesion) were generated, according to the statistical distribution for each random variable. The analysis was then run five thousand times, and a safety factor calculated for each sample. This resulted in a distribution of safety factors, from which the *probability of failure* was calculated. The Latin Hypercube Sampling scheme described in chapter 2 was used to sample the five thousand values for each random variable. The probabilistic analyses were carried out on the global minimum as determined from the deterministic analyses and not on the overall slope. What this means is that SLIDE would run a deterministic analysis with the mean parameters to find the slip surface (called global minimum surface). Afterwards, the input parameters were varied to obtain different values of FOS for the global minimum surface. No other surface was analysed in the probabilistic simulations. The *global minimum p*robabilistic analysis type, assumes that the Probability of Failure calculated for the (Deterministic) global minimum slip surface, is representative of the probability of failure for the entire slope. In many cases, this is a valid or reasonable assumption. This method results in much shorter computation times with very little loss in accuracy, Rocscience (2008).

3.2 Numerical modelling

Three different programs were used for the numerical modelling, depending on the model to be analysed. One finite element code (PHASE 2, Rocscience Inc), and two finite difference codes (FLAC and FLAC3D) were used. In all models, the recommendation in Wyllie and Mah (2004) by Loren Lorig, was adopted to ensure that boundaries were distant enough so as not to influence analysis results (Figure 3.1). Isotropic elasticity was assumed in all analyses, with the deformation properties of the materials being defined by the Young's modulus and Poisson's ratio.

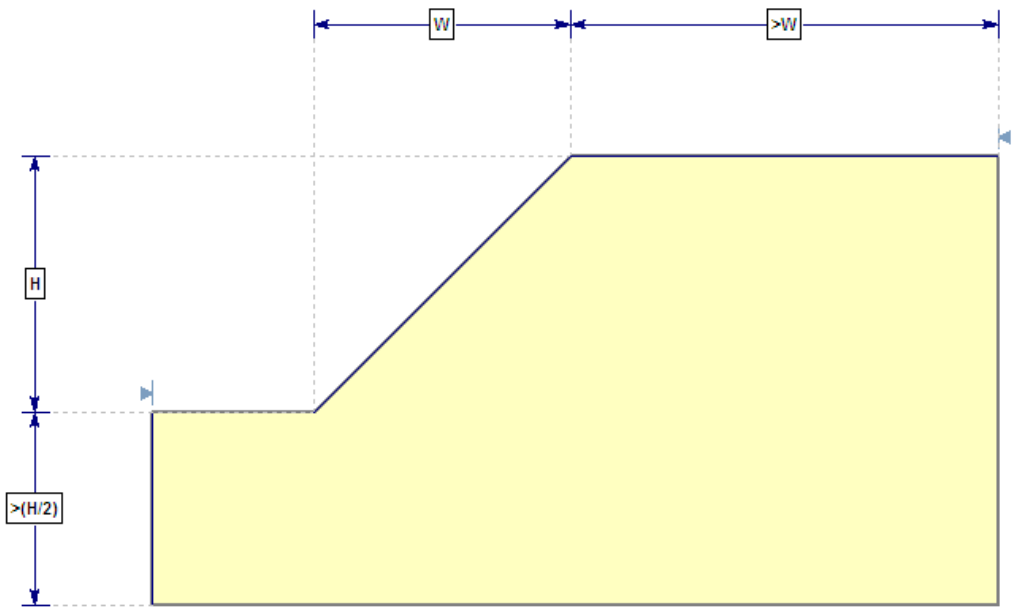

Figure 3.1 Recommended dimensions for numerical analysis to ensure boundaries do not influence analysis results, after Lorig and Varona (2004).

3.2.1 PHASE 2 (Finite Element Analysis)

Phase2 is a 2-dimensional elasto-plastic finite element program for calculating stresses and displacements around underground openings, and can be used to solve a wide range of mining, geotechnical and civil engineering problems. *Phase2* incorporates a 2 dimensional automatic finite element mesh generator, which can generate meshes based on either triangular or quadrilateral finite elements. For all the analyses that were carried out, 6 noded triangular elements were used. Figure 3.2 shows a typical 3 noded as well as a 6 noded element.

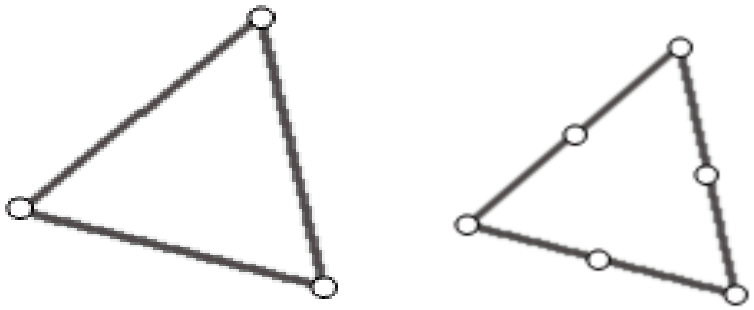

Figure 3.2 3 noded and 6 noded triangular elements for Finite Element Analysis

In general, elements with mid-side nodes (6-noded triangles or 8-noded quadrilaterals) will improve the accuracy of the results; however computation times and file sizes will increase accordingly. A uniform mesh was used throughout the entire Slope model. In each model elements of high aspect ratio (long "thin" elements) were avoided since the presence of such elements can have adverse effects on the analysis results. All the Phase2 analyses carried out in this work assumed plane strain conditions. Thus, the excavations were assumed to be of infinite length in the out-of-plane direction, thereby assuming zero strain in that direction. A Gaussian Elimination solver was used in solving the matrices produced in the finite element analysis. The absolute energy criterion was used to test for convergence during simulation, and an automatic step size was used in the Shear Strength Reduction scheme. The following briefly describes the settings used in all Phase2 models, unless specified otherwise.

In all the Phase2 models, the field stress represents the only loading imposed on the model. A gravitational field stress was specified, using the actual ground surface option. A k ratio (horizontal: vertical stress ratio) of 1 was used in all analyses for both the in-plane and out of plane directions. The only exception was in the models in which the effect of the k ratio on FOS was being investigated. The locked in stresses were kept at zero in all models, both in-plane and out-of-plane directions, except in the models which were investigating the effect of locked in stresses on FOS. The initial element loading was set as “field stress and body force”. All boundaries parallel to the y axis had their x displacements set at zero. The bottom boundary parallel to the x axis was restrained in both the x and y directions. The ground surface was left as a free boundary. Figure 3.3 shows the displacement boundary conditions imposed on all the Phase 2 models.

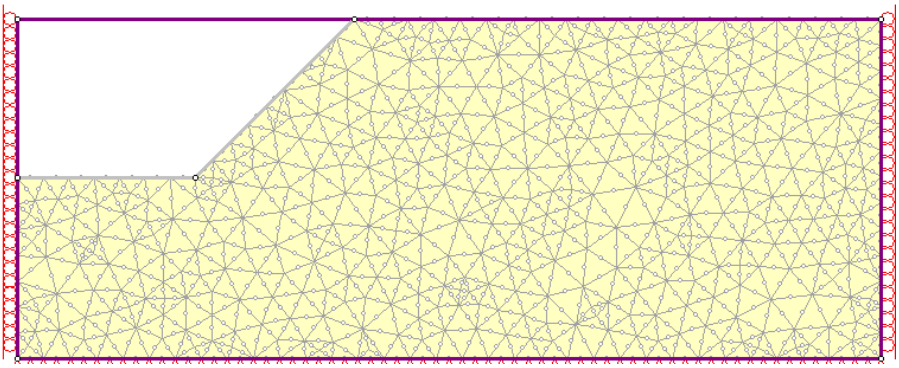

Figure 3.3 Displacement boundary conditions used in all 2D numerical models

3.2.2 FLAC (Finite Difference)

FLAC is a two-dimensional explicit finite difference program for engineering mechanics computation. This program simulates the behaviour of structures built of soil, rock or other materials that may undergo plastic flow when their yield limits are reached. Phase2 can only model Elastic perfectly-plastic and Elastic perfectly-brittle behaviour of the rock mass. FLAC was therefore used to investigate the effect of strain softening behaviour on the FOS of the slope. FLAC can model the effect of various strain softening parameters on the FOS using the strain softening constitutive model. FLAC was also used to build 2D models for comparison with full 3D analyses in FLAC3D. Since FLAC3D is a finite difference code, another finite difference code (FLAC) was chosen to analyse the 2D models so that any differences would not be due to differences in calculation logic but due to 3D effects. Thirdly, FLAC was used in analysing the slopes in the case study described in Chapter 5. These slopes include foliated rocks and Phase2 does not have a built-in constitutive model that can handle such cases. An option in Phase2 was to model the foliation planes with closely spaced deterministic joint sets. However, this approach results in a high percentage of poor quality elements in the mesh. Consequently, FLAC was chosen for modelling the slopes in the case study using the ubiquitous joint constitutive model. All FLAC models built in this work used the plane strain assumption.

3.2.3 FLAC3D (Finite Difference)

FLAC3D is the 3D counterpart of FLAC. The Finite Difference scheme is the same in both programs, with FLAC3D extending the logic into 3 dimensional space. FLAC3D was used to investigate the effects of slope curvature on slope stability. Only homogeneous slopes were modelled in FLAC3D.

3.3 Analyses Conducted

The analyses carried out in this research work comprised of 4 distinct stages. The first set of analyses was the verification of the response surface formulation as well as the selection of the proper parameters for use in the analysis. This was necessary since the RSM is not well documented in geotechnical literature, and a clear methodology has not yet been published by any author. The second set comprised of the comparison of the deterministic FOS values computed with the Limit Equilibrium program SLIDE with those computed using numerical tools. The third set of analyses involved comparing the POF values obtained from SLIDE with those from numerical models. Finally, the risk in terms of safety impact was calculated using results from the LE POF computations and from the numerical analysis POF computations.

3.3.1 Rock Mass Properties

The rock mass was characterised using the Generalised Hoek-Brown criterion. Nine different materials were characterised as shown in Table 3.1. The Geological Strength Index (GSI) is a measure of how blocky the rock mass is whereas the mi parameter is a measure of the frictional characteristics of the component minerals in the intact rock sample and it has a significant influence on the strength characteristics of rock, (Marinos and Hoek, 2001). D is a measure of the disturbance due to blasting with a value of 1 representing conditions of poor blasting. Such a choice of the D value gives the worst case scenario in slope design. The column labelled MR contains values of the modulus ratio, which is simply the ratio of the intact Young's modulus to the UCS of the rock. The rock named "homogeneous" was used for all models consisting of one rock unit (unless specified otherwise). The other 8 units were used in analyses involving many rock types. The values for UCS were selected so as to cover a wide spectrum ranging from weak (UCS < 50 MPa) to strong rocks (UCS > 200 MPa). Most of the values were taken from case studies of open pit slope designs.

Table 3.1 Hoek Brown strength parameters for the rock units used in the stability models

Rock Type	Unit Weight (kN/m^3)	Poisson Ratio	UCS(Mpa)	GSI	mi	D	MR
Hom o	27	0.25	80	50	10	1	400
cplx material 1	27	0.25	80	50	10	1	310
cplx material 2	27	0.25	215	45	10	1	431
cplx material 3	27	0.25	220	45	10	1	325
cplx material 4	27	0.25	50	45	10	1	273
cplx material 5	27	0.25	56	45	10	1	446
cplx material 6	27	0.25	30	30	24	1	1000
cplx material 7	27	0.25	70	30	20	1	100
cplx material 8	27	0.25	90	45	10	1	350

For models in FLAC and FLAC3D, the shear strength reduction (SSR) method cannot be used with the Hoek-Brown criterion. In Phase2 it is possible to use the Hoek-Brown criterion with the SSR method but so as to maintain uniformity; all models were implemented using the Mohr Coulomb criterion, which describes the strength of the rock using the cohesion and friction angle. Hence, all homogeneous models in this work were built using equivalent Mohr Coulomb parameters derived from the Hoek-Brown parameters (Table 3.2). The deformation modulus was calculated using the Hoek-Diederichs empirical relation (Hoek and Diederichs, 2006). The Poisson ratio was taken to be 0.25 in all numerical analyses. The tensile strength was calculated using the approach suggested by Hoek et al (2002).

Table 3.2 Mohr Coulomb and deformation properties derived from the Hoek-Brown parameters

Rock Type	c (kPa)	ϕ (°)	E (GPa)	σt (kPa)	v
Hom o	641	31	2.1	-68	0.25
cplx material 1	641	31	1.7	-68	0.25
cplx material 2	810	36	4.7	-114	0.25
cplx material 3	818	36	3.6	-117	0.25
cplx material 4	454	24	0.7	-27	0.25
cplx material 5	474	25	1.3	-30	0.25
cplx material 6	311	19	0.8	-2	0.25
cplx material 7	392	23	0.2	-4	0.25
cplx material 8	568	29	1.6	-48	0.25

Where c = rock mass cohesion; ϕ = friction angle; E = Young's modulus; σ_t = tensile strength; v = Poisson's ratio.

Converting Hoek-Brown parameters into equivalent Mohr Coulomb parameters requires knowledge of the expected maximum value of the minimum principal stress, σ3. Two approaches were used in coming up with an estimate of σ3 max. The first approach used the empirical relation proposed by Hoek et al (2002). The second approach involved performing an elastic analysis of the pit using the numerical modelling code Phase2. From the resulting contours of σ3, an estimate of $\sigma 3_{max}$ was then made. This resulted in a value of around 3 MPa for a 400m high slope and 7 MPa for a 1000m high slope. However, since an elastic analysis generally over-estimates the stresses (in a plastic analysis there is stress redistribution due to yielding), these values were downgraded to 1 -2 MPa for a 400m high slope, and 4-5 MPa for a 1000m high slope. To keep the work tractable, a constant value of $\sigma 3_{max}$ of 3 MPa was adopted for all pit depths. This value is an average of the elastic stress analysis and the empirical method by Hoek et al (2002) for a 400m deep pit.

3.3.2 Response Surface Methodology Verification

The probability of failure for the models was computed using the Response Surface Methodology (RSM). Since the RSM approach is not well documented in geotechnical literature, models to validate its use in probabilistic slope stability analysis were run. The following section gives a brief explanation of the RSM concept as well as a description of the models used to verify the accuracy of the RSM in probabilistic slope stability analysis. All the validation was done using the LE program SLIDE due to its ability to handle Monte Carlo simulations efficiently.

3.3.2.1 RSM Description

In the response surface method, with N uncertainties contributing to the distribution of FOS, this distribution could be viewed as being represented by a function

$$\boldsymbol{FOS = R(x_1, x_2, \dots, x_N)} \qquad \textbf{(3-1)}$$

In N-dimensional space, defined by variables x_1- x_N, R can be viewed as a surface (called the response surface). The response surface method assumes that the effects of each variable x_i on the FOS are independent of the other variables. Inaccuracies arise because this assumption is not true in general (Tapia et al, 2007). However, these inaccuracies are

minimised by calculating the best-estimate of FOS first using the best-estimates for each of the uncertainties x'_1, x_2',...,x'_N:

$$\boldsymbol{FOS_{bc}} = \boldsymbol{R}(\boldsymbol{x_1'}, \boldsymbol{x_2'}, \ldots, \boldsymbol{x_N'}) \quad \textbf{(3-2)}$$

where FOS_{bc} is the best-estimate value and is referred to as the base case. The sensitivity of the FOS to the various inputs is investigated by varying each variable while keeping the rest constant at their best estimate values as shown in Figure 3.4. A new FOS is then calculated using this new set of input variables with the aid of the relevant stability analysis tool like SLIDE or Phase2. This sensitivity is quantified by a parameter termed the sensitivity parameter, β, defined as:

$$\boldsymbol{\beta}(\boldsymbol{x_i} - \boldsymbol{x_i'}) = \frac{\boldsymbol{R}(\boldsymbol{x_i}, \boldsymbol{x_2'}, \ldots, \boldsymbol{x_N'})}{\boldsymbol{FOS_{bc}}} \quad \textbf{(3-3)}$$

The sensitivity parameter, β, is defined twice for each variable; One point on each side of the best estimate (referred to as the "-"and "+" case). A plot of β against the normalised variable is made and regression techniques used to fit a 2nd order polynomial that gives the value of β for any given value of the normalised variable. These regression lines can also be defined using piece-wise linear functions.

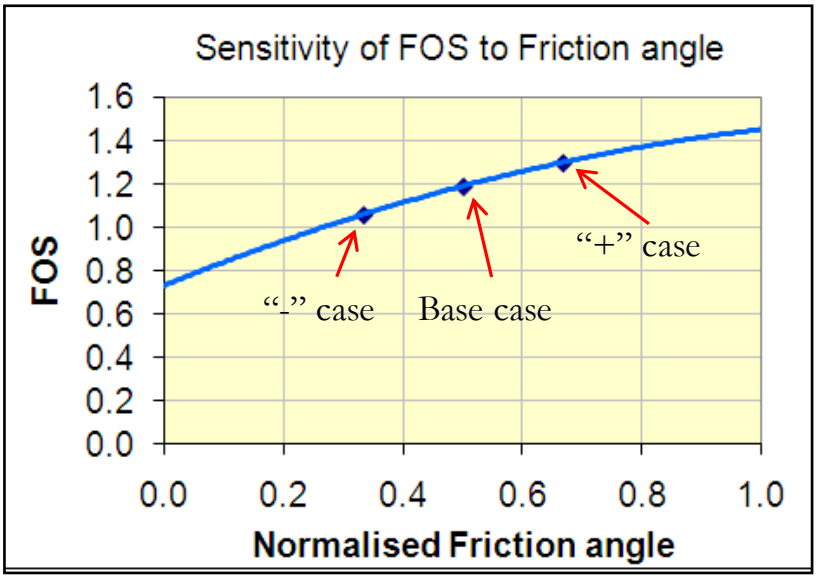

Figure 3.4 Sensitivity of FOS to friction angle showing the locations of the "-"case, the "+" case, and the base case

The points at which the "-" and "+" case are evaluated can be located anywhere in the region of interest. However, for most problems using points located at "-" and "+" one

standard deviation gives good results. When modelling a system with N variables, N 2nd order equations relating β to the variable are formed. For any random combination of the input variables, a value of the factor of safety (FOS_i) is obtained by:

$$\boldsymbol{FOS_i = FOS_{bc} \times \beta_{1i} \times \beta_{2i} \times \ldots \times \beta_{Ni}} \qquad \textbf{(3-4)}$$

Multiple Monte Carlo simulations (numbering up to fifty thousand) in a spreadsheet package like Microsoft Excel, using the various probability distributions of the uncertainties, results in a distribution of FOS from which the POF can be calculated as:

$$\boldsymbol{POF = P(FOS < 1)} \qquad \textbf{(3-5)}$$

Figure 3.5 illustrates the definition of the probability of failure from Monte Carlo simulations. In essence, the RSM approach seeks to replace the slope stability analysis tool with a model constructed using only a few runs of the stability model and regression techniques. Full Monte Carlo simulations are then executed by randomly sampling the input variables and estimating the FOS from the RSM model and not the actual stability model. The RSM requires 2N + 1 runs of the stability model in order to create the response surface. As a result, the RSM approach is very efficient in terms of computational times.

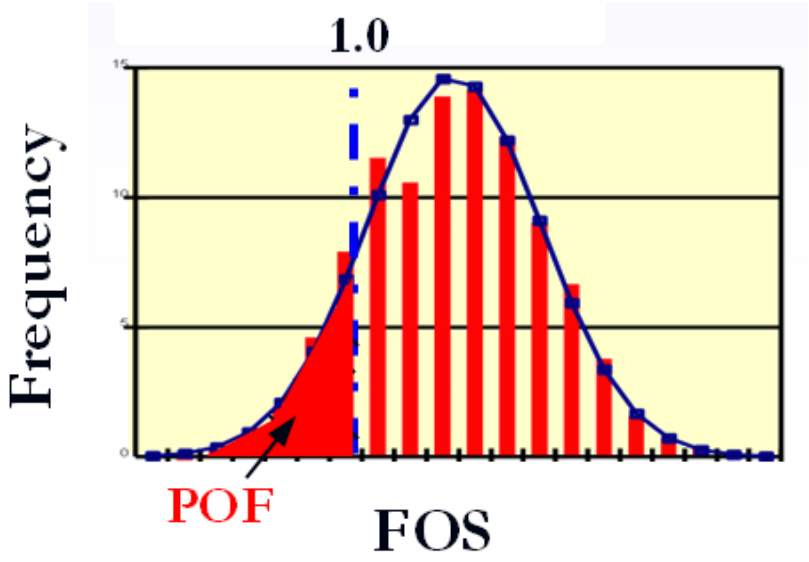

Figure 3.5 Graph showing the distribution of FOS from Monte Carlo simulations and definition of the probability of failure.

3.3.2.2 Verification Approach and Models

The verification of the RSM formulation involved doing a full Monte Carlo simulation in SLIDE (simply called SLIDE Monte Carlo in this section) and comparing the results with the RSM approximation. In other words, the first approach involved running 10,000 models of SLIDE with randomly sampled strength parameters. The POF was then defined as the number of models that resulted in a FOS of less than one divided by the total number of models, which were 10,000 in this case. The RSM approximation involved running only a few SLIDE runs (5 or 13, depending on the slope geometry) and using the results to create the response surface as explained in the previous section. Monte Carlo simulations were then done in Excel to come up with the POF. The two POF values obtained using the 2 different approaches were then compared.

Two different models were used for the analyses; a homogeneous slope and a slope consisting of 3 materials. Figure 3.6 shows the 2 different models. In the model with more than one rock type, the slope limits were placed so as to force the slip surface to pass through all rock units. For the analyses, only the cohesion and friction angle were regarded as uncertain parameters.

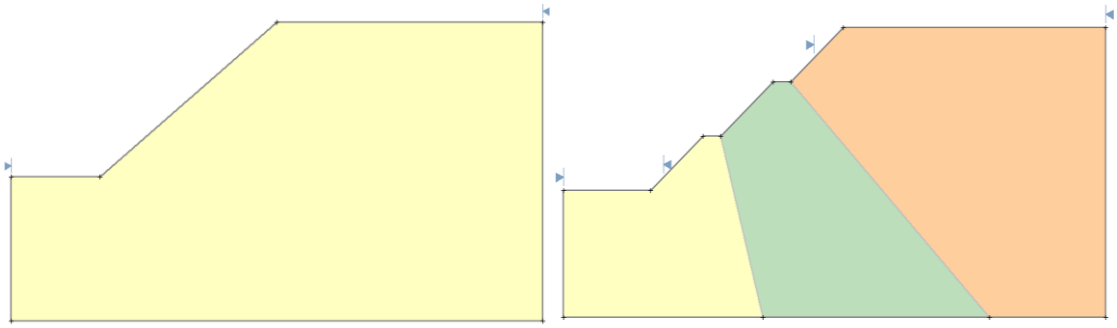

Figure 3.6 The Slope geometries used for validating the RSM approach to probabilistic slope design; (a) homogeneous slope (b) heterogeneous slope

Since some parameters used in slope stability analysis are known to be correlated in some way (cohesion and friction angle for example), the ability of the RSM formulation to handle correlated variables was investigated. To achieve this, different levels of correlation between the friction angle and the cohesion were specified. The analyses were divided into 3 classes with correlation coefficients (CC) between the friction angle and the cohesion of 0.5, 0, and -0.5 so as to cover conditions of positive correlation, independent variables, and negative correlation respectively. In addition to the CC, another parameter that was varied

during the analyses is the coefficient of variation (CV). The CV is simply the ratio of the standard deviation to the mean and is a measure of the spread of the distribution. A low CV implies a distribution with the data points concentrated around the mean, whereas a high CV implies wide scatter amongst the data.

The normal distribution is an open distribution which allows the variable to assume negative variables. However, most of the input parameters in geotechnical analyses, like cohesion and friction angle, cannot take on negative values and are better modelled using lognormal distributions (Baecher and Christian, 2003). The ability of the RSM in handling non-normal variables was therefore studied by assuming lognormal distributions to the cohesion and friction angle in some of the homogeneous models.

3.3.2.3 Strength properties

Table 3.3 gives a summary of the mean values of the cohesion and friction angle of the materials used in the RSM verification models. The material named "homogeneous" refers to the material constituting the homogeneous model. Materials A to C refer to the materials making up the heterogeneous slope consisting of three materials.

Table 3.3 Strength parameters used for the SLIDE RSM verification models

Rock Type	c (kPa)	ϕ (°)	γ (kN/m^3)
Homogeneous	500	30	27
material A	35	22	27
material B	85	27	27
material C	120	25	27

Four different distributions were created by varying the CV from 0.1 to 0.3, keeping the mean values constant in all models. Since the normal distribution is an open distribution, the sampling was done in the region encompassing 3 standard deviations both sides of the mean (99.7% of the data in a normal distribution lie within ± three standard deviations from the mean).

When using the lognormal distribution unrealistically high values can be sampled due to the fact that the lognormal distribution does not have an upper bound. There is need to truncate the distribution at a value which is representative of the maximum that can

realistically occur for that variable. However, estimating the maximum value for the input parameter is not very straight forward when working with the lognormal distribution. The approach adopted in this work was to first convert the lognormal distribution to its underlying normal variate. From the normal variate the maximum was then simply estimated as:

$$\boldsymbol{Max = mean + (3 \times standard\ deviation)} \qquad \textbf{(3-6)}$$

This value was then converted back to the lognormal distribution by taking its exponential and the distribution was then truncated at this maximum value in the SLIDE Monte Carlo simulations. No truncation is necessary for the lower limit of a lognormal distribution since by definition it cannot have values less than zero.

3.3.2.4 Implementation of Response Surface Methodology

The RSM was implemented using an Excel spreadsheet, together with a commercial add-in, Crystal Ball (Oracle Inc.). In all cases, the model was evaluated at two points placed at ±1 standard deviation from the mean, as was described earlier. A piecewise linear interpolation/extrapolation scheme was used in the RSM. Monte Carlo simulation on the response surface was done using 50,000 trials, with a Latin Hypercube sampling scheme.

3.3.3 Deterministic FOS calculations

Different slope geometries were set up to compare the FOS results from LE (SLIDE) and from numerical analyses. The goal was to determine those parameters, not included in LE analyses, which have an influence on FOS. Table 3.4 is a summary of the analyses that were conducted in this phase of the research. In the table, the column labelled “No. of models” refers to the number of models built for each analysis type. For example, if the number of models is given as 5, it means five models were built in SLIDE and another five in Phase2. Unless specified otherwise, the Phase2 models assumed a k ratio of one, a dilation angle of zero, no locked in stresses, an elastic-perfectly plastic strength model, and mining modelled in one step.

Table 3.4 Summary of conducted analyses for deterministic FOS comparisons

Investigated parameter	Geology	No of models	LE program	Numerical program
Slope angle	Homogeneous	5	SLIDE	Phase2
Pit depth	Homogeneous	5	SLIDE	Phase2
k ratio	Heterogeneous	5	SLIDE	Phase2
Locked in stress	Heterogeneous	5	SLIDE	Phase2
Dilation Angle	Heterogeneous	5	SLIDE	Phase2
Tensile strength	Homogeneous	5	SLIDE	Phase2
Sequential mining	Homogeneous	5	NA	Phase2
Strain softening	Homogeneous	5	NA	FLAC
Concave slope	Homogeneous	4	NA	Phase2
Bathtub	Homogeneous	4	NA	FLAC/FLAC3D

In addition to the FOS, an attempt was made to estimate the expected failure volumes from the model results. This task was complicated by the fact that 2D models assume that the slope geometry extents to infinity in the out of plane direction, and the same applies for the predicted failure surface. In real life, the extent of the failure in the out of plane direction will be constrained to form a semi spherical shape. The approach adopted in this work was to determine the volume of rock defined by the failure surface for a distance of 1m in the out of plane direction. This volume was then used as an indicator of the relative size of the failure volume predicted by the 2D model.

SLIDE gives the failure volume for unit slope length in the out of plane direction directly but Phase2 does not. To estimate this failure “volume” in Phase2 the failure surface in Phase2 was therefore defined by the maximum shear strain contours as shown in Figure 3.7, a poly line was used to approximate the failure surface, and this poly line surface subsequently exported into AutoCAD (AutoDesk Inc.) where the surface area was calculated. This surface area is equal to the volume for a unit length of the slope in the out of plane direction. Figure 3.7 shows an example of the poly line superimposed on top of maximum shear strain contours. The image to the right of Figure 3.7 shows the deformation vectors at the point of failure. These deformation vectors confirm the validity of using the maximum shear strain contours as an indicator of the failure surface.

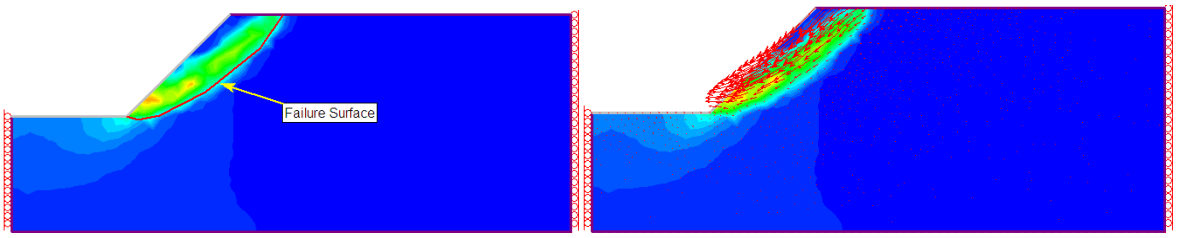

Figure 3.7 Phase2 result image showing (left) maximum shear strain contours with polyline drawn to approximate the surface and (right) deformation vectors

For FLAC and FLAC3D analyses, a modified approach was adopted in calculating the failure volumes. Comparing the failure volumes from 3D and 2D models was complicated by the fact that the 2D models do not give 'volumes' but simply the surface area of the failing material. To simplify the comparison, the depth of the failure surface was used as an indication of the failure 'volume'. Thus the actual shape of the FLAC3D failure surface was not considered. The failure surfaces in these two codes were defined using the shear strain increment contours. Unlike Phase2 these two programs do not have the ability to export dxf files. Therefore, the result files from FLAC and FLAC3D were saved as jpeg files which were subsequently imported into Phase2 wherein the failure surfaces were approximated using poly lines. These poly lines were then exported as dxf files into AutoCAD from where the failure volumes were determined.

Models were built assuming a homogeneous and a heterogeneous slope. The heterogeneous slope used for the models is as shown in Figure 3.8. It consisted of 7 rock units, cplx material 1 to cplx material 7 in Table 3.1. The slope height was 470m and the slope angle was 41°. The homogeneous slope consisted of the material named "homo" in Table 3.1.

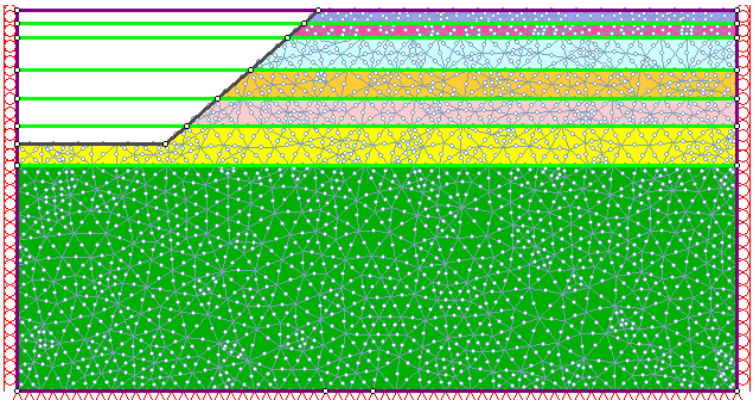

Figure 3.8 Heterogeneous slope used for the models to test the effect of locked-in stress, tensile strength, and dilation angle on slope stability

1) Slope Angle

A 600m deep pit was modelled at five different slope angles; 30°, 40°, 50°, 60°, and 75°. Five models were run in SLIDE and Phase 2 for the different slope angles. The slopes were homogeneous using the material “homo” in Table 3.1.

2) Pit Depth

An overall slope angle of 45° was used for varying pit depths. SLIDE and Phase2 were used for the LE and numerical analyses. The pit depths considered were 400m, 600m, 800m, 1000m, and 1200m. The slope was homogeneous consisting of the material “homo” in Table 3.1.

3) k ratio

The effect of the horizontal to vertical stress ratio on stability was investigated by building five Phase2 models of the heterogeneous slope in Figure 3.8 using five different k ratio values; 0.5, 1, 2, 3, 4. The same slope was analysed in SLIDE but only one model was necessary since the k ratio is not an input parameter in SLIDE.

4) Locked-in stresses

The effect of the locked-in stresses on stability was also investigated by building five Phase2 models of the heterogeneous slope in Figure 3.8. The values of locked-in stresses used were 0, 1, 5, 10, and 20 MPa. The same slope was analysed in SLIDE but only one model was necessary since k ratio is not an input parameter in SLIDE.

5) Dilation Angle

The purpose of this set of analyses was to study the effect of the dilation angle on the FOS values. The heterogeneous slope of Figure 3.8 was modelled in Phase2 with five different dilation angles of 0°, 10°, 15°, 20°, and 25°. The same slope was analysed in SLIDE but only one model was necessary since dilation angle is not an input parameter in SLIDE.

6) Tensile Strength

An 800m high homogeneous slope, with a slope angle of 45° was modelled in Phase2 for five different values of tensile strength; 0, 50, 70, 100, and 200 KPa. The slope consisted of the material "homo" in Table 3.1.

7) Sequential Mining

The effect of the number of mining steps simulated was investigated using a homogeneous slope at varying pit depths. The slope angle was kept constant at 45°. For each value of pit depth, two scenarios were modelled in Phase2. In the first scenario, the pit was mined out in one step, and in the second model the pit was mined out in seven steps. The results were then plotted to see the effect of sequential mining on slope stability.

8) Strain Softening

To study the effect of strain softening behaviour of the rock on slope stability, the program Phase 2 was used. Two models were built for each of five different mining depths. The first model used an elastic perfectly plastic strength type while the second used a strain softening material type. Pit depths of 400m, 600m, 800m, 1000m, and 1200m were used and the strength parameters were according to Table 3.5 below.

Table 3.5 Peak and residual strength parameters for the strain softening model

Parameter	Peak	Residual
Cohesion (kPa)	640	450
Friction angle (°)	30	25

9) Concave Geometry

In this set of analyses a perfectly conical pit was analysed in 2D and 3D with the aim of determining the effect the radius of curvature has on the stability of a slope with concave geometry in plan, Figure 3.9. The pit, which was homogeneous, 500m high, and with a slope angle of 65° was modelled in Phase2 using the plane strain assumption to provide a

2D solution. The same slope was then modelled in Phase2 using the axi-symmetric assumption at varying values of radius of curvature. For concave slopes, the radius of curvature is defined as the distance between the axis of revolution and the toe of the slope. The values for the radius of curvature were 100m, 400m, 800m, and 1500m. The slope consisted of the material "homo" in Table 3.1.

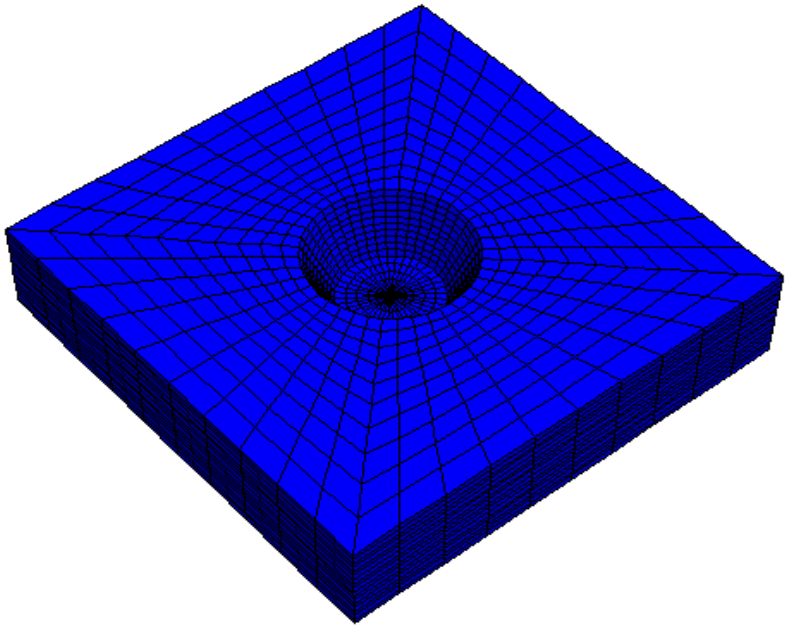

Figure 3.9 3D image of the pit used to analyse the effects of concave curvature on slope stability. The image was generated in FLAC3D but analysis done with Phase2.

10)Bathtub Geometry

In this analysis, an "elliptical" pit was considered and the influence of the concave geometry at the ends was studied with distance from the ends. The geometry was as shown in Figure 3.10. The pit was 500m deep and the slope angle was 50°. The sections were arbitrarily taken at distances of 250m, 500m, 750m, and 1500m from the pit end. Table 3.6 gives the material properties used for the slope.

Table 3.6 Material properties for the Bathtub models

Property	Value
Bulk Modulus (GPa)	0.2
Shear Modulus (GPa)	0.1
Cohesion (KPa)	744
Friction angle (°)	24
Tensile Strength (KPa)	42

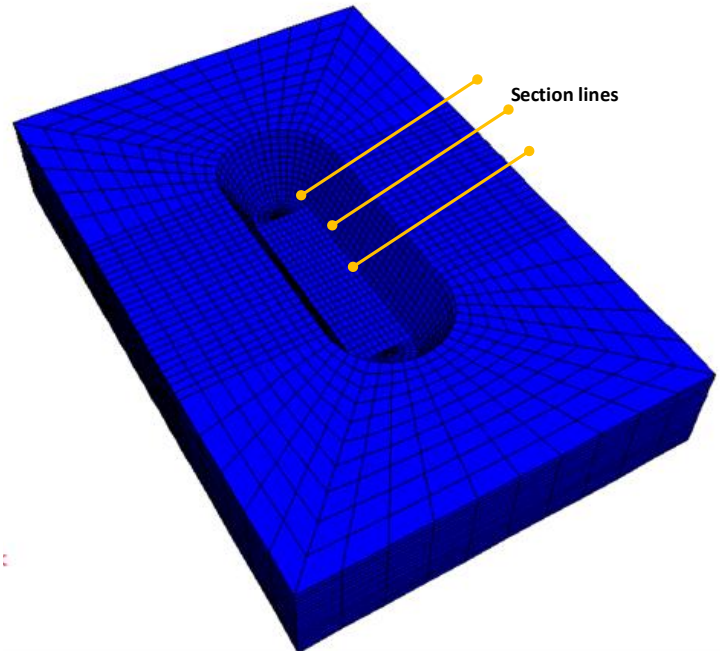

Figure 3.10 Elliptical pit in FLAC3D showing positions of sections considered, at various distances from the curved ends.

3.3.4 Probabilistic Analysis

The models described in the previous section were also used to calculate the probability of slope failure. Full Monte Carlo simulations are possible within SLIDE itself but not within the numerical models. So, to ensure a fair comparison of the POF values, the same method (RSM) was used in calculating all POF values. The verification of the accuracy of the RSM that was done using the models described in section 3.3.2, enabled the RSM to be used with confidence in this work. The parameters included as uncertain variables in the probabilistic analyses were cohesion, friction angle, dilation angle, and the k ratio. The probabilistic analysis comparison was done in 2 generic categories; Limit Equilibrium vs. Numerical models, and 2D vs. 3D models. All models used in the probabilistic analysis were homogeneous.

3.3.4.1 Limit Equilibrium vs. Numerical Models

The POF computed from SLIDE models was compared with the POF from Phase 2 models. Table 3.7 gives the input values used for the probabilistic analysis. The columns labelled

model 1, model 2, and model 3 refer to three different model categories analysed. The geometries for the three models were identical, an overall slope angle of 45° and slope height of 600m, Figure 3.11.

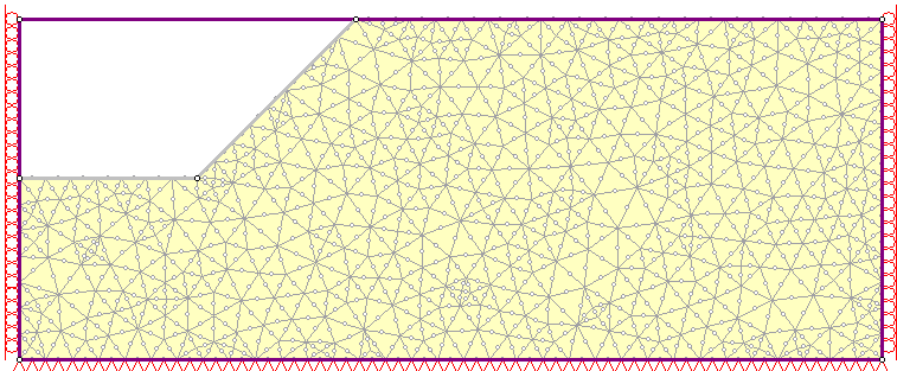

Figure 3.11 Phase2 model showing geometry used for the comparison of SLIDE and Phase2 POF computations.

The cohesion and friction angle were also the same in all the three models. The only difference was in the values of dilation, k ratio, and the locked-in horizontal stresses. In all the SLIDE models, only the cohesion and friction angle were considered as uncertain variables. The number of uncertain parameters in the Phase 2 models varied from two to four. Consequently the analyses were divided into two groups, depending on the number of uncertain variables assumed for the Phase2 models. The purpose for having different numbers of variables was so as to investigate the effect of the variability of the different input parameters on the computed POF. Table 3.7 shows the assumed variables in the different sets of analyses. In all analyses a coefficient of variation of 0.3 was assumed for every variable.

Table 3.7 Uncertain Input parameters for models used to compare POF values computed with LE models and POF values computed with Numerical models.

Parameter	Model 1	Model 2	Model 3
Cohesion (kPa)	640	640	640
Friction angle (°)	30	30	30
Dilation angle (°)	0	7	15
k ratio	1	2	3
Locked-in stress (MPa)	0	1	3

The first set of analyses assumed that there were only two uncertain parameters, the cohesion and the friction angle. Thus the dilation angle and the k ratio were assumed to be known deterministically. The POF was determined using the RSM, which requires 2N + 1 model runs. Hence, for each POF computed, five models were evaluated. Different values were assumed for the correlation coefficient (CC) between cohesion and friction angle; -1, -0.5, 0, 0.5, and 1. For each CC value a POF was computed for the SLIDE model as well as model 1, model 2, and model 3 using Phase2.

The second set of analyses considered the cohesion, friction angle, dilation angle and the k ratio as uncertain variables. In this case, the same CC was assumed between cohesion and friction angle, as well as between dilation angle and friction angle. For each POF value nine models were run so as to create the response surface.

3.3.4.2 2D vs. 3D models

FLAC and FLAC3D were used in comparing the POF values computed with 2D models and those from 3D analyses. The bathtub geometry of Figure 3.10 was used for the comparison. Three section lines were created along the straight portion of the pit geometry. The distances of these section lines from the pit end were 250m, 750m, and 1500m. For each section, the POF was evaluated at five different values of correlation coefficient between -1 and 1.

3.3.5 Risk Analysis

The consequences of slope failures are generally classed into safety and economic categories. Results from the probabilistic analyses were used together with assumed consequences to give an assessment of the risk levels. The approach in carrying out a risk analysis is the same for both safety and economic impact. Only the economic impact was assessed in this work, but the conclusions derived from the economic impact analysis can be extended to the safety impact analysis. Since most of the analyses carried out in this work were 2D in nature, the reported volumes are for a slice of unit thickness in the out of plane direction as explained in section 3.3.3. To enable realistic risk analyses to be carried out, the extent of the failure in the out of plane direction had to be estimated. The length of slope failures along the strike of the pit excavation is generally proportional to the height of the failure and a ratio of 1:3 is a reasonable assumption (Contreras, pers. comm.).

Thus, using the failure height and failure volume of unit length of slope, the expected failure volumes could be estimated for each model. It was this expected volume that was used for the consequence analysis.

3.3.5.1 Economic Impact

The event tree applicable for the consequences of a slope failure in an open pit mine can be represented as shown in Figure 3.12.

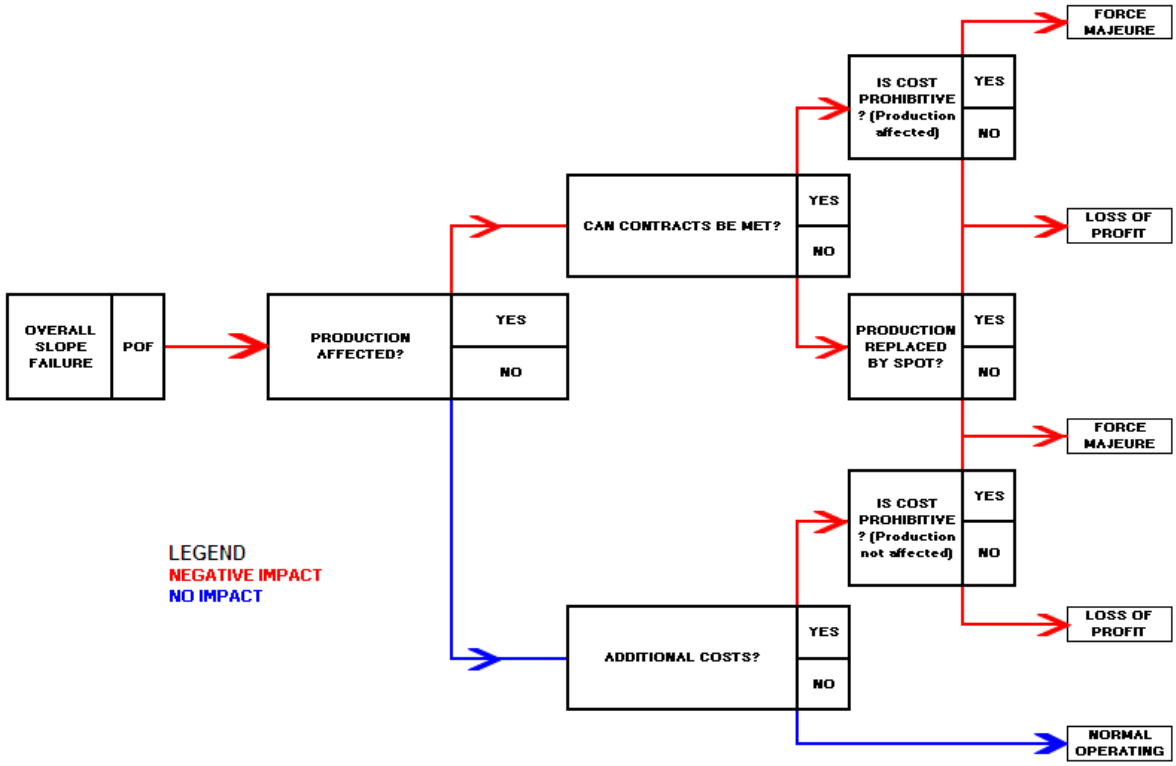

Figure 3.12 The event tree developed for the evaluation of economic impact of slope failures. The risk evaluation considered 3 different consequences; Normal operating conditions, Loss of Profit, and Force Majeure. (after Steffen et al, 2006)

The probabilities associated with each branch of the event tree in Figure 3.12 are given in Table 3.8. These were probabilities adopted in a risk analysis for a specific copper mine (SRK, 2009). These values are specific to a particular mine and are not dependent on the analysis method used for slope design. Hence the same values were used for all risk analyses. The probability of overall slope failure was taken from the probabilistic analyses in section 3.2.3. Other sources of variability, like mining methods and geology, not accounted for in the stability analysis were ignored.

Table 3.8 Probability values used in the event tree used to determine probabilities of occurrence of various economic consequences.

LIKELY EVENT	Probability	
	YES	NO
Production Affected?	0.7	0.3
Can Contracts be met?	0.5	0.5
Additional costs?	0.2	0.8
Is cost prohibitive?	0.2	0.8
Production replaced by spot?	0.9	0.1

Of the three possible economic consequences in Figure 3.12, only the loss of profit was considered in this work. The reason for this was simply to keep the work tractable. Moreover, any trends reflected by the loss of profit consequence will also be reflected in the other consequences such as the Force Majeure consequence. Since the goal of this work is simply a comparison of the assessed risk when LE and numerical tools are used, it is apparent that ignoring Force Majeure impacts will in no way affect the conclusions of the study.

For the purposes of the current investigation, the total loss of profit was assumed to be made up of two components; the cost of cleaning up after a failure and the cost due to production delays. The assumption is that the slope being modelled is just above an access ramp which happens to be the only access into the pit. Therefore, any slope failure will result in delays to production until the failed volume has been cleared. This was just a hypothetical scenario in order to compare the risk determined from the two stability analysis methods without confusing the analysis with financial calculations that would cloud the main issue under investigation. Other contributors to loss of profits such as damage to equipment were not included in the analysis. Table 3.9 shows the hypothetical costs associated with different tasks resulting from a slope failure. It is important to note that the choice of these costs has no bearing on the final comparison between the risk assessed using LE methods and that from numerical methods. In other words, the relative comparison of the results is independent of the values used in Table 3.9. However, the values have been chosen to reflect typical costs associated open pit mining operations. The rate of clearing was assumed to be 5,000 ton/hr.

Table 3.9 Costs involved with actions performed after a slope failure

Task	Value (ZAR)
Cost of clearing (Rand / m^3)	500
Lost production cost (Rand / hr)	100,000

Once the total loss of profit was determined for any model, it was multiplied with the probability of loss of profits to come up with a risk quantity. It is this quantity which was used to compare the risk assessed by the different modelling tools. Technically speaking, this risk quantity is the expected loss of profits.

$$\boldsymbol{Risk = P(Loss\ of\ Profit) \times Loss\ of\ profit} \qquad \textbf{(3-7)}$$

This risk quantity was considered to be representative of the economic risk associated with the mining operation.

3.3.5.2 Risk Models

The risk models were grouped into two categories depending on the comparison being investigated. The first category dealt with models comparing the risk assessed by LE models with that from numerical models. The second category compared the risk determined from 2D slope stability models with that determined from 3D models.

a) LE vs. Numerical Models

Three SLIDE models and three Phase2 models were used for the comparison. The models were selected from the analyses carried out in section 3.3. The selected models had 2 uncertain parameters (cohesion and friction angle) and a correlation coefficient of zero. The probabilities of failure computed previously were input into the event tree of Figure 3.12. This gave the probability of incurring a loss of profit due to the failure. Secondly, the failure volumes were used in conjunction with the parameters in Table 3.9 to calculate the total loss in profit due to the failure. Multiplying the probability of loss of profit and the total loss of profit gave the risk level according to the description above.

b) 2D vs. 3D Models

The FLAC and FLAC3D models described in section 3.3.4 were used in the risk analyses to compare 2D and 3D models. The event tree of Figure 3.12 was used to calculate the probability of incurring a loss of profit due to the failure, and consequently to calculate the risk.

CHAPTER 4

4 RESULTS AND DISCUSSION

This Chapter presents the results of the analyses conducted on the models described in Chapter 3. The results have been organised according to the following structure:

- Response Surface Methodology Verification
- Deterministic FOS comparisons
- Probabilistic analyses comparisons
- Risk analyses comparisons

At the end of the Chapter a summary of all the results is given.

4.1 Response Surface Methodology Verification

The models for verifying the RSM approach were divided into three categories depending on whether the slope was homogeneous or heterogeneous and whether the uncertain variables followed a normal or lognormal distribution. As described in section 3.3.2, the comparisons were carried out for three different levels of correlation and three different levels of scatter in the data, represented by different values of the correlation coefficient and coefficient of variation respectively.

4.1.1 Homogeneous slope (Assuming Normal Distributions for c and Φ)

The first verification models considered a homogeneous slope with the variability in the cohesion and friction angle following normal distributions. Table 4.1 gives a summary of the results from these analyses. The column labelled "SLIDE" refers to the results obtained by performing Monte Carlo Simulation within the SLIDE model itself. Δ refers to the difference between the SLIDE Monte Carlo and RSM results.

Table 4.1 Summary of POF results for models run to compare Monte Carlo simulation in SLIDE and the Response Surface Methodology.

CV	CC = -0.5			CC = 0			CC =0.5		
	SLIDE	RSM	Δ	SLIDE	RSM	Δ	SLIDE	RSM	Δ
0.1	1%	2%	-1%	5%	5%	0%	8%	8%	0%
0.2	14%	15%	-1%	20%	21%	0%	23%	24%	0%
0.3	24%	25%	-1%	29%	29%	0%	31%	32%	-1%

The results show remarkably good agreement between the SLIDE Monte Carlo simulation and the RSM formulation. The maximum difference between the two methods is just 1%. This agreement is true for both correlated and uncorrelated variables. Figure 4.1 shows the results graphically.

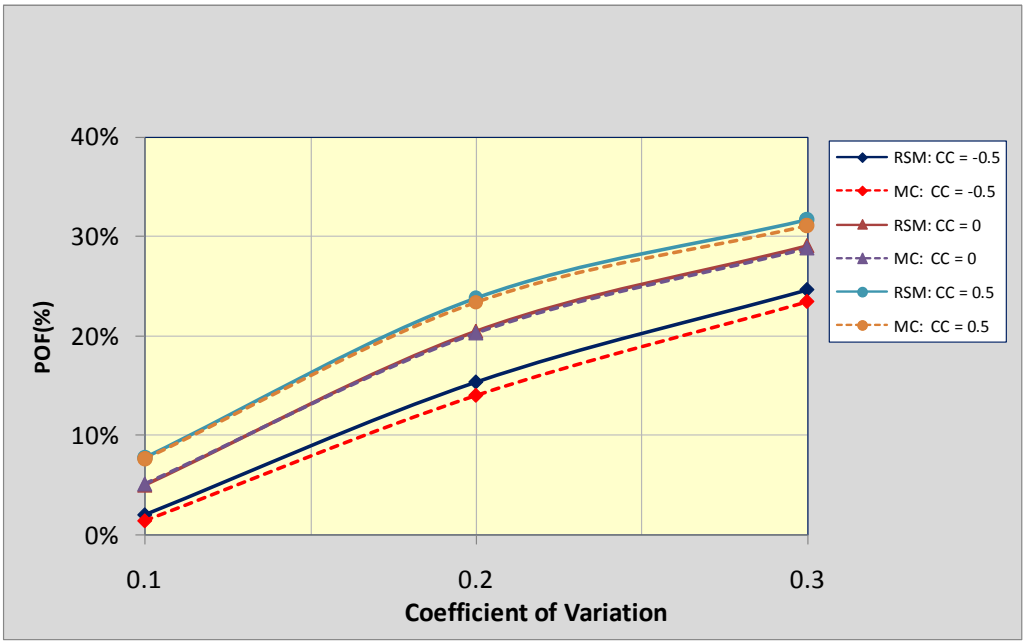

Figure 4.1 Comparison of POF values (for normally distributed variables) calculated using Monte Carlo Simulation in SLIDE (MC) and the RSM formulation for different levels of correlation between c and Φ.

10,000 SLIDE models were run to obtain the POF using the SLIDE Monte Carlo simulation method. On the other hand only five SLIDE models were run to create a response surface on which Monte Carlo simulations were carried out in Excel. This highlights the computational efficiency of the RSM approach, a feature that makes it particularly well suited for use with numerical models.

4.1.2 Homogeneous slope (Assuming Lognormal Distributions for c and Φ)

These models considered the same homogeneous slope used in section 4.1.1 with both the cohesion and friction angle following lognormal distributions. Table 4.2 gives a summary of the results from these analyses.

Table 4.2 Summary of POF results for models run to compare Monte Carlo simulation in SLIDE and the Response Surface Methodology.

CV	CC = -0.5			CC = 0			CC =0.5		
	SLIDE	RSM	Δ	SLIDE	RSM	Δ	SLIDE	RSM	Δ
0.1	1%	1%	0%	4%	4%	0%	7%	7%	0%
0.2	13%	15%	-1%	21%	21%	0%	24%	25%	-1%
0.3	25%	26%	-2%	32%	31%	0%	35%	35%	1%

The results also show good agreement between the two methods. The maximum discrepancy is just 2% for a CV of 0.3 and CC of -0.5. Graphically the comparison is shown in Figure 4.2.

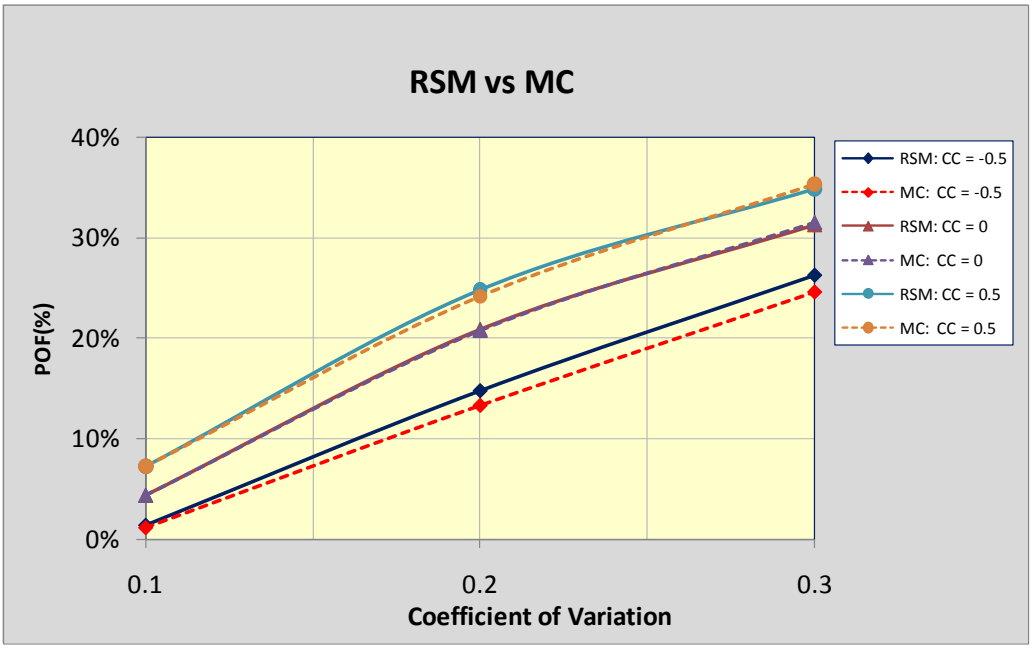

Figure 4.2 Comparison of POF values (for lognormally distributed variables) calculated using Monte Carlo Simulation in SLIDE (MC) and the RSM formulation for different levels of correlation between c and Φ.

4.1.3 Heterogeneous slope (Assuming Normal Distributions for c and Φ)

The third class of verification models considered a heterogeneous slope with both the cohesion and friction angle following normal distributions. Table 4.3 gives a summary of the results from these analyses. Even for this slope with three different materials, the RSM still agrees very well with SLIDE Monte Carlo simulation. The graphs of Figure 4.3 show the comparison of the results.

Table 4.3 Summary of POF results for heterogeneous models run to compare Monte Carlo simulation in SLIDE and the Response Surface Methodology.

CV	CC = -0.5			CC = 0			CC =0.5		
	SLIDE	RSM	Δ	SLIDE	RSM	Δ	SLIDE	RSM	Δ
0.1	0%	0%	0%	2%	1%	0%	3%	3%	1%
0.2	8%	8%	0%	12%	13%	0%	16%	16%	0%
0.3	20%	21%	-1%	25%	25%	0%	28%	27%	1%
0.4	25%	26%	-1%	29%	30%	-1%	32%	33%	-1%

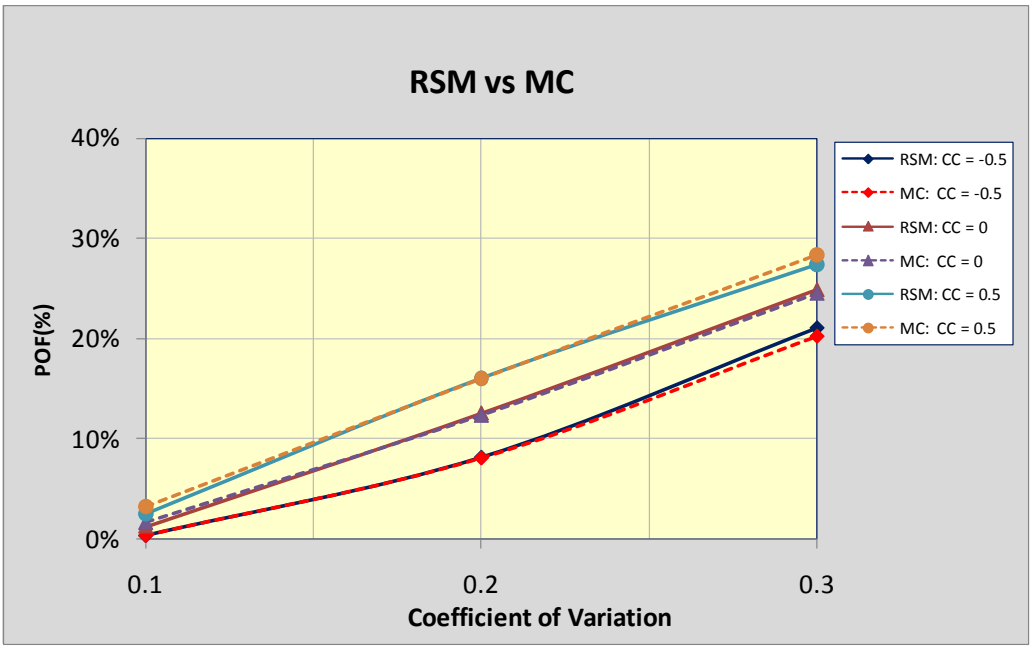

Figure 4.3 Comparison of POF values (for normally distributed variables) calculated using Monte Carlo Simulation in SLIDE (MC) and the RSM formulation for different levels of correlation between c and Φ.

4.1.4 Summary

The comparison of the RSM and full Monte Carlo simulations in SLIDE shows remarkable agreement. The RSM requires significantly fewer runs and hence becomes an attractive tool for use with computationally expensive analysis tools like numerical models. The results suggest that the RSM can be used both with correlated and uncorrelated variables. The methodology gave satisfactory results for varying degrees of scatter in the input distributions. Additionally, the RSM results compared well with Monte Carlo simulations in SLIDE for both normal and non-normal variables. Thus, the verification has indicated that the RSM can be used with confidence in probabilistic slope stability analysis.

4.2 Deterministic Analysis

The purpose of the deterministic analyses was to evaluate the effect of various parameters on slope stability. Most of these parameters are not included in Limit Equilibrium analyses hence the need to verify their effect on the FOS. The LE program SLIDE and the numerical modelling program Phase2 were used for the comparisons. In addition to the FOS, failure volumes were also calculated. The two methods of slices, Bishop simplified and Janbu corrected, were used in the LE analyses. The failure surfaces predicted by Bishop's method and Janbu's corrected method are nearly identical. Hence, the same failure volume is assumed for both methods in this work. As explained in section 3.3.3 the Phase2 models assumed a k ratio of one, a dilation angle of zero, no locked in stresses, an elastic-perfectly plastic strength model, and mining modelled in one step, unless specified otherwise.

4.2.1 Slope Angle

The FOS and failure volume for a homogeneous slope were computed using SLIDE and Phase2 for varying slope angles. Table 4.4 shows the FOS and failure volumes for the various slope angles for the LE and numerical models.

Table 4.4 Sensitivity of FOS to variations in slope angle with all other parameters kept constant

Slope angle (°)	FOS			Failure Volume ($10^3 m^3$)	
	Bishop simplified	Janbu corrected	Phase2	SLIDE	Phase2
30	1.58	1.58	1.61	187	286
40	1.22	1.22	1.25	127	220
50	0.99	0.99	1.00	100	172
60	0.81	0.81	0.84	83	160
75	0.58	0.65	0.58	61	133

The FOS and failure volumes decrease with an increase in slope angle for both SLIDE and Phase2. The FOS values are basically identical but the Phase2 failure volumes are higher than those from SLIDE. In fact, for all slope angles the Phase2 failure volumes are between 1.5 and 2 times those obtained from SLIDE. As the slope angle increases, the failure surfaces predicted by both codes become shallower, though the slope becomes less stable, Figure 4.4.

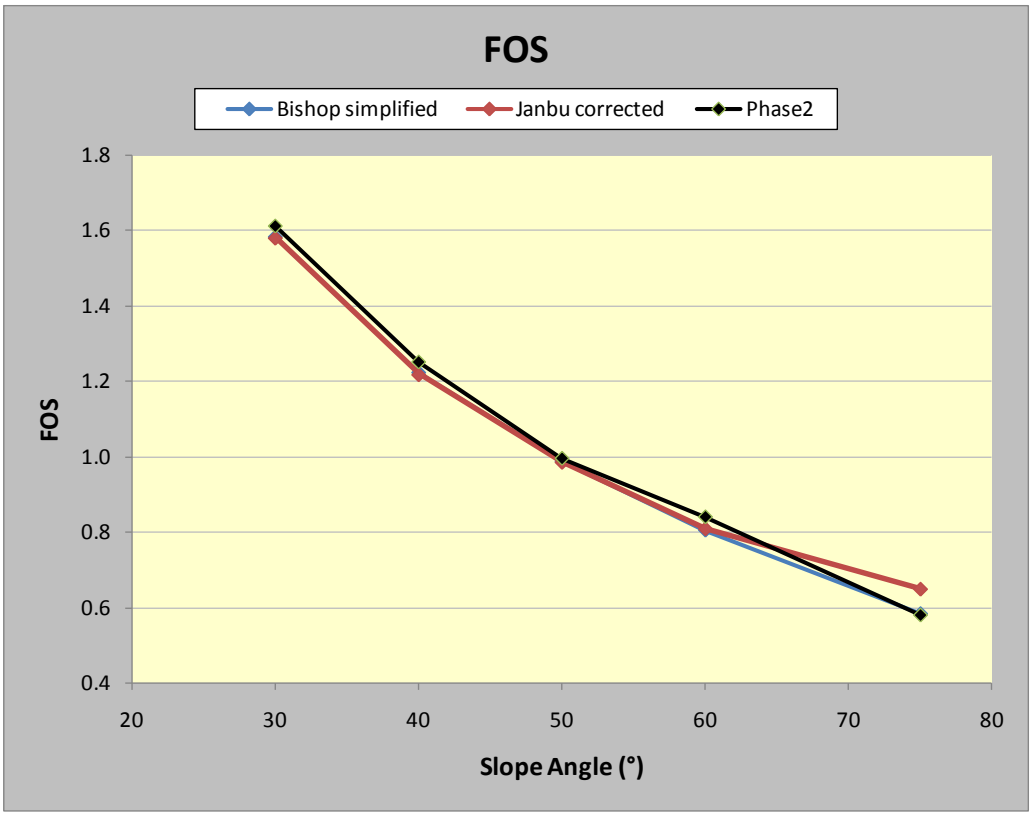

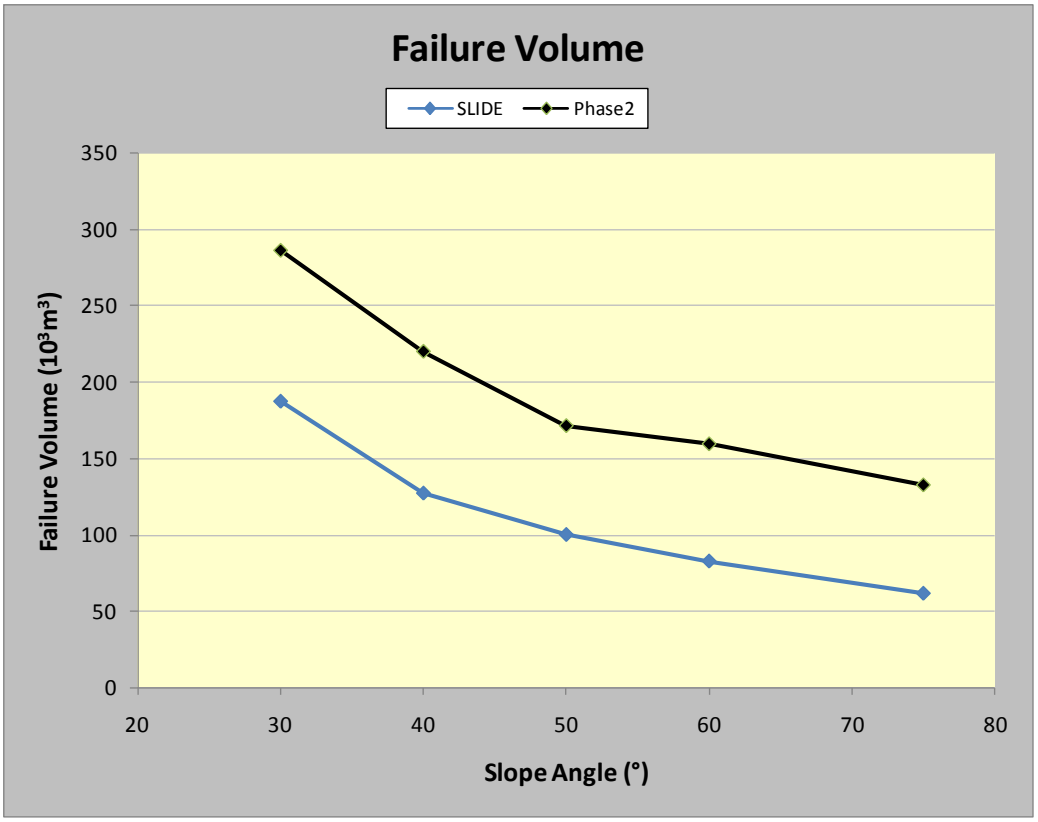

Figure 4.4 (top) Predicted FOS values with SLIDE and Phase2 for varying slope angles, (bottom) predicted failure volumes

4.2.2 Pit Depth

The FOS and failure volume for a homogeneous slope were computed using SLIDE and Phase2 for varying pit depths at a constant slope angle. Table 4.5 shows the FOS and failure volumes for the various slope angles for the LE and numerical models.

Table 4.5 Sensitivity of FOS to variations in pit depth. All other parameters were kept constant

Pit Depth (m)	FOS			Failure Volume ($10^3 m^3$)	
	Bishop simplified	Janbu corrected	Phase2	SLIDE	Phase2
400	1.25	1.25	1.31	59	87
600	1.09	1.09	1.13	110	173
800	1.01	1.00	1.04	172	281
1000	0.95	0.94	1.00	245	429
1200	0.91	0.90	0.94	326	638

Both SLIDE and Phase2 show the same trend of FOS decreasing with increasing depth, Figure 4.5(a). The differences between the reported FOS values are quite small, with the Phase2 result consistently higher. However, the predicted failure volumes are quite different, Figure 4.5(b). SLIDE predicts much lower failure volumes than Phase2. The difference between the volumes increases with increasing pit depth.

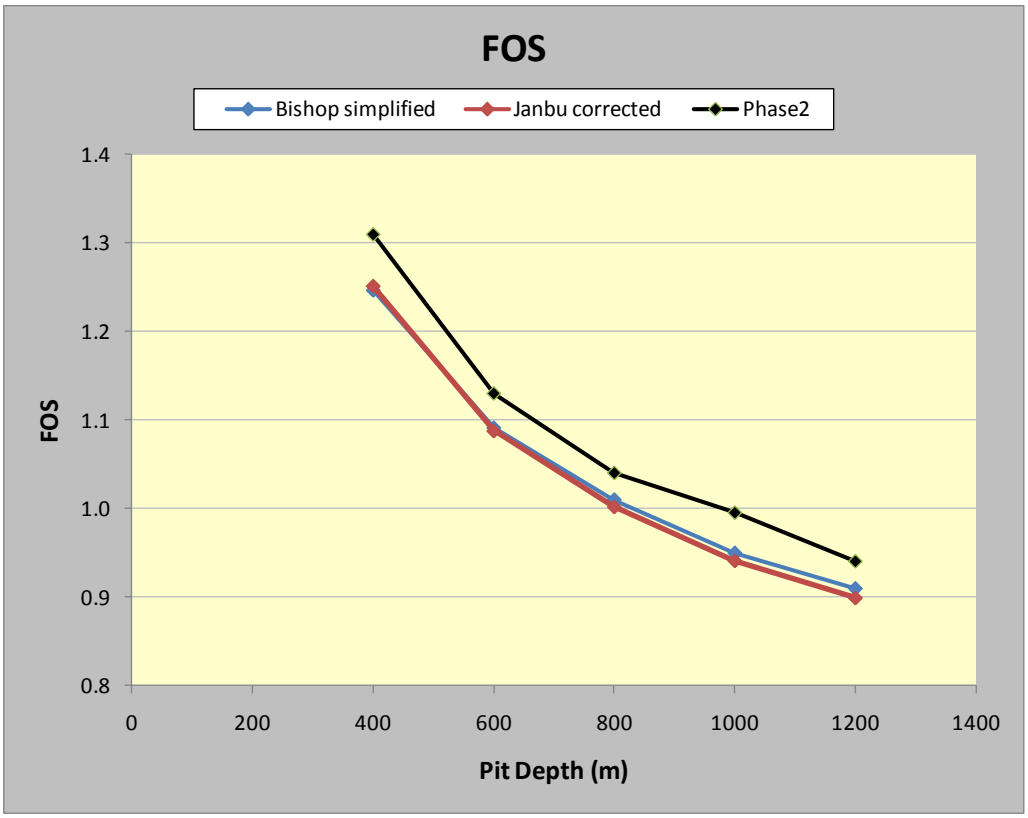

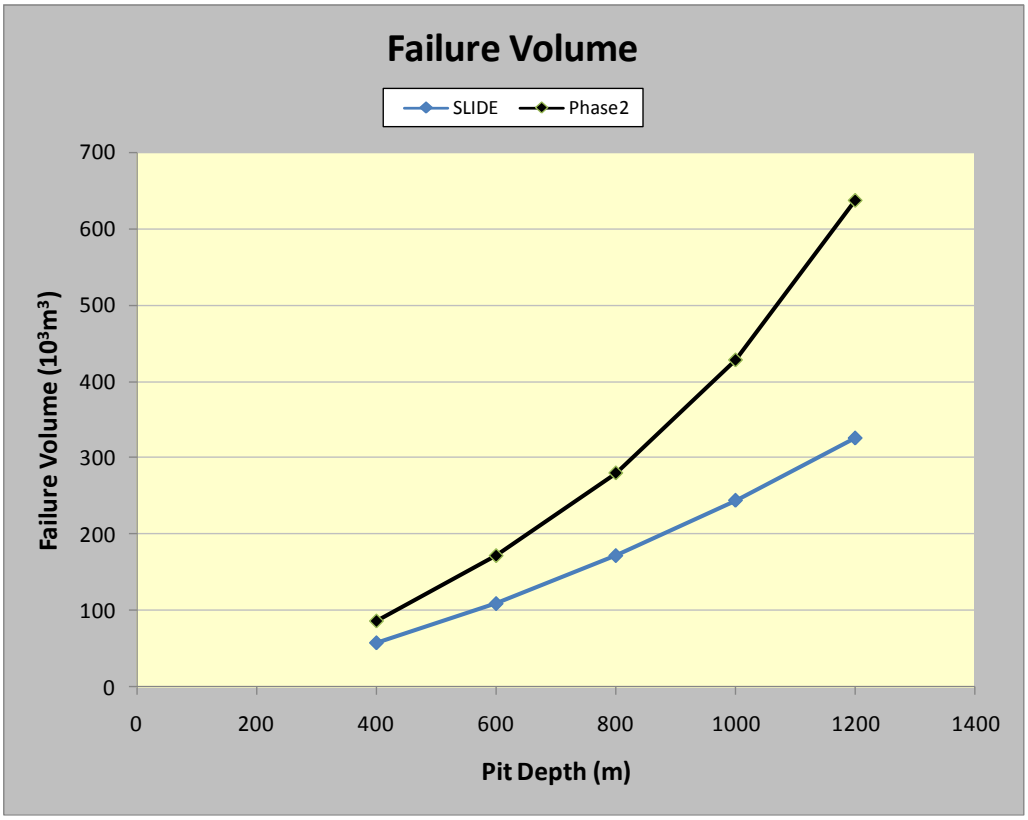

Figure 4.5 (top) Predicted FOS values with SLIDE and Phase2 varying pit depths, (bottom) predicted failure volumes

4.2.3 k ratio

The FOS and failure volume for a heterogeneous slope were computed using SLIDE and Phase2 for varying k ratios, at constant values of pit depth and slope angle. Table 4.6 shows the FOS and failure volumes for the various k ratios. Since the k ratio is not included in LE analyses, the SLIDE results are the same for all values of k ratio.

Table 4.6 Sensitivity of FOS to variations in k ratio. All other parameters were kept constant

k ratio	FOS			Failure Volume ($10^3 m^3$)	
	Bishop simplified	Janbu corrected	Phase2	SLIDE	Phase2
0.1	1.16	1.19	1.20	93	145
1.0	1.16	1.19	1.20	93	137
2.0	1.16	1.19	1.23	93	156
3.0	1.16	1.19	1.25	93	147
4.0	1.16	1.19	1.25	93	146

For the Phase2 models, changes in the k ratio are reflected in the FOS and failure volumes. As the k ratio increases from 0.1 to 4 the stability of the slope increases from an FOS of 1.20 to 1.25. The stability seems to reach a maximum at a k ratio of 3 after which any increases in the k ratio had no effect on FOS. The Phase2 FOS is consistently higher than the SLIDE FOS, though the differences are small. These results are summarised graphically in Figure 4.6. The failure volumes from Phase2 exhibit some scatter but the trend reveals an average value about 1.5 times the SLIDE failure volume.

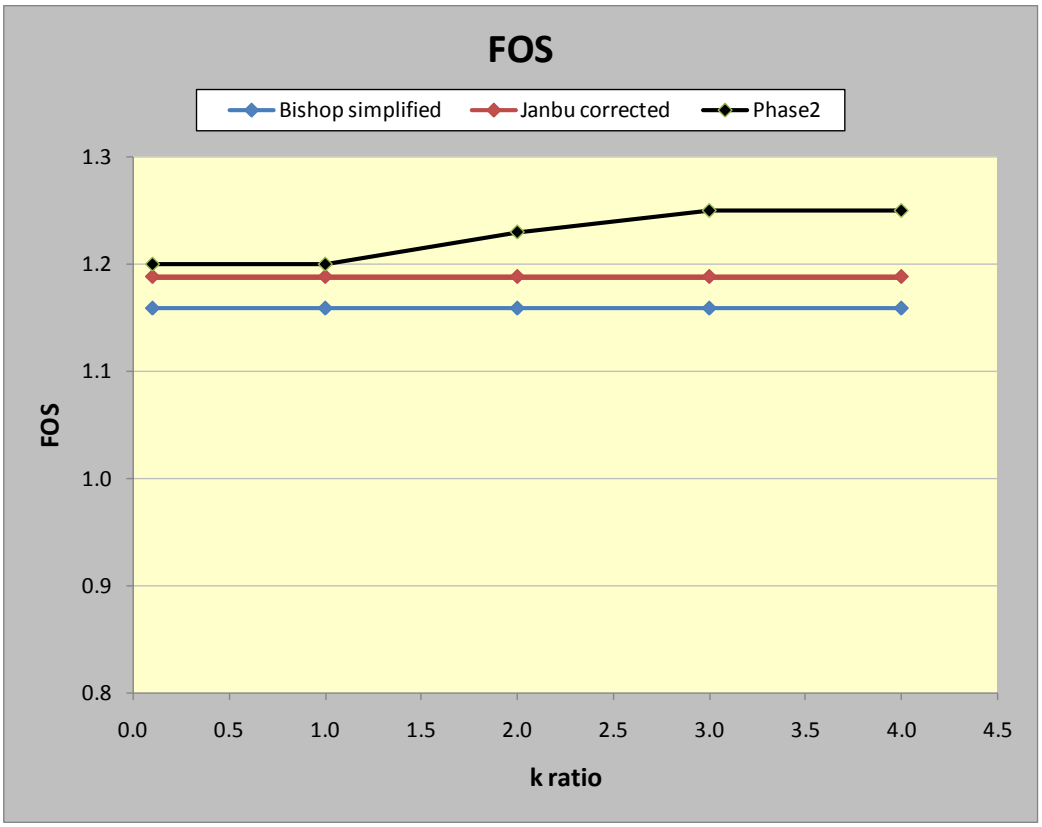

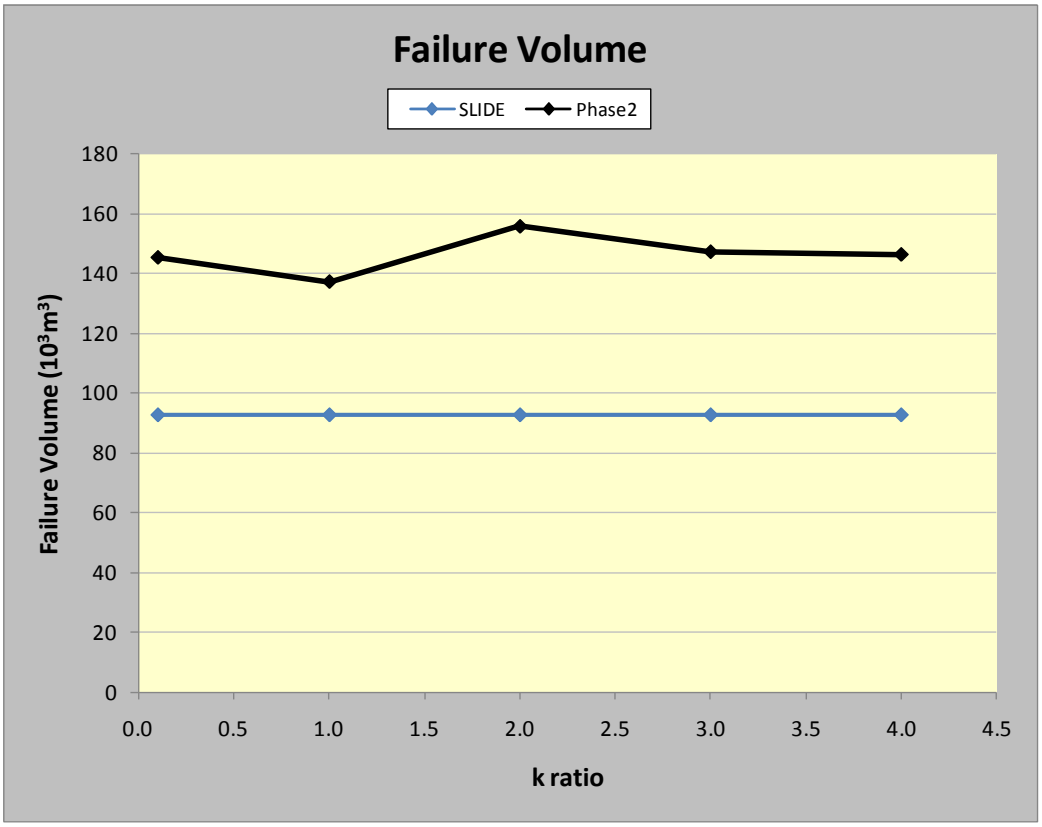

Figure 4.6 (top) Predicted FOS values with SLIDE and Phase2 for varying k ratio values, (bottom) predicted failure volumes

4.2.4 Locked-in Horizontal Stresses

The FOS and failure volume for a heterogeneous slope were computed using SLIDE and Phase2 for varying Locked in horizontal stress (LIS) values. Table 4.7 shows the FOS and failure volumes for the various LIS values. Since the LIS is not included in LE analyses, the SLIDE results are the same for all values of LIS.

Table 4.7 Sensitivity of FOS to variations in locked-in stresses. All other parameters were kept constant

Stress (MPa)	FOS			Failure Volume ($10^3 m^3$)	
	Bishop simplified	Janbu corrected	Phase2	SLIDE	Phase2
0	1.16	1.19	1.20	93	139
1	1.16	1.19	1.20	93	133
5	1.16	1.19	1.21	93	141
10	1.16	1.19	1.23	93	131
20	1.16	1.19	1.23	93	158

As the locked-in horizontal stresses increase from 0 to 10 MPa, the FOS increases from 1.20 to 1.23. Any further increases in the LIS have no effect on the stability. The failure volumes from Phase2 show some variability around an average value, which is approximately 1.5 times the SLIDE failure volume, (Figure 4.7).

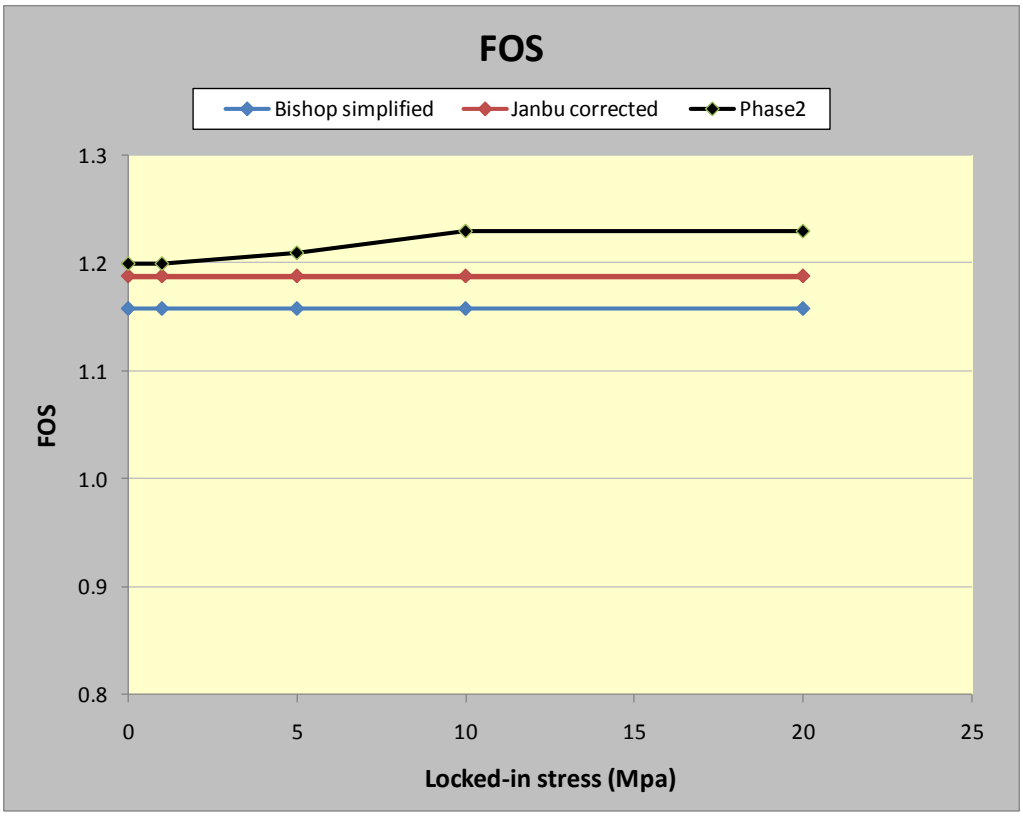

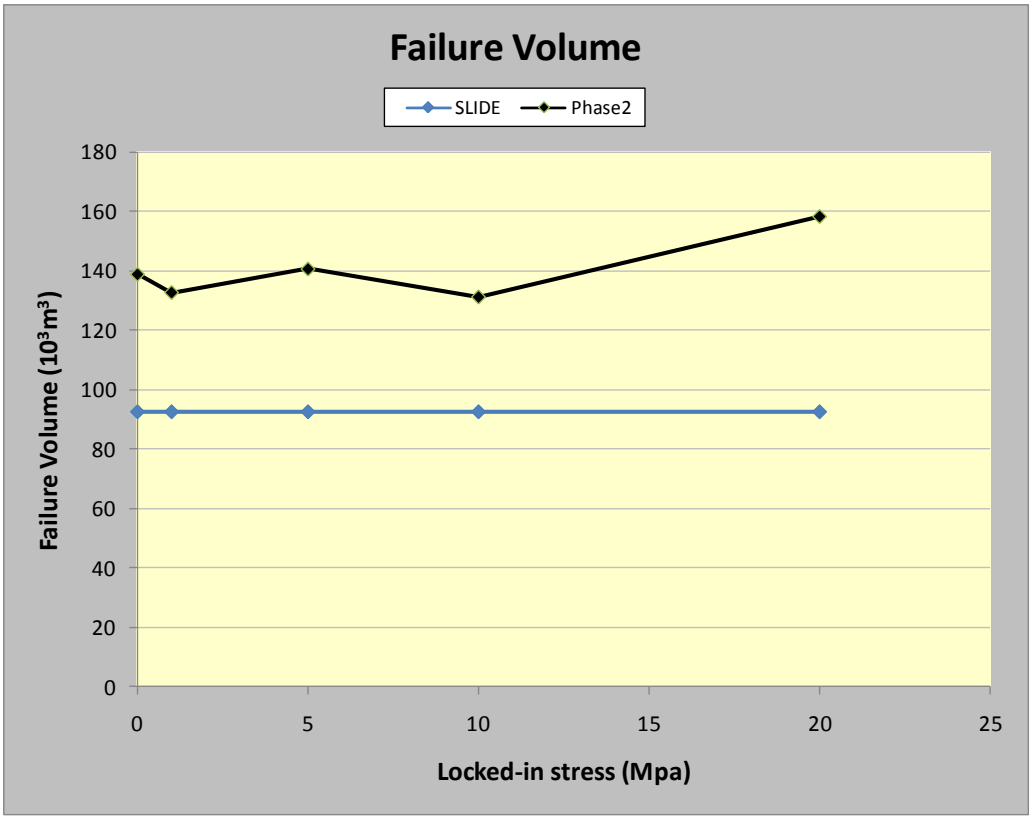

Figure 4.7 (top) Predicted FOS values with SLIDE and Phase2 for varying Locked-in horizontal stress values, (bottom) predicted failure volumes

4.2.5 Dilation Angle

The FOS and failure volume for a heterogeneous slope were computed using SLIDE and Phase2 for varying dilation angle values. Table 4.8 shows the FOS and failure volumes for the various values of dilation angle. Since the dilation angle is not included in LE analyses, the SLIDE results are the same for all values of dilation angle.

Table 4.8 Sensitivity of FOS to variations in dilation angle. All other parameters were kept constant

Dilation angle (°)	FOS			Failure Volume ($10^3 m^3$)	
	Bishop simplified	Janbu corrected	Phase2	SLIDE	Phase2
0	1.16	1.19	1.20	93	120
10	1.16	1.19	1.24	93	121
15	1.16	1.19	1.24	93	123
20	1.16	1.19	1.26	93	128
25	1.16	1.19	1.28	93	128

The FOS increased with increasing dilation angle values. The FOS predicted by SLIDE and Phase2 are roughly the same for a dilation angle of zero. As the dilation increases, Phase2 indicates improved stability conditions, (Figure 4.8). The failure volumes from Phase2 are higher than those from SLIDE. However, the failure volumes do not change significantly with increases in the dilation angle.

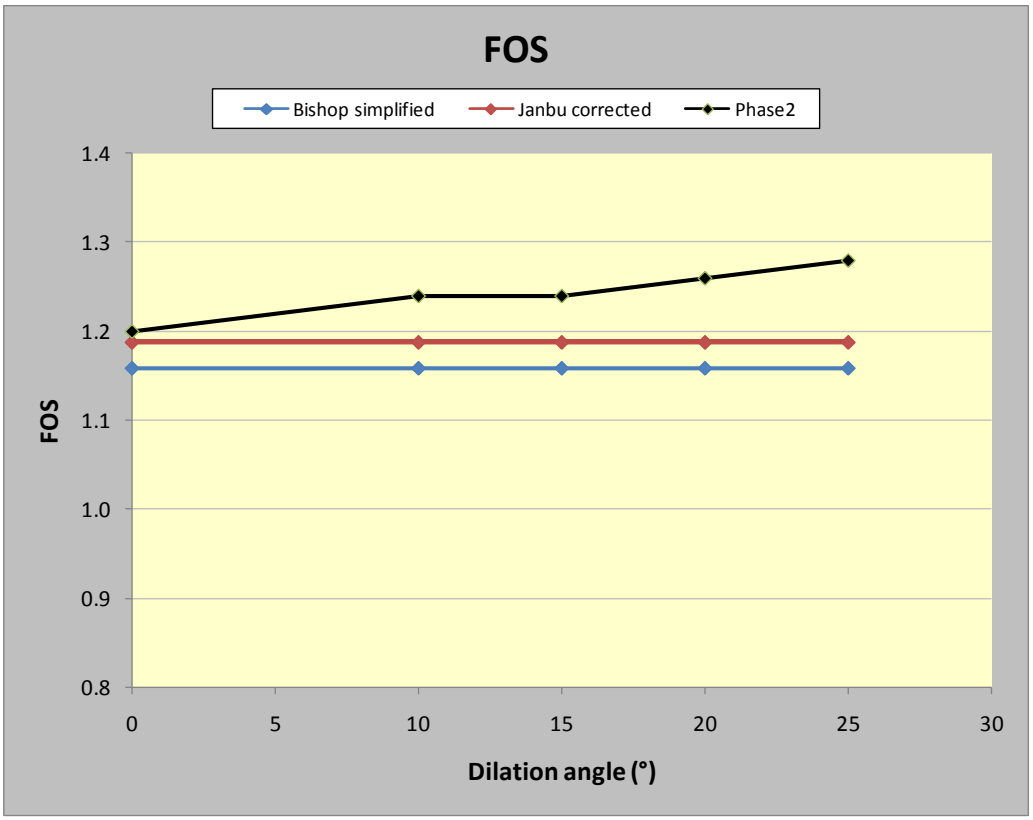

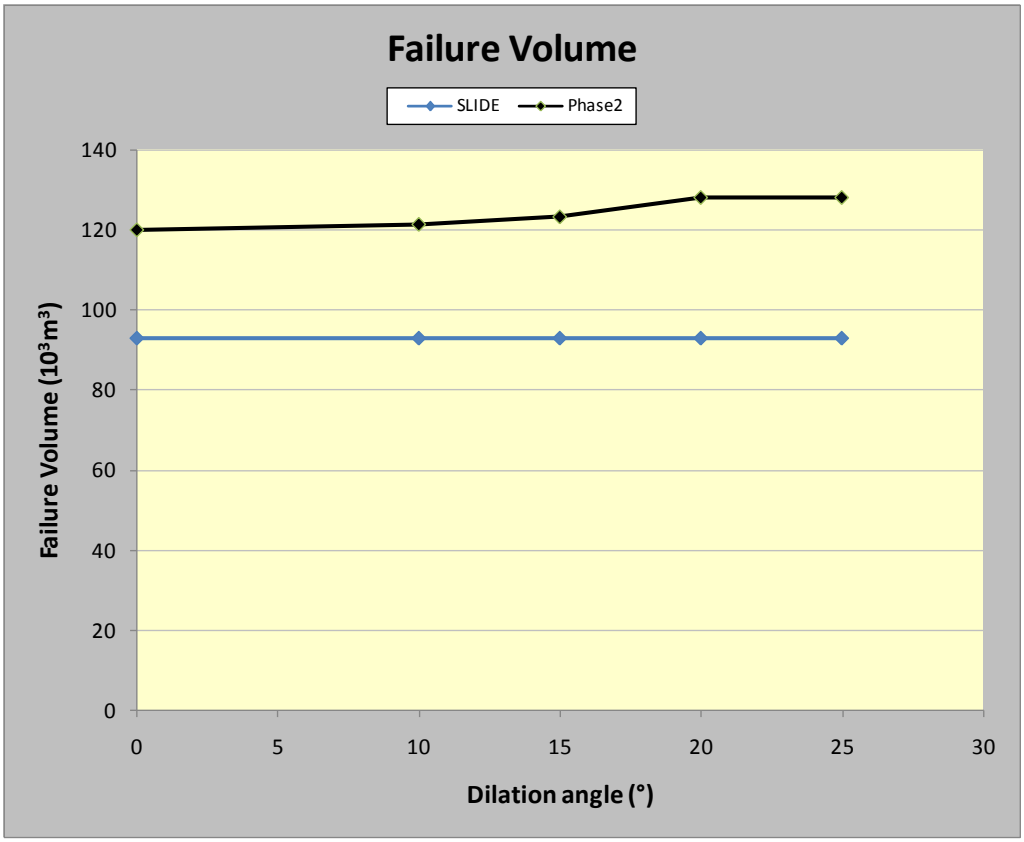

Figure 4.8 (top) Predicted FOS values with SLIDE and Phase2 for varying Dilation angle values, (bottom) predicted failure volumes

4.2.6 Tensile Strength

The FOS and failure volume for a heterogeneous slope were computed using SLIDE and Phase2 for varying tensile strength values. Table 4.9 shows the FOS and failure volumes for the various values of tensile strength. Since the tensile strength is not included in LE analyses, the SLIDE results are the same for all values of tensile strength.

Table 4.9 Sensitivity of FOS to variations in tensile strength. All other parameters were kept constant

Tensile strength (kPa)	FOS			Failure Volume ($10^3 m^3$)	
	Bishop simplified	Janbu corrected	Phase2	SLIDE	Phase2
0	1.01	1.00	1.03	172	317
50	1.01	1.00	1.03	172	326
70	1.01	1.00	1.03	172	319
100	1.01	1.00	1.03	172	325
200	1.01	1.00	1.03	172	332

Increasing the tensile strength of the rock in Phase2 produced no difference in the FOS result. The failure volumes were also nearly constant at values which were roughly double those predicted by the LE methods, Figure 4.9.

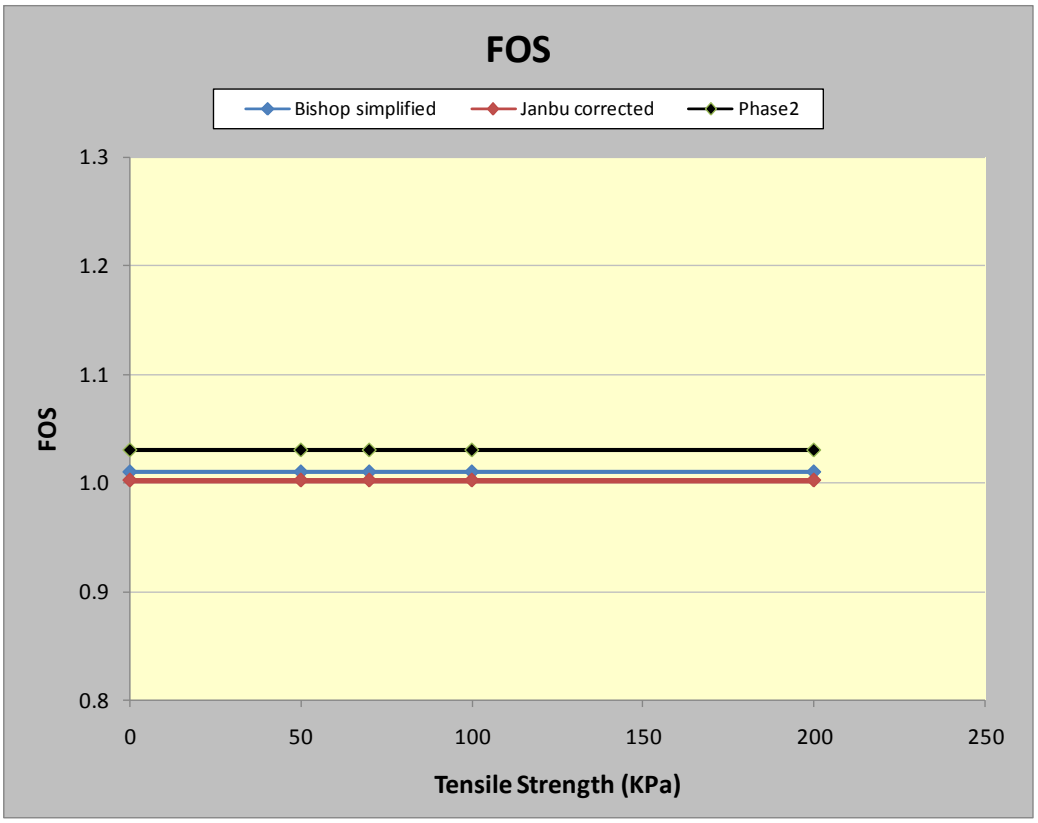

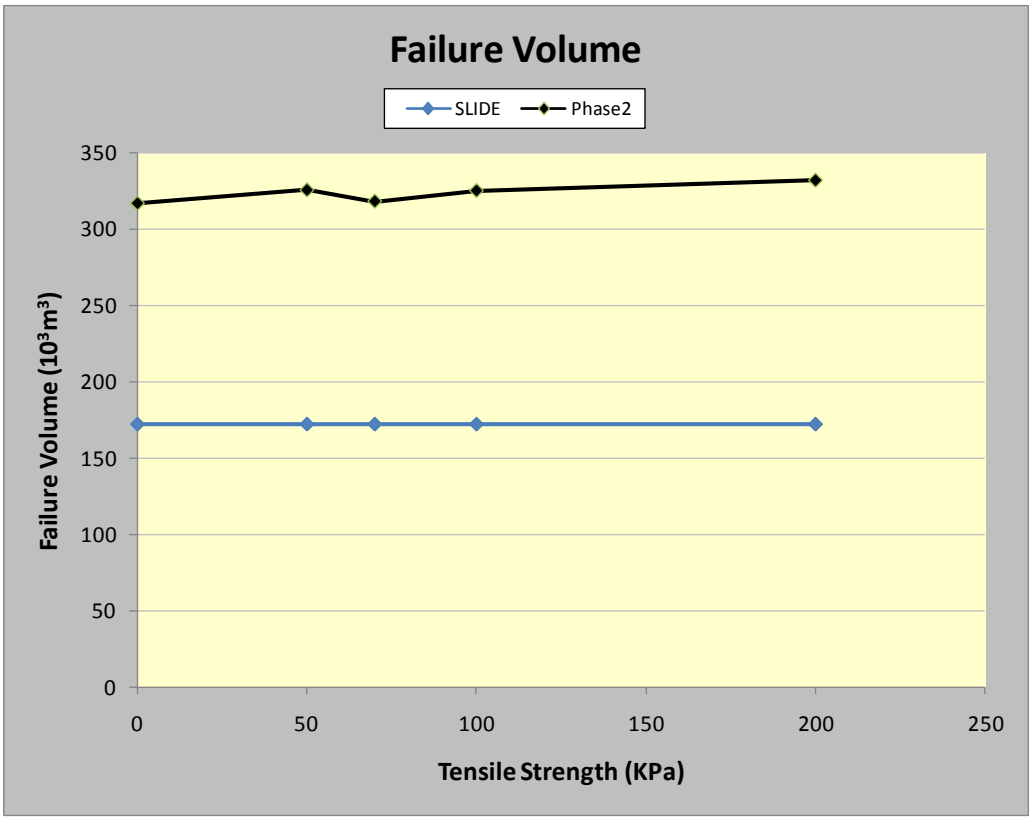

Figure 4.9 (a) Predicted FOS values with SLIDE and Phase2 for varying Dilation angle values, (b) predicted failure volumes

4.2.7 Sequential Mining

The result of mining a homogeneous slope in one step was compared with the effect of simulating the mining in seven steps. Both models were carried out in Phase2 at varying depths of mining. Table 4.10 gives the results. Both the FOS and failure volumes are almost identical in the two models. Figure 4.10 gives a visual comparison of the two modelling approaches. This implies that the mining sequence has a small effect on slope stability. However, the analyses ignore the effect that time may have on the strength of the rock (the rock and discontinuity strengths decrease with time).

Table 4.10 Comparison of mining in one step and mining in seven steps

Pit Depth (m)	FOS		Failure Volume ($10^3 m^3$)	
	One step	7 steps	One step	7 steps
400	1.29	1.28	87	84
600	1.12	1.12	175	204
800	1.03	1.04	281	319
1000	0.99	0.97	429	488
1200	0.92	0.90	533	576

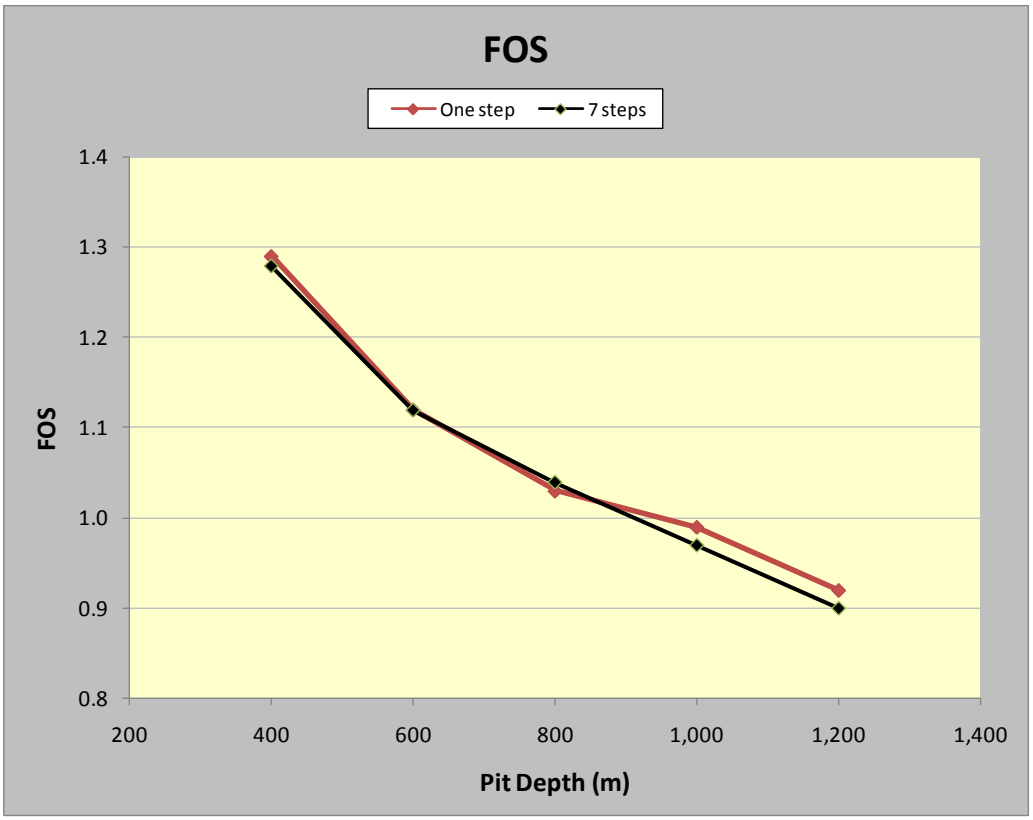

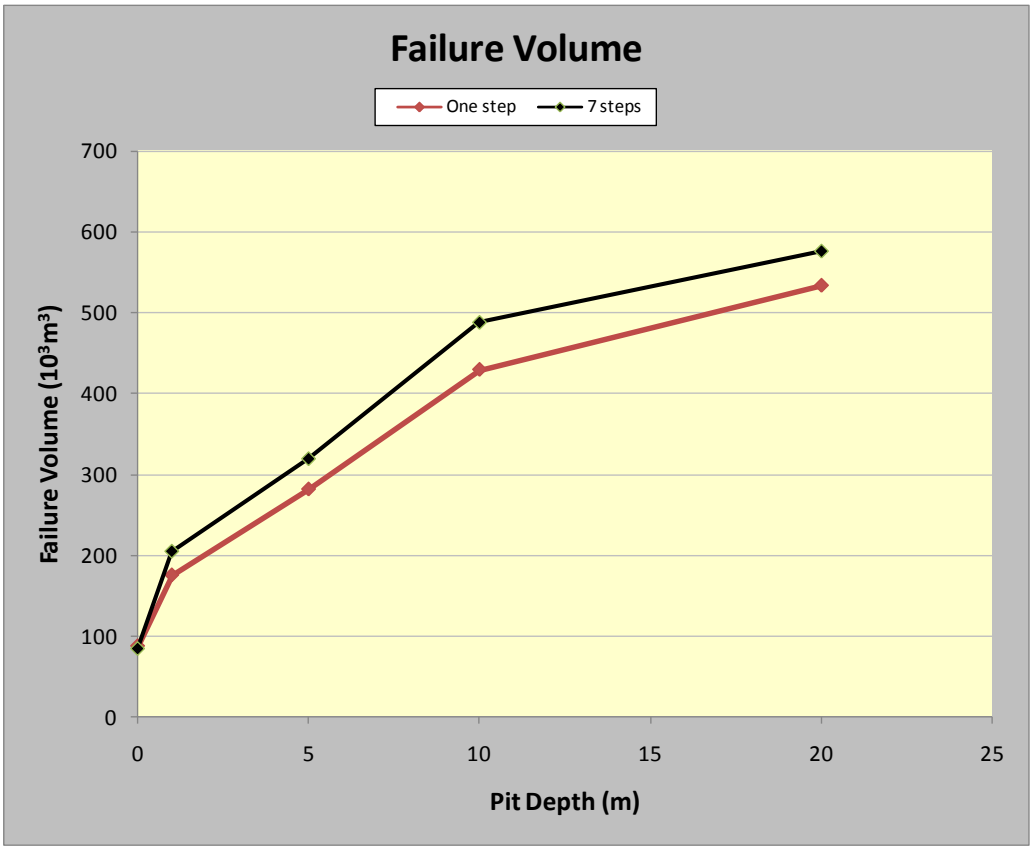

Figure 4.10 (top) Predicted FOS values with SLIDE and Phase2 for varying Pit depths simulating the mining in 1 step and in seven steps, (bottom) predicted failure volumes

4.2.8 Strain Softening

The elastic-perfectly plastic strength type was compared with the strain softening model in Phase2 and the results are summarised in Table 4.11 as well as Figure 4.11 and Figure 4.12.

Table 4.11 Comparison of FOS / failure volumes obtained with a perfectly plastic vs. strain softening model

Pit Depth (m)	FOS		Failure Volume ($10^3 m^3$)	
	Perf. Plas	Strain Soft	Perf. Plas	Strain Soft
400	1.31	1.00	87	87
600	1.13	0.88	173	173
800	1.04	0.81	281	281
1000	1.00	0.77	429	429
1200	0.94	0.73	638	638

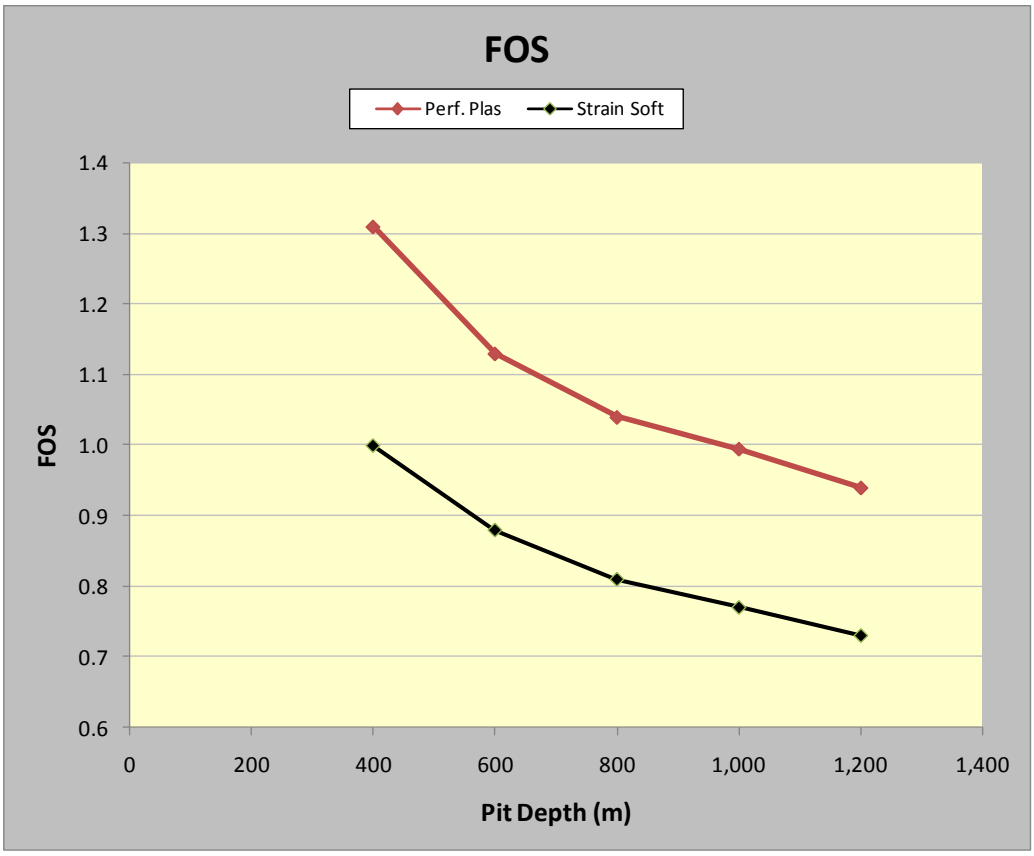

Figure 4.11 Predicted FOS values Phase2 for varying Pit depths using a perfectly plastic and strain softening model

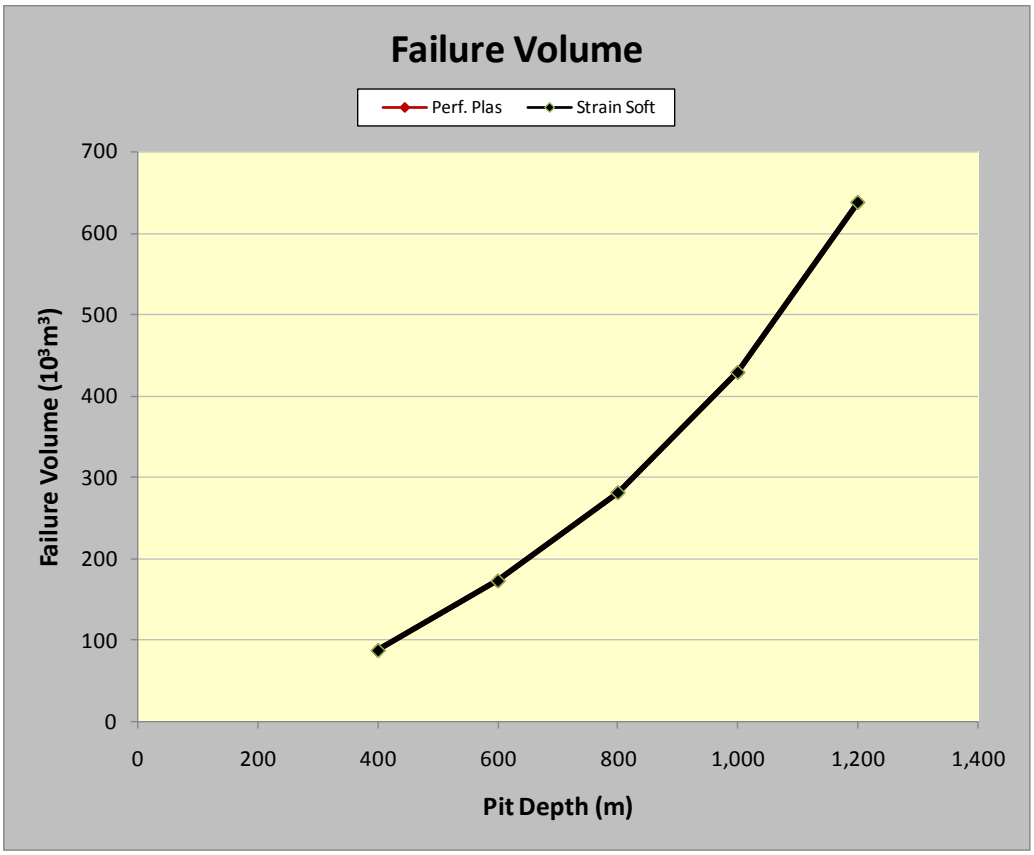

Figure 4.12 Predicted Phase2 failure volumes for varying Pit depths using a perfectly plastic and strain softening model

The results show that using an elastic perfectly plastic model gives an optimistic estimate of the failure volume as compared to the strain softening model. The greater the strain softening effect, the lower the stability will be. However, the failure volumes remain the same regardless of which material strength type is adopted.

4.2.9 Concave Geometry

To determine the effect of slope curvature on stability, axisymmetric models were compared with plane strain models. The analyses were carried out using Phase2, on a 3D circular pit with a slope height of 500m, at varying radii of curvature. The results are summarised in Table 4.12. The results of the plane strain are the same for all values of radius. This is due to the fact that increasing the radius of curvature does not change the 2D plane strain cross-section of the slope.

Table 4.12 Sensitivity of FOS to variations in radius of curvature. All other parameters were kept constant

Radius of curvature (m)	FOS		Failure Volume ($10^3 m^3$)	
	Plane Strain	Axi symmetric	Plane Strain	Axi symmetric
100	0.79	1.26	82	73
400	0.79	1.00	82	66
800	0.79	0.92	82	65
1500	0.79	0.83	82	65

For small radius of curvature values, the plane strain models produced conservative FOS results as compared to the axisymmetric models. As the radius of curvature increases, the FOS from the axisymmetric models approached that from the plane strain models (Figure 4.13). This means that a 2D plane strain analysis is adequate if the radius of curvature is large enough. For a slope with radius of curvature equal to 1000m, Figure 4.13 shows that the difference in the axisymmetric and plane strain FOS values is about 12%. Hoek and Bray (1981) recommended that if the radius of curvature is in excess of twice the slope height (1000m in this case), the slope angle given by a conventional stability analysis should be used. This recommendation seems to be in agreement with the results of Figure 4.13. The failure volumes from the axisymmetric models are consistently lower than those from the plane strain models.

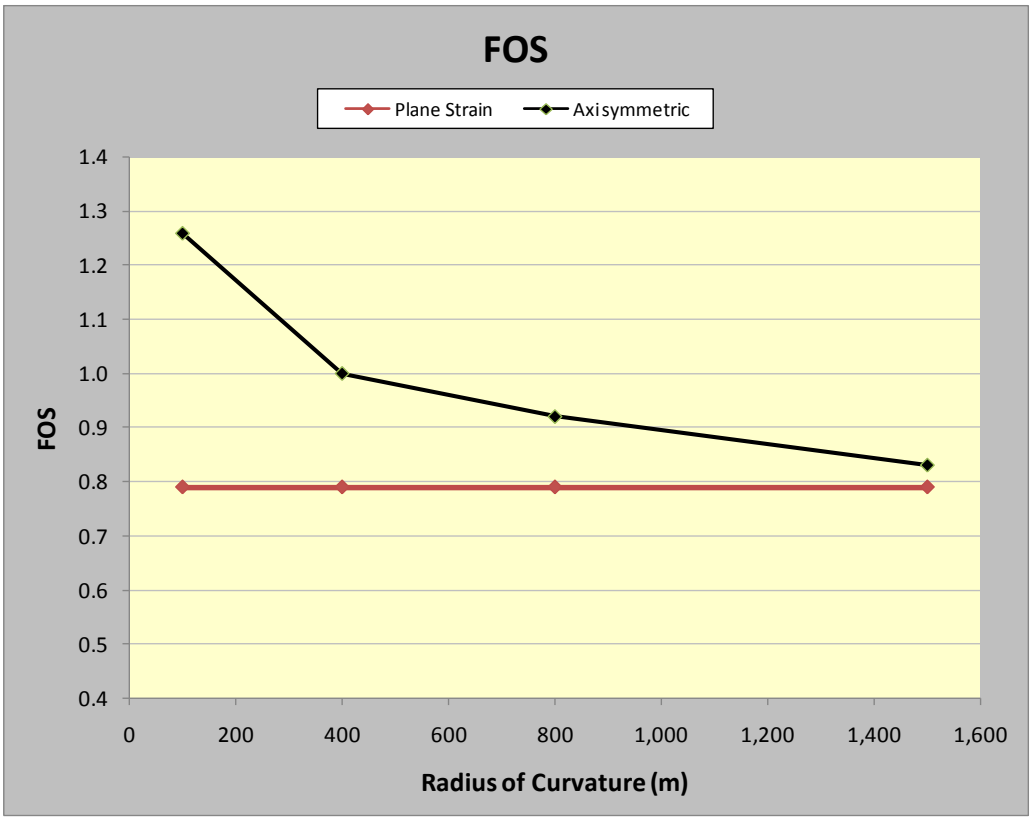

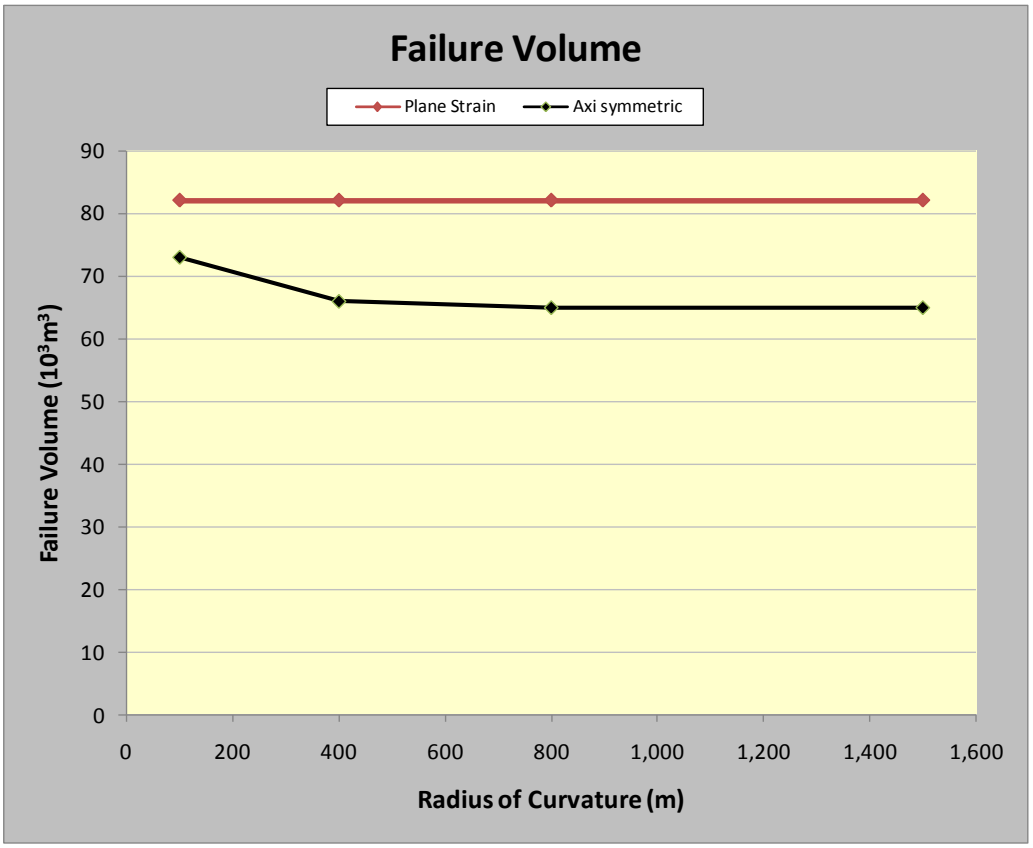

Figure 4.13 (top) Predicted FOS values with Plane strain and axisymmetric models in Phase2 for varying radii of curvature, (bottom) predicted failure volumes

4.2.10 Bathtub Geometry

The stability was evaluated along four sections at different distances from the curved ends of an elliptical pit using FLAC and FLAC3D. The FLAC models assumed plane strain conditions along the section. Table 4.13 contains a summary of the results.

Table 4.13 Sensitivity of FOS to variations in the distance from curved end of elliptical pit. All other parameters were kept constant

Distance (m)	FOS		Failure Volume ($10^3 m^3$)	
	FLAC	FLAC3D	FLAC	FLAC3D
250	1.00	1.20	134	171
500	1.00	1.10	134	177
750	1.00	1.07	134	170
1500	1.00	1.03	134	162

Since the cross sections at the various distances from the end of the pit are identical, the FLAC result is the same. As the distance from the ends increases, FLAC3D reports decreasing values of FOS. The further from the end, the closer the 2D and 3D analysis results approach each other. Figure 4.14 portrays the results graphically. 2D stability analyses can therefore be used at large distances from the concave ends, but nearer the ends they give conservative results.

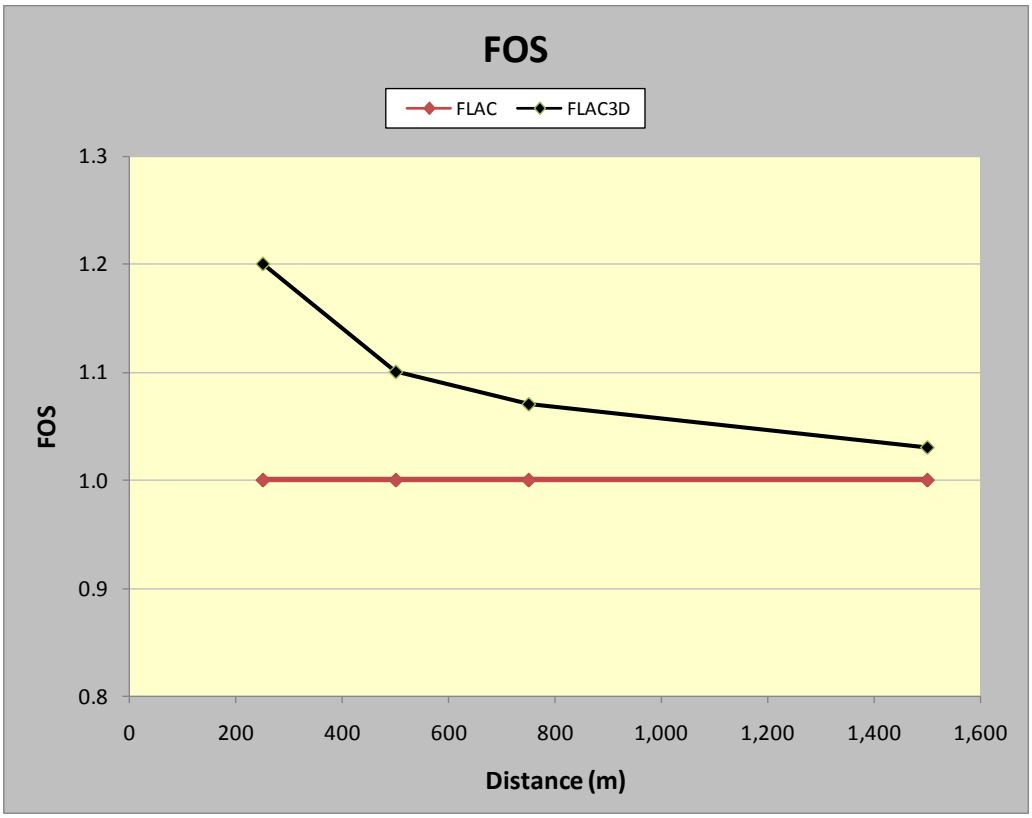

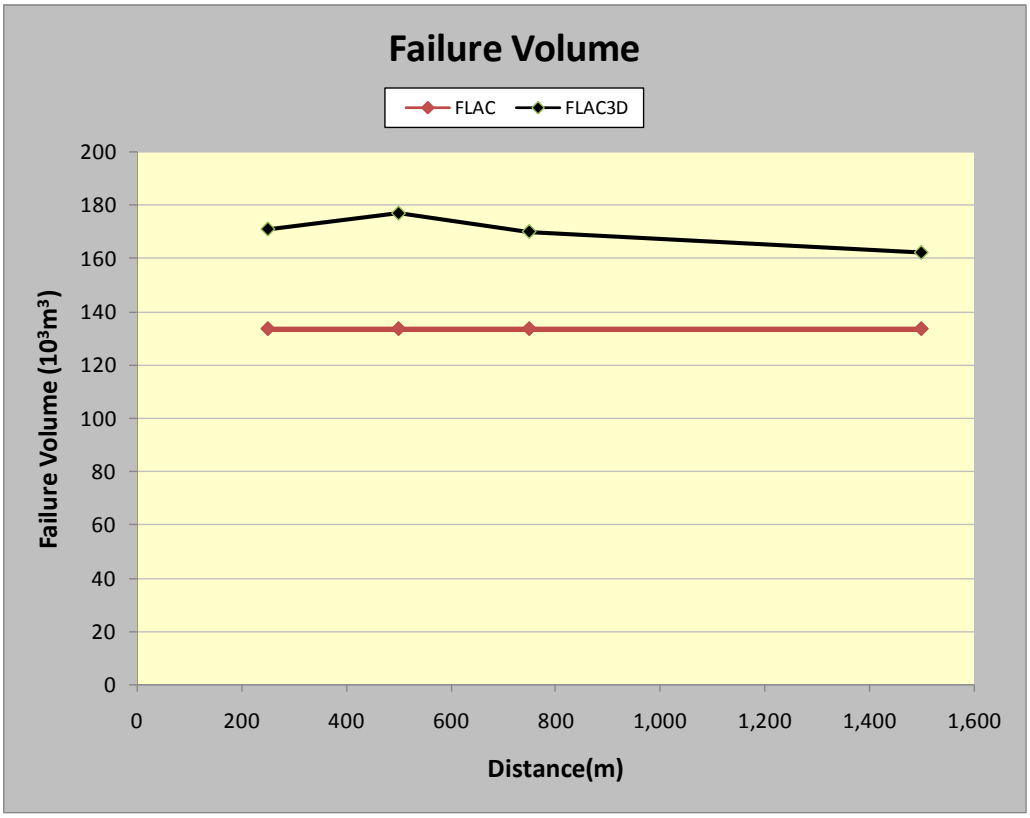

Figure 4.14 (a) Predicted FOS values with FLAC and FLAC3D at varying distances from the concave ends of an elliptical pit, (b) predicted failure volumes

4.3 Probabilistic Analysis

The results of the probabilistic analyses were grouped into 2 categories viz a comparison of LE and numerical models in probabilistic analysis, and a comparison of 2D and 3D models. All probabilities of failure were calculated using the response surface methodology as described earlier in section 3.3.4.

4.3.1 LE vs. Numerical Models

One SLIDE and three Phase2 models were analysed according to the description in section 3.3.4 above. Table 4.14 is a summary of the results of the analyses for the case where only the cohesion and friction angle were treated as uncertain inputs. Models 1 to 3 refer to different model parameters used in the Phase2 models as explained in section 3.3.4. All the Phase2 models used the same Mohr-Coulomb strength parameters as the SLIDE models. Model 1 assumed a k ratio of 1, dilation angle of zero, and locked in stresses of zero. In model 2 and model 3 the k ratio, dilation angle, and locked in stresses were increased to the values shown in Table 3.7.

Table 4.14 Probabilities of failure from SLIDE and Phase2 for the scenario with 2 variables.

CC	model 1			model 2			model 3		
	SLIDE	Phase2	Δ	SLIDE	Phase2	Δ	SLIDE	Phase2	Δ
-1.0	30%	31%	-1%	30%	16%	14%	30%	13%	17%
-0.5	36%	36%	0%	36%	21%	14%	36%	17%	19%
0.0	39%	38%	1%	39%	25%	14%	39%	20%	19%
0.5	39%	38%	1%	39%	27%	12%	39%	22%	17%
1.0	40%	39%	1%	40%	29%	11%	40%	24%	16%

The SLIDE result is similar to the Phase2 result for model 1 but not models 2 and 3, (Figure 4.15). Increasing the k ratio, dilation angle, and locked in stresses in model 2, had the effect of improving the stability of the slope. Consequently the POF values for model 2 are lower than the SLIDE result. Further increases in the dilation angle, k ratio, and LIS resulted in the POF curve labelled model 3 in Figure 4.15. Regardless of the correlation coefficient between the input parameters, comparison of the LE and numerical models gives the same conclusion. These results show that parameters like the k ratio, the dilation angle, and the locked in stresses do have a substantial influence on the calculated probability of failure of

a slope. Since these parameters are not included in an LE analysis, the consequence is that the LE and numerical modelling POF values for the same slope can differ as indicated by Figure 4.15. A very important observation is that the base case FOS changes significantly from model 1 to model 3. It is this change in the base case FOS that results in the lower POF for models 2 and 3.

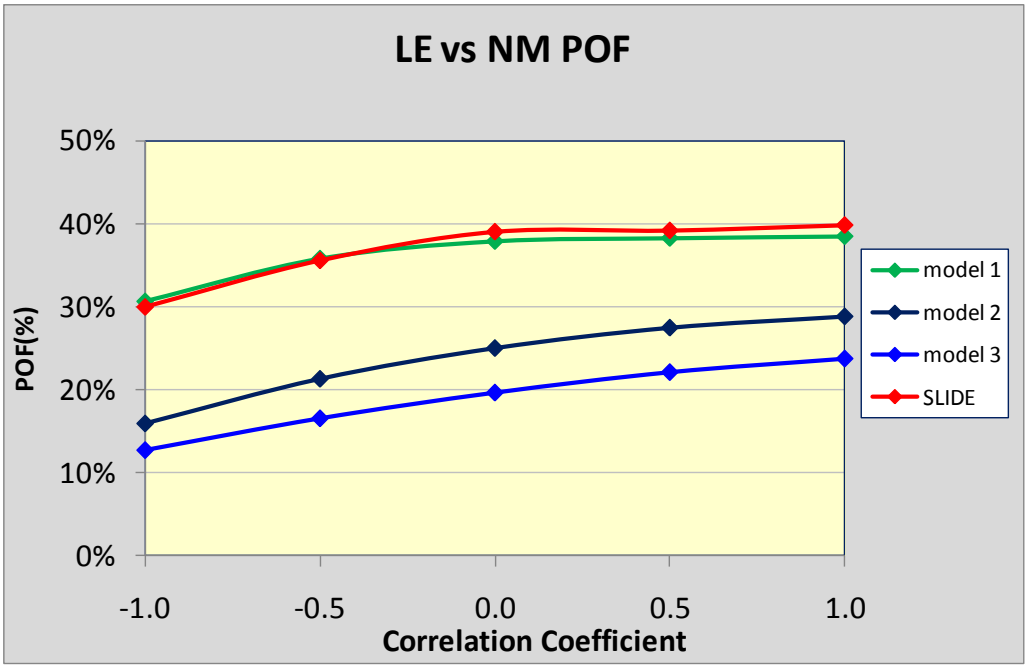

Figure 4.15 A comparison of the POF determined from SLIDE and three Phase2 models for different levels of correlation between the cohesion and friction angle.

4.3.1.1 Sensitivity Analysis

In the previous results the only variable inputs were the cohesion and friction angle. Two more scenarios were considered to investigate the major contributors to the uncertainty in slope stability. In the first scenario, the dilation angle was added as a third variable and in the second scenario the k ratio was added as a fourth variable. A coefficient of variation of 0.3 was assumed for all input variables. The results for the analysis, using 'model 3', are shown in Figure 4.16.

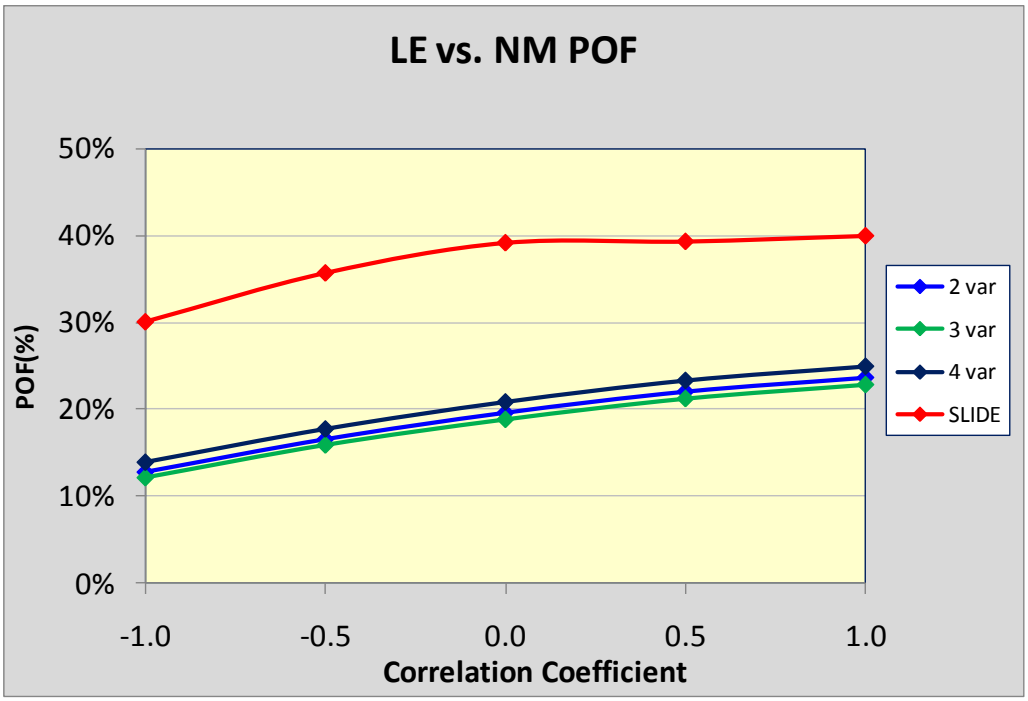

Figure 4.16 The effect on POF of increasing the number of uncertain variables from two to four.

The graphs show that increasing the number of variables has little effect on the POF. It is important to note that the contribution to the POF of an input parameter depends on two things; the variability of the parameter (measured by the coefficient of variation) and the influence the parameter has on the stability of the slope. Results from a sensitivity analysis for one model with four variables are shown in Figure 4.17. Since all the four parameters had the same coefficient of variation of 0.3, the differences in contribution to variance were solely due to differences in the influence the input parameters have on the stability of the slope. The sensitivity plot shows that the strength parameters, cohesion and friction angle, have a greater influence on the POF than the other variables like k ratio and dilation angle. This then explains the fact that including the k ratio and dilation angle as uncertain variables does not significantly change the computed FOS, (Figure 4.15). Increasing the variance of the other parameters like dilation angle will certainly increase their relative contribution to the POF but the relative influence will still be small compared to the strength parameters like cohesion and friction angle. The implications of these results is that when carrying out a probabilistic analysis with numerical models, the number of uncertain variables can be reduced by ignoring the variability in parameters like the k ratio and dilation. This means that fewer runs of the numerical models will be needed to create the response surface from which the POF is determined. It should be noted, however, that this conclusion is valid for cases in which shear failure of the rock is the failure mechanism at play. Assuming a different failure mechanism may result in different dominant parameters in the probabilistic analysis.

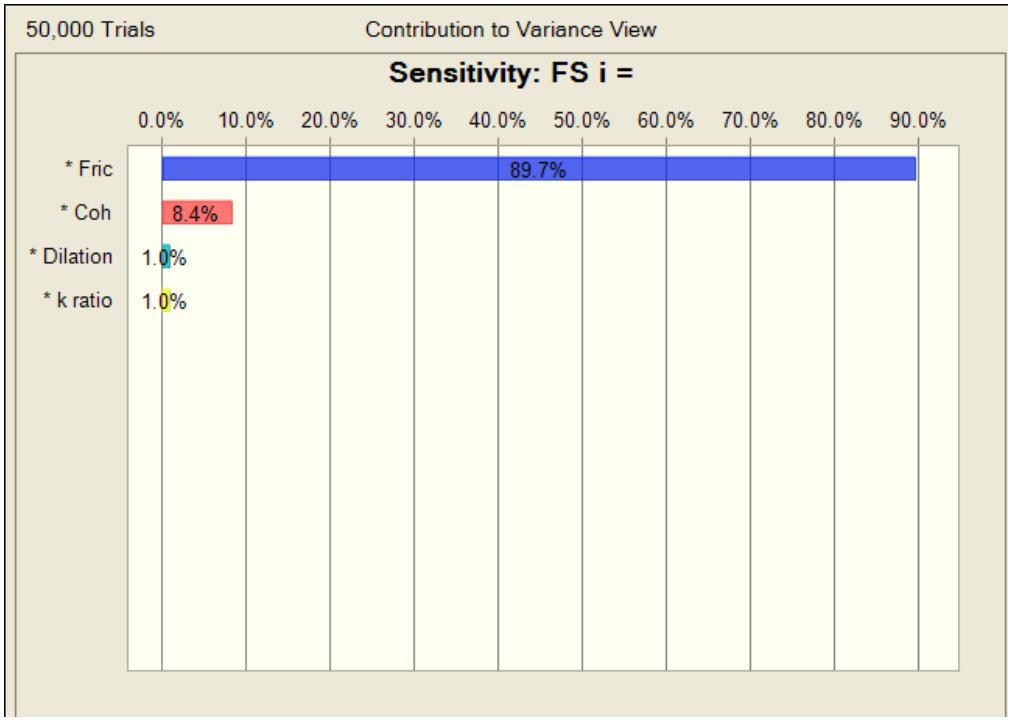

Figure 4.17 Results from sensitivity analysis for model 3 showing the relative contribution to variance of the various input parameters.

4.3.1.2 Calibrated SLIDE models

For routine probabilistic slope stability analysis it is desirable to use the fastest available tools to carry out the probabilistic analysis. For probabilistic analysis using numerical models, even though the RSM approach reduces the required runs of the numerical model, time constraints can still demand that the analyses be carried out quicker. For example, for some complex models, five runs of a numerical model can still take more than a day or even days to complete. An approach often used involves calibrating a SLIDE model to give the same base case FOS (FOS with all parameters at their mean values) as the numerical tool being used, say Phase2. The probabilistic analysis is then carried out using the calibrated SLIDE model instead of the Phase2 models. This makes the probabilistic analysis much faster than when directly using the Phase2 models. The results from the sensitivity analysis in Figure 4.17 seem to suggest this approach might be valid. To investigate the validity of this approach, two SLIDE models were calibrated so that the base case FOS values agreed with the Phase2 base case FOS values for 'model 2' and 'model 3'. The un-calibrated SLIDE model already gave a base case FOS equal to Phase2 model 1, hence there was no need for calibration in the case of 'model 1'. The calibration involved changing the

cohesion and friction angle until the FOS equalled that from the Phase2 analysis. The adjustment of the cohesion and friction angle was carried out using a trial and error approach until the desired FOS was obtained.

Table 4.15 gives the changes in the strength parameters for model 1 and model 2. The calibrated SLIDE models were used in a probabilistic analysis assuming that the cohesion and friction angle were the only uncertain inputs. The RSM analysis was carried out for five different levels of correlation between the input variables. The results are shown summarised in Table 4.16 and graphically in Figure 4.18. The calibrated SLIDE models give probabilities of failure almost identical to the Phase2 models. This is essentially due to the fact that the major contributors to variance in the FOS result are those parameters included in an LE analysis (strength parameters) and not those parameters which are not accounted for in a LE analysis (k ratio , dilation angle, and so forth).

Table 4.15 New strength parameters for the calibrated SLIDE models.

Parameter	Original value	Calibrated value	
		Model 2	Model 3
Cohesion (kPa)	640.0	655.0	694.5
Friction angle (°)	30.0	34.0	36.0

Table 4.16 POF results when using calibrated SLIDE models

CC	model 1			model 2			model 3		
	SLIDE	Phase2	Δ	SLIDE	Phase2	Δ	SLIDE	Phase2	Δ
-1.0	30%	31%	-1%	16%	16%	0%	12%	13%	-1%
-0.5	36%	36%	0%	21%	21%	0%	16%	17%	-1%
0.0	39%	38%	1%	25%	25%	0%	19%	20%	0%
0.5	39%	38%	1%	27%	27%	0%	22%	22%	0%
1.0	40%	39%	1%	28%	29%	0%	24%	24%	0%

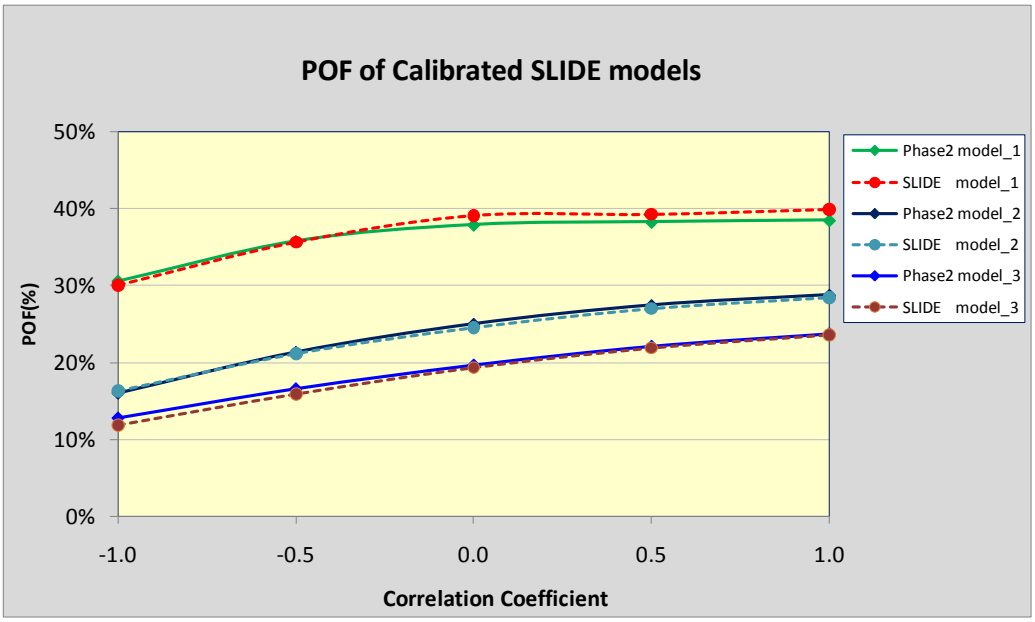

Figure 4.18 POF curves for calibrated SLIDE models (dotted lines) compared to the POF from Phase2 models.

4.3.1.3 Overall Trends

The plot in Figure 4.19 summarises the findings from the comparison of the POF determined with LE and Phase2 models. The graph is for models assuming only two uncertain inputs, cohesion and friction angle, and complete independence between those inputs. The curves labelled "SLIDE" and "SLIDE calibrated" refer to the SLIDE models before and after calibration. When parameters not included in an LE analysis (like dilation angle) are set at values that eliminate their effect, such as by setting dilation angle at zero, the POF from the Phase2 and un-calibrated SLIDE models will be the same. However, if these parameters take up other values, the POF from Phase2 will deviate significantly from the SLIDE result as shown in the case of model 2 and model 3 in Figure 4.18. These differences can be significant as the result for model 3 shows; 40% POF from SLIDE compared with 20% from Phase2. If a calibrated SLIDE model is used instead, the POF from the Phase2 and SLIDE models becomes the same for all scenarios. However, it is probable that for slopes with complex geometries and loading conditions, the calibrated SLIDE model will not provide an accurate representation of the POF. Moreover, the calibrated models are limited in their scope of application. They are only applicable to slopes with the same geometry and geology.

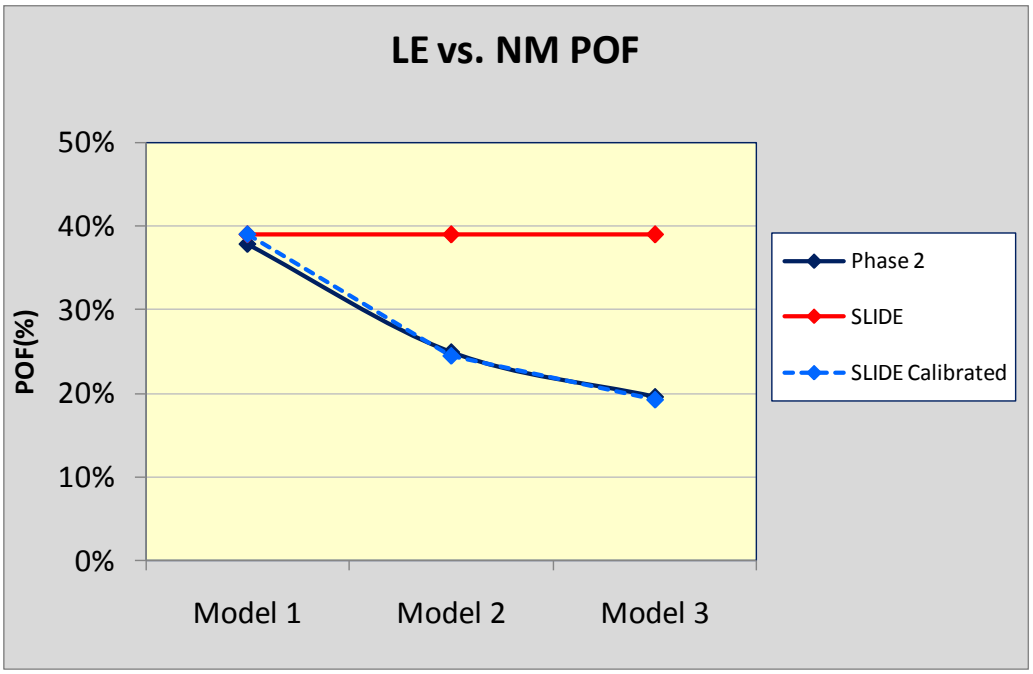

Figure 4.19 SLIDE and Phase2 POF results for models with 2 independent input variables

4.3.1.4 Failure Volumes

The failure volumes that resulted when all input parameters were at their mean values were taken to be representative of the expected failure volume in the risk analysis. In fact, increasing or decreasing the values of the input parameters about their mean values did not significantly change the failure surface. The only change was in the computed FOS value. A comparison of the failure volumes for the three Phase2 models and the SLIDE models is shown in Figure 4.20. The results show that changing the value of dilation angle, the k ratio, and locked-in horizontal stresses did not change the failure surface significantly. The only thing that changed was the FOS. In the case of failure volumes, the SLIDE calibrated models gave very similar results to the un-calibrated ones. The Phase2 models gave much higher failure volumes than the SLIDE models.

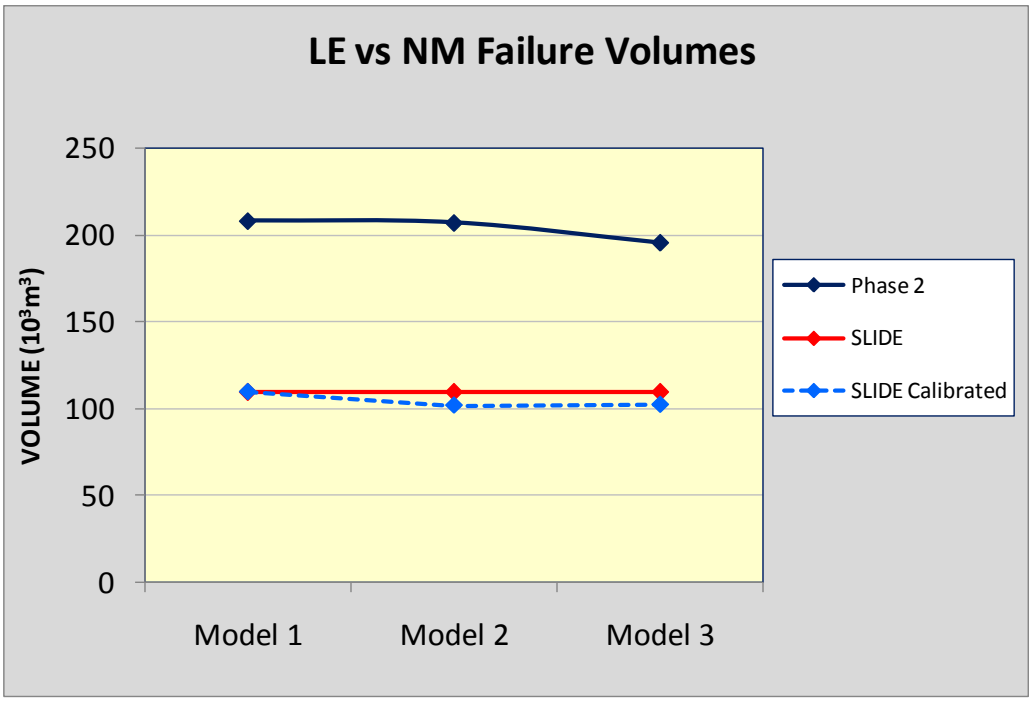

Figure 4.20 Failure volumes from SLIDE and Phase2 for scenarios where all inputs are at their mean values.

4.3.2 2D vs. 3D Models

The comparison of POF derived from 2D models and 3D models was carried out assuming complete independence between the cohesion and friction angle. 2D plane strain models for the bathtub geometry of Figure 3.10 were analysed using FLAC while 3D analyses were carried out using FLAC3D as described in section 3.3.4. The correlation coefficient has no effect on the relative comparison of the POF from LE and numerical models. Table 4.17 gives the summary of results for the analyses.

Table 4.17 Comparison of the POF and failure volumes from FLAC and FLAC3D models

Section	POF		Volumes (10^3m^3)	
	FLAC	FLAC3D	FLAC	FLAC3D
Section A	53%	24%	134	221
Section B	53%	41%	134	244
Section C	53%	46%	134	246

The 2D model analysed in FLAC was the same for all the 3 sections and therefore the POF and failure volumes are the same. The POF trend shows that as one moves away from the

concave end of the pit the POF from FLAC3D increases, approaching the result from a 2D plane strain analysis. Figure 4.21 shows this information graphically.

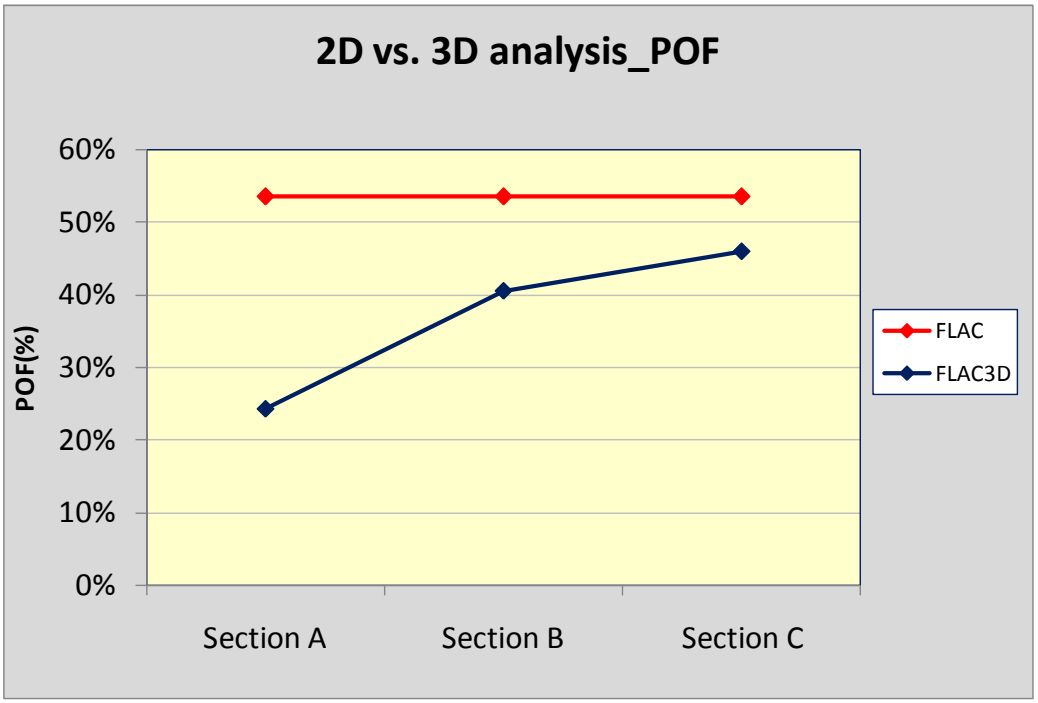

Figure 4.21 POF curves from FLAC and FLAC3D for three different sections along the pit slope

The failure volumes for the base case scenarios are shown in Figure 4.22. The differences in volumes are small from one section to the other. It appears that as the distance from the end increases, the failure volume also increases up to a limiting distance after which the failure volume becomes constant. However, the increases in volumes are just marginal.

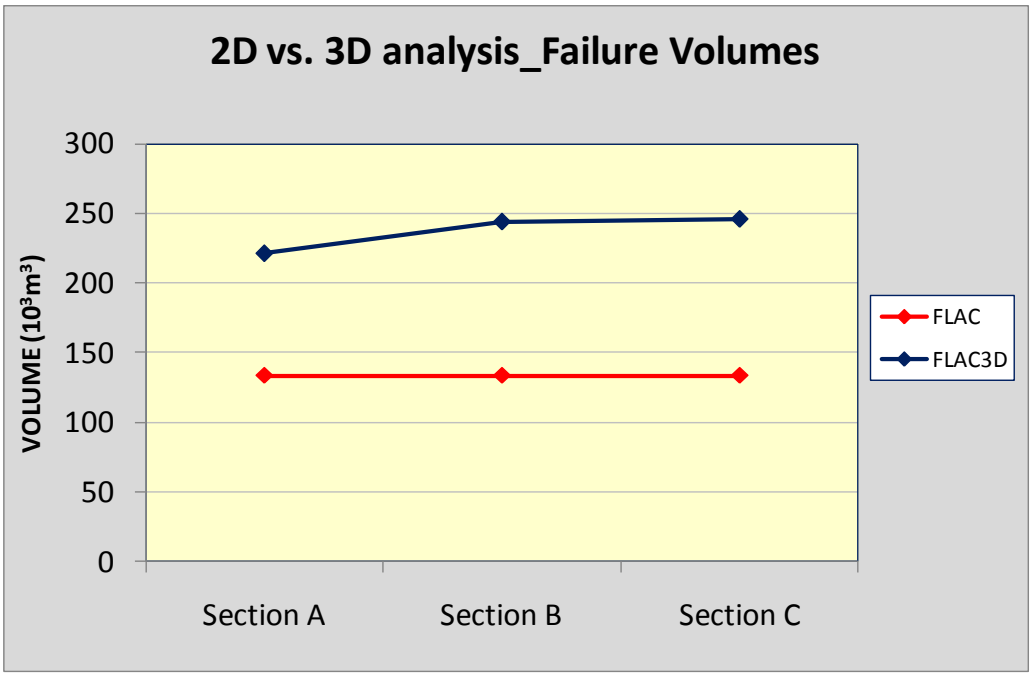

Figure 4.22 Failure volumes from FLAC and FLAC3D for the base case scenarios at 3 cross sections along the pit wall.

4.4 Risk Analysis

In carrying out the risk analysis, the event tree of Figure 3.12 was used together with the probability of failure values obtained from the models in section 4.3. As in the case of the probabilistic models, the results in this section are in two groups; comparison of LE and numerical methods as well as the comparison of 2D and 3D models. Only the economic impact of the slope failures was considered in the risk analysis, assuming that the probability of loss of profit is representative of all the economic consequences of the slope failure.

4.4.1 LE vs. Numerical Models

The POF results from section 4.3.1 were input into the event tree of Figure 3.12 so as to determine the probability of incurring a loss of profits. The results for models with 2 independent variables are shown in Table 4.18.

Table 4.18 Adjustment of the probability of overall slope failure from Phase2 and SLIDE to give the probability of loss of profits.

Model	Overall Slope Failure		P(Loss Of Profits)	
	SLIDE	Phase2	SLIDE	Phase2
Model 1	39%	38%	25%	24%
Model 2	39%	25%	25%	16%
Model 3	39%	20%	25%	13%

Since a slope failure can result in three different economic consequences (normal operating conditions, loss of profits, and force majeure), the probability of loss of profit is always less than or equal to the probability of overall slope failure. Figure 4.23 shows a comparison of the probability of overall slope failure and probability of loss of profits for the SLIDE and Phase2 models.

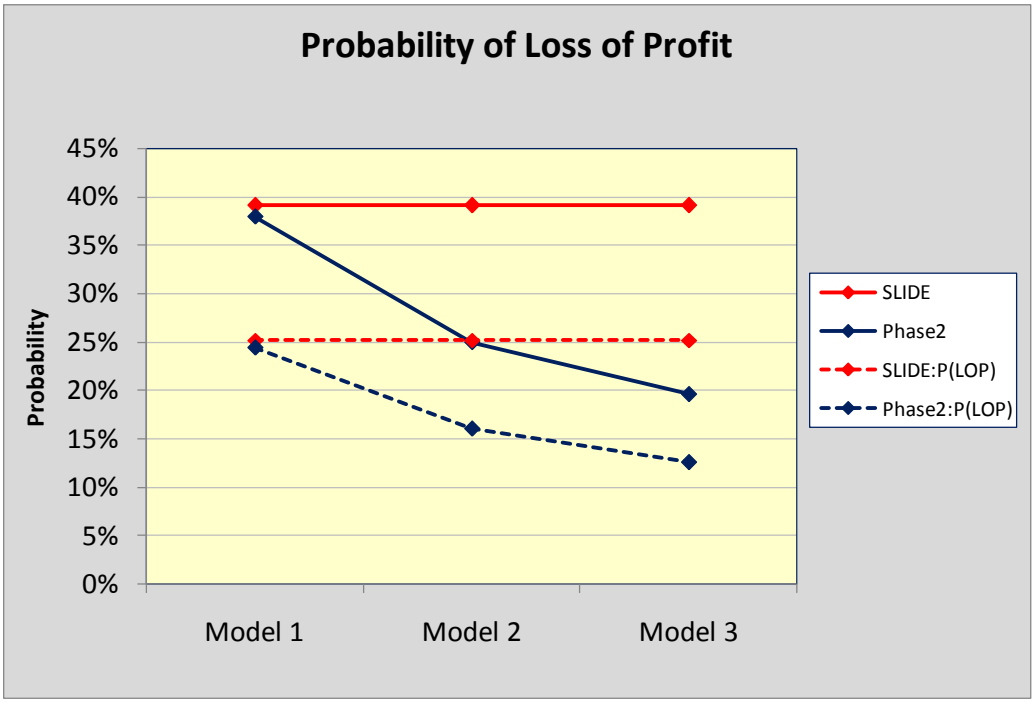

Figure 4.23 Adjustment of the probability of overall slope failure to the probability of loss of profit, P (LOP), for the SLIDE and Phase2 models.

The failure volumes were combined with the parameters of Table 3.9 (the costs associated with slope failure) to determine the total loss of profit in the event of a slope failure. It was this total loss of profit that was multiplied by the probability of loss of profit to give a risk quantity. This risk quantity is, technically speaking, the expected loss of profit. The results are in Table 4.19 and shown graphically in Figure 4.24. The important point is the relative

comparison of the assessed risk and not the absolute monetary values since the inputs were all hypothetical figures.

Table 4.19 Calculation of the expected loss of profit (risk) for the various models analysed using Phase2 and SLIDE.

Statistic	Model 1		Model 2		Model 3	
	SLIDE	Phase2	SLIDE	Phase2	SLIDE	Phase2
Failure Volume (10^3m^3)	110	208	110	207	110	196
Failure Height (m)	600	600	600	600	600	600
Clean up time (hrs)	11880	22513	11880	22398	11880	21174
Clean up cost (MZAR)	11	21	11	21	11	20
Production loss (MZAR)	1,188	2,251	1,188	2,240	1,188	2,117
Total LOP (MZAR)	1,199	2,272	1,199	2,261	1,199	2,137
P(LOP)	25%	24%	25%	16%	25%	13%
Risk (MZAR)	**301**	**554**	**301**	**363**	**301**	**270**

MZAR = Million South African Rands

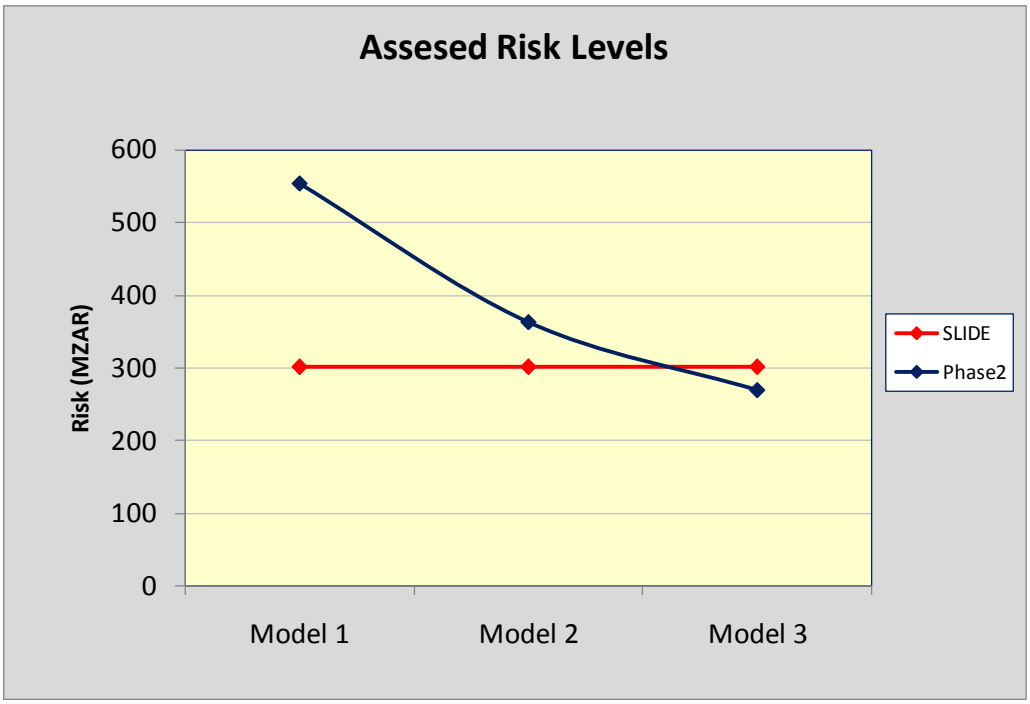

Figure 4.24 Overall risk associated with the slope determined using SLIDE and Phase2 stability models.

The expected loss of profits is larger with Phase2 in models 1 and 2. In model 3, Phase2 gives a risk assessment slightly less than the SLIDE result. The SLIDE model and Phase2 model 1 both gave an almost similar POF. However, because Phase2 always predicts larger

failure volumes, Phase2 gives a much larger risk than SLIDE for model 1. Actually, the Phase2 risk is almost double the SLIDE risk. The model 2 Phase2 POF is lower than that of the SLIDE model but again the risk is higher due to the higher failure volume reported by Phase2. The POF from Phase2 for model 3 was sufficiently small to reduce the risk to levels lower than those predicted by SLIDE.

If the calibrated SLIDE models described in earlier are used in the risk analysis the plot in Figure 4.25 is produced. The calibrated SLIDE models consistently give much lower expected loss of profits than both the Phase2 and un-calibrated SLIDE models. The reason is that the calibrated SLIDE models give probabilities of failure lower than the un-calibrated SLIDE models (but nearly equal to the Phase2 POF) and failure volumes less than both the calibrated SLIDE and Phase2 models. The aggregate effect of this is that the resultant risk is lower with the calibrated SLIDE models.

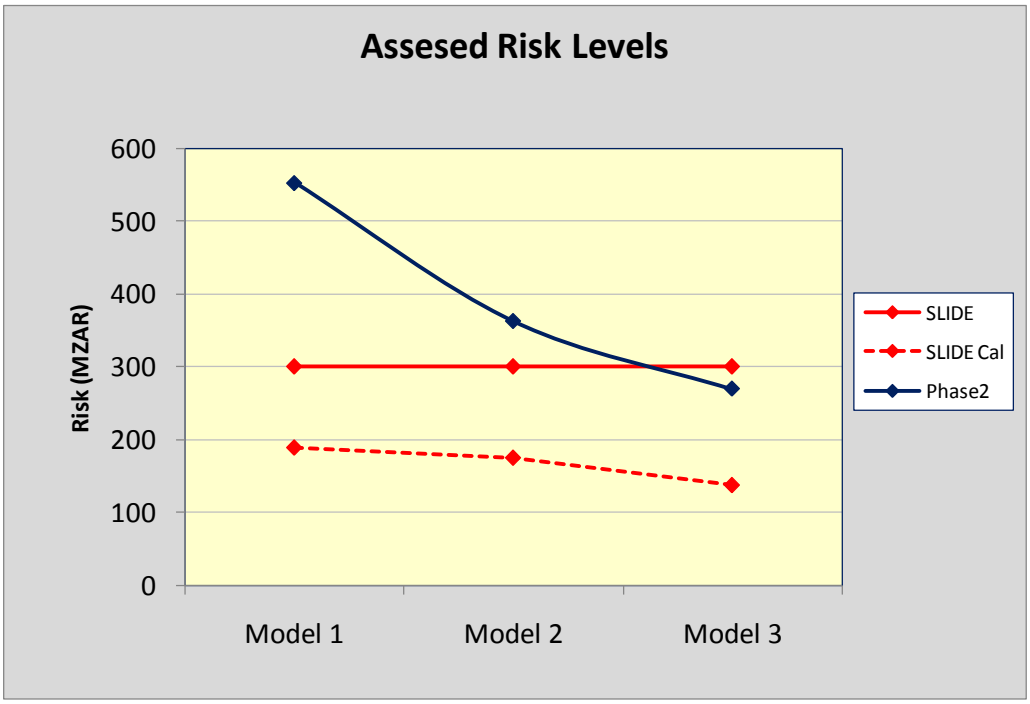

Figure 4.25 Plot of how the risk determined from calibrated SLIDE models (dotted curve) compares with that from the un-calibrated SLIDE models and Phase2 models.

4.4.2 2D vs. 3D Models

The POF results from the FLAC and FLAC3D models in section 4.3.2 were input into the event tree of Figure 3.12 so as to determine the probability of incurring a loss of profits. The results for models with two independent variables are shown in Table 4.20.

Table 4.20 Adjustment of the probability of overall slope failure from FLAC and FLAC3D to give the probability of loss of profits.

Section	Overall Slope Failure		P(Loss Of Profits)	
	FLAC	FLAC3D	FLAC	FLAC3D
Section A	53%	24%	34%	16%
Section B	53%	41%	34%	26%
Section C	53%	46%	34%	30%

Figure 4.26 shows a comparison of the probability of overall slope failure and probability of loss of profits for the FLAC and FLAC3D models. The probability of overall slope and the probability of loss of profits follow the same trend.

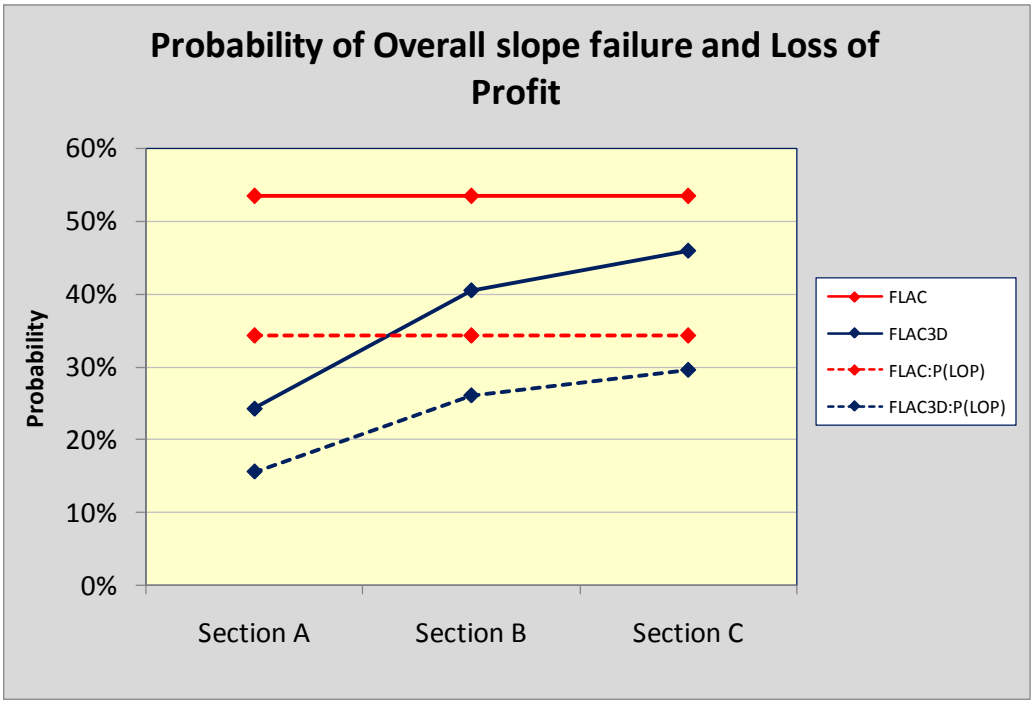

Figure 4.26 Adjustment of the probability of overall slope failure to the probability of loss of profit, P (LOP), for the FLAC and FLAC3D models.

Table 4.21 summarises the results of the risk analyses for the FLAC and FLAC3D models. The results of the risk analysis (expected loss of profits) show that for Section A (closer to the concave end) the risk determined from FLAC3D is lower than that from 2D analyses with FLAC, (Figure 4.27). For sections B and C, the risk from FLAC3D becomes greater than that from FLAC. The POF determined from FLAC3D for all sections was lower than that from FLAC but the failure volumes were greater in FLAC3D, Figure 4.22. The failure volumes from FLAC3D do not show a big variance from one section to the next but the FOS

show a big reduction moving from section A to section C. Consequently the risk computed with FLAC3D shows an increase from section A to section C.

Table 4.21 Calculation of the expected loss of profit (risk) for the various models analysed using FLAC and FLAC3D.

Statistic	Section A		Section B		Section C	
	FLAC	FLAC3D	FLAC	FLAC3D	FLAC	FLAC3D
Failure Volume (103m3)	134	221	134	244	134	246
Failure Height (m)	500	500	500	500	500	500
Clean up time (hrs)	12027	19916	12027	21961	12027	22131
Clean up cost (MZAR)	11	18	11	20	11	20
Production loss (MZAR)	1,203	1,992	1,203	2,196	1,203	2,213
Total LOP (MZAR)	1,214	2,010	1,214	2,216	1,214	2,234
P(LOP)	34%	16%	34%	26%	34%	30%
Risk (MZAR)	**418**	**313**	**418**	**578**	**418**	**661**

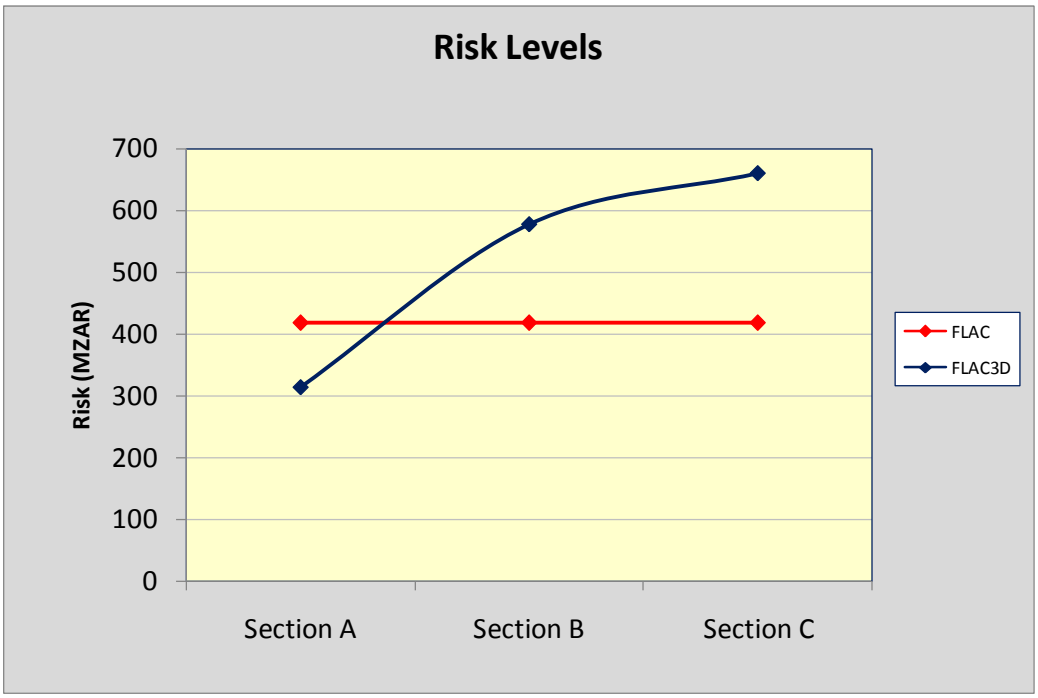

Figure 4.27 Overall risk associated with the slope as determined using FLAC and FLAC3D.

4.5 Summary of results

4.5.1 Response Surface Methodology

The calibration of the response surface methodology was carried out by comparing its results with those obtained from Monte Carlo simulations within SLIDE itself. The results show very remarkable agreement, validating the use of RSM in probabilistic slope stability analysis. The main advantage of the method is the requirement for only a few model runs as compared to the traditional Monte Carlo methods that require thousands of model runs. For example, in determining the POF for a homogeneous slope with two uncertain inputs, five SLIDE runs were used to create a response surface. The POF was then determined by carrying out Monte Carlo simulation using the response surface instead of the SLIDE model. This gave the same POF as 10,000 Monte Carlo SLIDE runs produced within the SLIDE program. This outstanding efficiency makes the RSM a very practical method of incorporating numerical models directly into probabilistic analysis. Other interesting conclusions from the calibration were that the RSM formulation can be used with correlated or independent variables, as well as with non-normally distributed variables.

4.5.2 Deterministic Analysis

There are parameters not included in a Limit Equilibrium analysis which do have an effect on slope stability. Examples of these are the dilation angle, the horizontal to vertical stress ratio (k ratio), and the locked-in horizontal stresses. Generally these parameters have the tendency of improving the stability of the slope, thus making LE analyses somewhat conservative. Other parameters such as the tensile strength of the rock and the mining sequence showed very little impact on computed FOS.

One consistent result was that the numerical models almost always predict greater failure volumes than the LE models. The failure surface indicated by Phase2 is always flatter at the top than the SLIDE surface. Figure 4.28 gives a typical comparison of the failure surfaces predicted by the two programs. The reason for this result is that the limit equilibrium solution only identifies the onset of failure, whereas the numerical solution includes the effect of stress redistribution and progressive failure after movement has been initiated. Thus, numerical models are better tools for determining the failure surfaces for a slope failure.

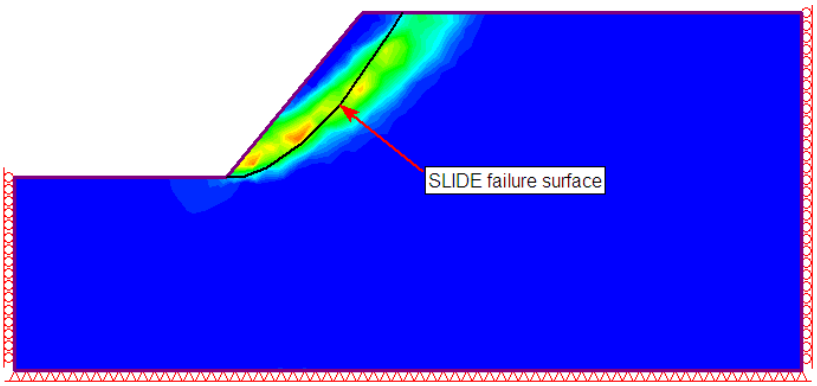

Figure 4.28 Phase2 result image showing contours of maximum shear strain which depict the failure surface. The SLIDE failure surface has been superimposed onto the image.

The comparison between 2D and 3D analysis revealed that 2D models greatly underestimate the stability of concave geometries of slopes. As the distance from a curved end of an elliptically shaped pit increases, 2D analyses become more and more applicable.

4.5.3 Probabilistic Analysis

Those parameters, such as dilation angle, not accounted for in LE analyses tend to lower the probability of failure of slopes. This means that the probabilities of failure reported by LE programs are generally on the conservative side. However, the chief contributors to variance in the FOS results remain the strength parameters (c and ϕ in the Mohr Coulomb failure criterion; UCS, m, s, a in the Hoek-Brown failure criterion etc) and the other parameters (dilation angle, k ratio etc) contribute little uncertainty in the FOS. It is the effect of the "other" parameters on the deterministic FOS that lowers the POF, not their variance. The implication of this observation is that the probabilistic analysis can be carried out with fewer parameters, by assuming inputs such as dilation angle and the k ratio to be constant, thereby reducing the number of runs required in the RSM implementation. Another important thing revealed by the results of the analyses is that the failure volumes in Phase2 for models with the same geometry but different strength parameters are generally the same. In other words, the different strength parameters improve or decrease the FOS but rarely alter the failure surface.

2D plane strain analyses will always overestimate the POF compared to axisymmetric or full 3D analyses for concave geometries. However, as the distance from the concave sections increases, the 2D assumption becomes more valid, with the 3D analysis result

converging to the 2D result. The failure volumes increase slightly on moving away from the concave ends but the differences are marginal.

4.5.4 Risk Analysis

The assessed risk for a LE analysis is generally different from that obtained using numerical tools. The results show that for some models the risk from numerical models is greater than that from LE analyses whereas for other models the risk determined from numerical models is less than that from LE methods. The risk from calibrated SLIDE models is consistently less than that from both the un-calibrated SLIDE models and Phase2 models. Even though the calibrated SLIDE models give estimates of POF in agreement with Phase2 models, the predicted failure volumes are much lower, hence resulting in the low assessed risk.

The comparison of 2D and 3D analyses shows that the risk assessed from 2D models differs from that assessed with 3D models. The results show that for some models the risk from 2D models is greater than that from 3D analyses whereas for other models it is the opposite.

CHAPTER 5

5 CASE STUDY (MINE X)

5.1 Introduction

To validate the findings from the hypothetical models used in the previous chapters, a real life case study of Mine X was used. Deterministic FOS and probabilistic analyses were carried out using the LE program SLIDE and the numerical modelling code FLAC. Risk analyses were then carried out and the results from the two analysis methods compared. This Chapter begins by giving some background information concerning the geology and hydrogeology of Mine X, followed by brief descriptions of how the rock mass and joint strength properties that were used in the analyses were determined. The FOS, POF, and risk models are then described and finally the results of the analyses are presented.

5.2 Geology and Hydrogeology

Mine X is a diamond open pit operation located in Paleoproterozoic aged sedimentary rocks of the Pretoria Group of the Transvaal Supergroup. Underlying these sedimentary rocks is the Malmani Subgroup of the Chuniespoort Group. The rock strata dip between 10° and 40° towards the NW. Variations in dip are due to rotations on large-scale structure-bounded blocks, and due to local folding. The top of the stratigraphic column are Kalahari aged sands and calcretes. Immediately below, an often gradational contact with the calcrete is the uppermost Timeball Hill Formation. It comprises a complex mixture of laminated shales, quartzitic shales, siltstones and sandstones, and carbonaceous shales. The upper most stratigraphic units have simply been lumped into one laminated shale unit (LS). A relatively consistent carbonaceous shale (CS) layer marks the base of the Timeball Hill Formation (SRK, 2008).

The structural geology is dominated by NE-SW striking faults with a strong normal dip slip shear sense component. These faults are down-thrown to the SE and compartmentalize the shallow to intermediately NW dipping strata into domains, which have been used as the geotechnical domains for slope design (SRK, 2008).

An extensive hydrogeological investigation program was implemented at the mine by a consultant in order to model the pore pressure distribution in the rock mass. Borehole piezometers were installed and monitored. The results from the monitoring program were coupled with numerical analyses using the finite element program Phase2 to estimate the pore pressure distribution in the rock mass. The major conclusion from the investigation of water regimes was that the water levels were very low and therefore had very little, if any, impact on slope stability.

5.3 Rock Mass and Structural Properties

The estimation of the rock mass strength parameters was carried out based on a geotechnical borehole log database and on the results of laboratory testing programmes that were available. Mohr-Coulomb parameters (c and ϕ) based on the Hoek-Brown criterion were assessed to represent the rock mass strengths. The methodology followed uses the geological strength index (GSI), the intact rock strength (IRS) and mi values as key inputs to characterize the rock mass. The strength characteristics of joints have been represented by Mohr-Coulomb parameters based on the Barton-Bandis criterion (Barton, 1976; Barton and Choubey, 1977; Barton and Bandis, 1990) and the evaluation has been focussed in particular on the joints associated with the foliation in the shale units. In this case average values of residual friction angle (ϕ_{res}) from laboratory testing results, the joint roughness coefficient (JRC) and the joint compressive strength (JCS) were used as the key inputs to characterize joints.

5.3.1 Rock mass characterisation

The geotechnical characterization of the lithological units at Mine X was carried out utilising Laubscher's Rock Mass Rating (RMR) classification system. The older version of the system is based on the calculation of the RMR and MRMR indexes as described by Laubscher (1990). The rock mass strength characterization for the purpose of the slope stability assessment of the present study was based entirely on the RMR estimation. The borehole database considered for the analysis included 148 boreholes drilled during different investigation campaigns. The data base comprises a total of 4,102 geotechnical intervals corresponding to 70.2 km of core. This information was further converted to 5,857 records corresponding to weighted averages of values representing 12 metre rock intervals (bench height). The rock types were grouped into the six basic lithological units indicated in Table 5.1, which were used as the geotechnical units for slope design.

Table 5.1 Summary of lithological units

Geotechnical Unit Description	Code	n raw int.	n 12m int.	Core length (m)
Carbonaceous Shale	CS	244	189	2,268
Dolomite	DM	656	1,029	12,348
Dolerite	DOL	369	310	3,720
Kimberlite	KIM	838	1,525	18,300
Laminated Shale	LS	222	142	1,704
Quartzitic Shale	QS	1,773	2,662	31,944

5.3.2 Rock mass strength parameters

Mohr-Coulomb parameters (c and ϕ) based on the Hoek-Brown criterion were assessed to represent the rock mass strengths. The methodology followed is illustrated in the diagram of Figure 5.1, with the abbreviations as defined in the list of symbols given at the beginning of this dissertation.

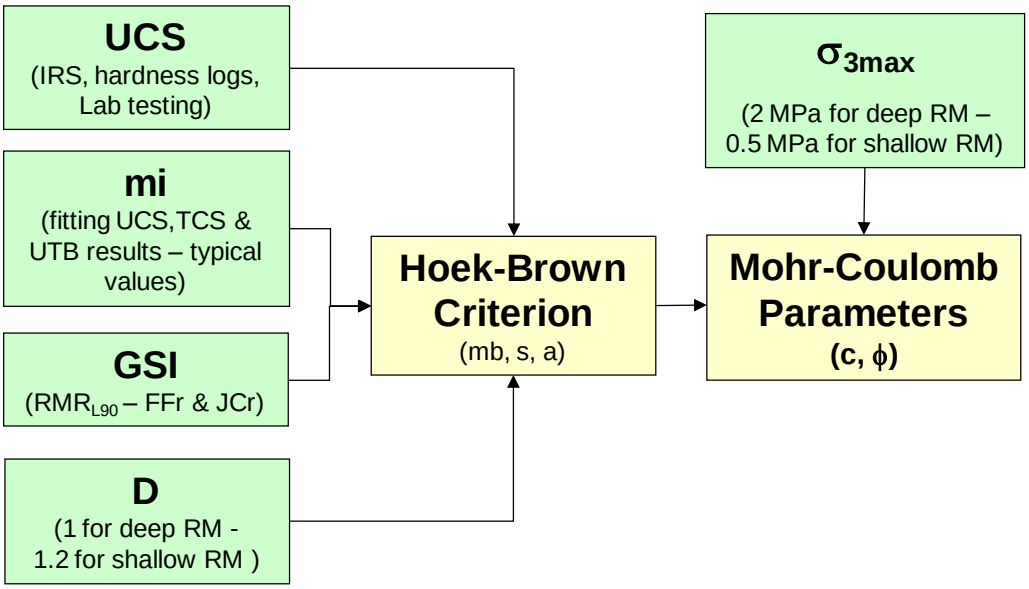

Figure 5.1 Methodology for the estimation of rock mass strength parameters

In terms of the UCS input, an attempt was made to combine the hardness field estimates with the lab UCS data. For this purpose five statistical indicators of the hardness and UCS data populations were used to establish a correlation between these two parameters. The estimation of mi values was based on fitting Hoek-Brown failure envelopes with the results of UCS, triaxial and Brazilian tensile strength tests for each geotechnical unit. The results of this analysis showed good agreement with the typical values of mi reported in the literature for the associated rock types. The estimation of the Geological Strength Index (GSI) from the Laubscher classification system was based on selecting the smaller value resulting from applying two different criteria. The first criterion consisted in assuming that

GSI is equivalent to RMR_{L90} – 5, which is based on the original definition of GSI that used Bieniawski's RMR ratings for its estimation. The second criterion is based on the translation of Laubscher's indices, Joint Condition rating (JCr) and Fracture Frequency rating (FFr), into Hoek's scales for Surface Condition and Structure of the GSI chart as indicated in Figure 5.2 (Contreras, 2009). The logic was coded using the programming language Visual Basic for Applications (VBA) and then implemented as a macro in Microsoft Excel. Appendix A gives the VBA code used for this purpose. The disturbance due to blasting was estimated as D=0.8 and the stress level as σ3max=2.0 MPa.

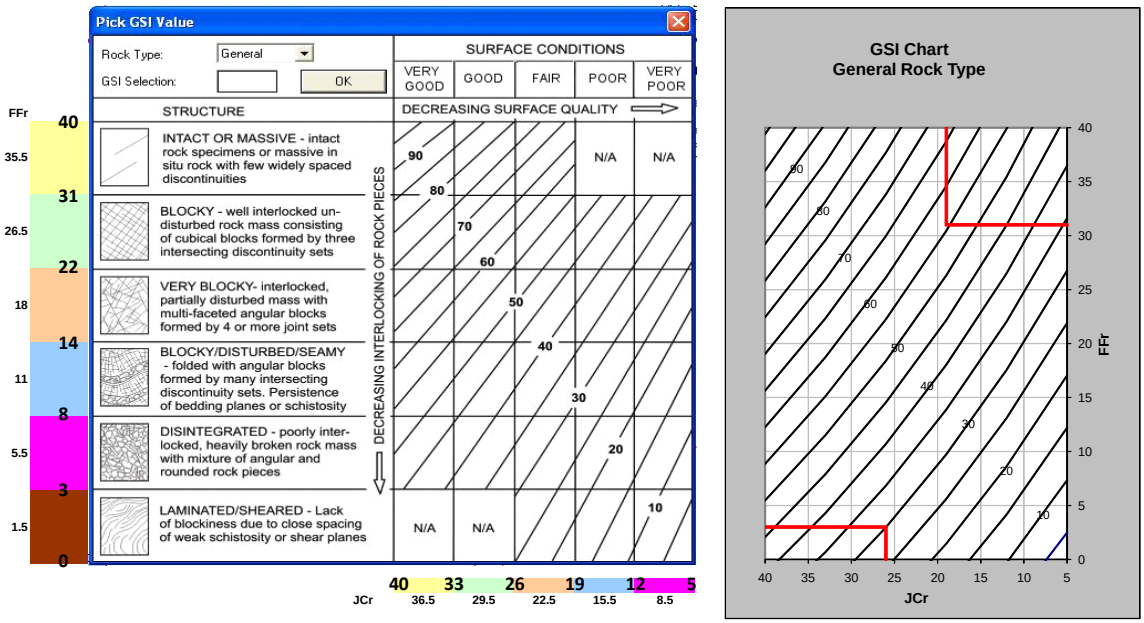

Figure 5.2 Conversion from rock structure in Laubscher 1990 to GSI (Contreras, 2009)

The Hoek-Brown characterisation parameters were converted into equivalent Mohr-Coulomb parameters using the equations in Hoek et al (2002). A summary of the estimated Mohr-Coulomb strength parameters for each geotechnical unit is presented in Table 5.2. The graph in Figure 5.3 shows the average values of the estimated parameters for deep and shallow rock mass conditions. The parameters for the calcrete unit (CAL) were assumed equal to those that had been used in an earlier (2007) design.

Table 5.2 Summary of rock mass strength parameters

Code	UCS (MPa)	mi	RMR	GSI	c (kPa)	Φ (˚)
CS	121	5	54	47	654	32
DM	218	13	66	54	1,467	50
DOL	237	9	61	49	1,168	44
KIM	39	9	55	50	437	30
LS	79	5	44	39	373	26
QS	173	5	60	47	864	36
CAL	NA	NA	NA	NA	318	35

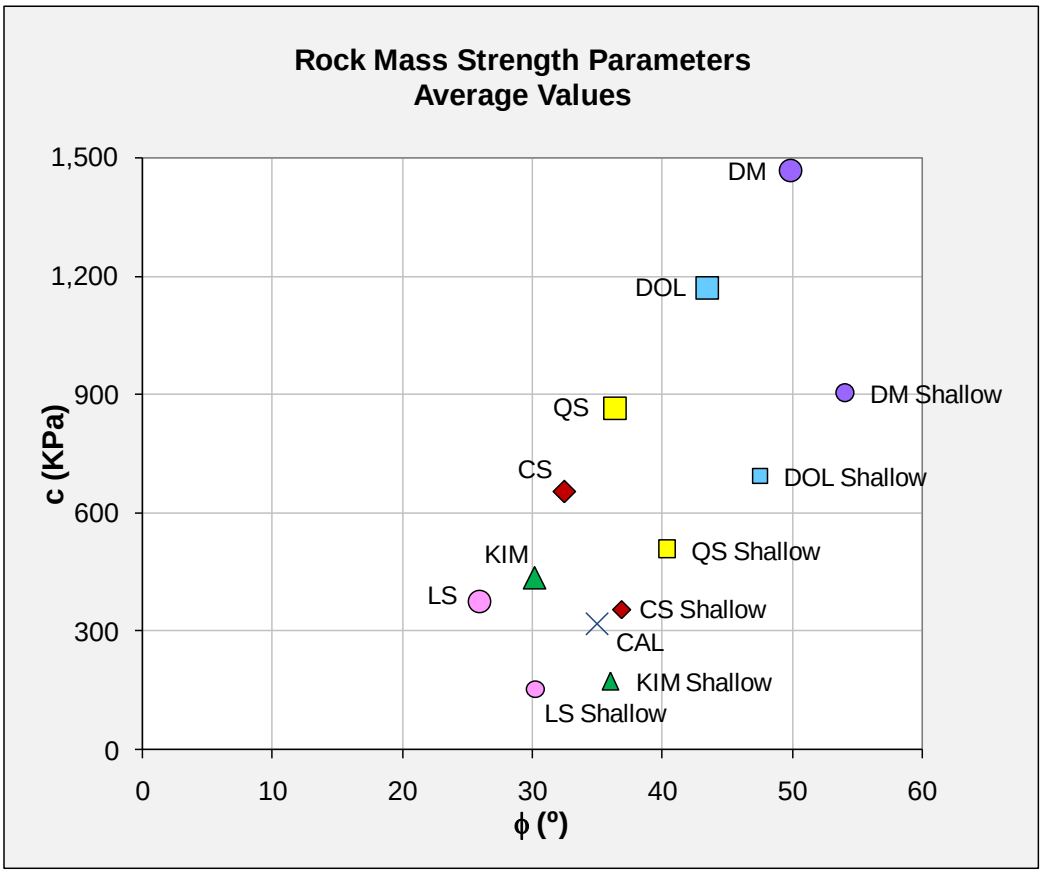

Figure 5.3 Rock mass strength parameters used for the design of slopes at Mine-X

5.3.3 Joint (Foliation) strength parameters

The estimation of strengths along joints, in particular those associated with the foliation in the shale units, was based on the Barton-Bandis criterion which enabled the estimation of equivalent Mohr-Coulomb parameters (c and ϕ) for a defined maximum level of normal stress. The methodology followed is illustrated in the diagram of Figure 5.4. The estimated strengths were compared with the results of the numerous direct shear tests carried out

on open and closed (welded) foliation joints in order to confirm the validity of the estimations.

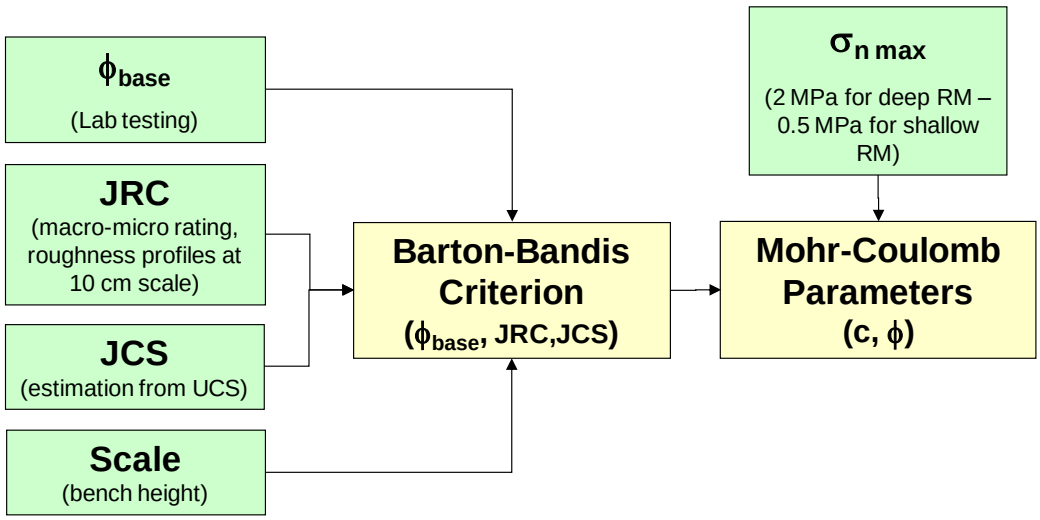

Figure 5.4 Methodology for the estimation of Joint (foliation) strength parameters

Average values of base friction angle (BFA) and residual friction angle (RFA) were obtained from the results of a laboratory testing programme. Representative values of the joint roughness coefficient (JRC) were estimated from the small scale joint expression data from the logs. A scale dimension consistent with the bench height (12 m) was assumed for the estimation of the JRC values representative of field conditions. The joint compressive strength (JCS) values representative of field conditions were estimated by applying the scale factor correction from Bandis (Barton and Bandis, 1990) to the average values of UCS defined with the laboratory testing programme for each rock unit. The maximum normal stress (σ_{nmax}) acting on the joints was estimated to be 2.0 MPa. A summary of the estimated strength parameters for joints is presented in Table 5.3 and these results are illustrated in Figure 5.5.

Table 5.3 Summary of joint strength parameter estimates

Code	UCS (MPa)	RFA (˚)	JRC log	JCS Field (MPa)	JRC Field	c (kPa)	Φ (˚)
CS	115	30	4	65	2.7	20	34
DM	214	29	6	90	3.4	25	34
DOL	222	32	4	125	2.7	22	37
KIM	36	30	4	20	2.7	20	33
LS	56	30	4	32	2.7	20	34
QS	173	31	4	98	2.7	21	36

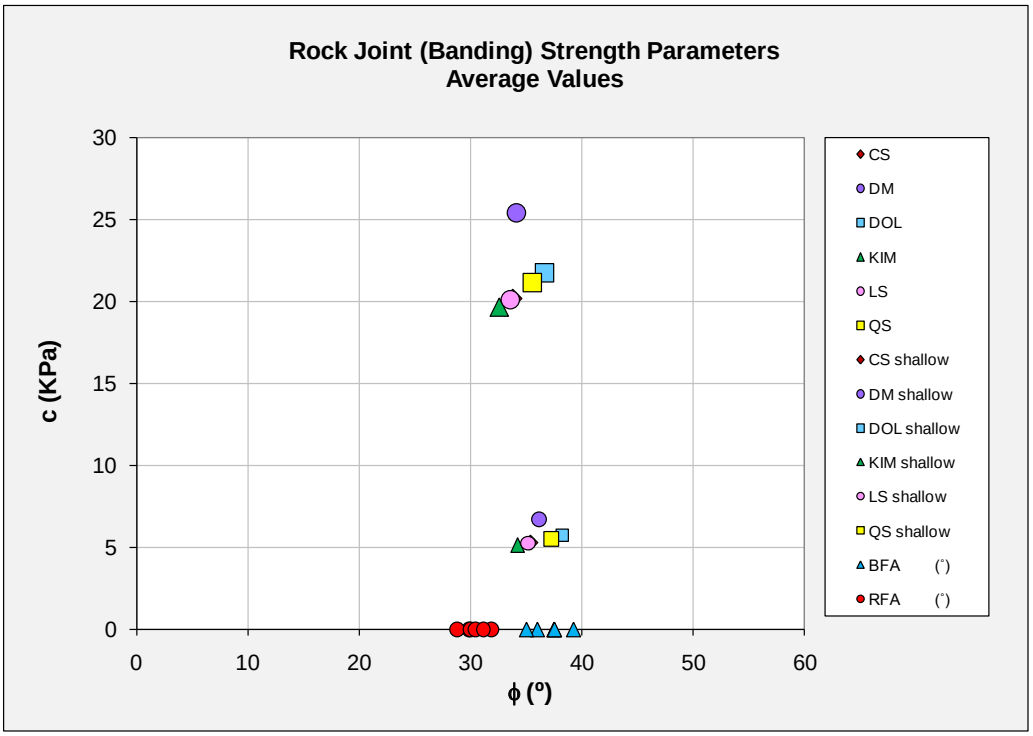

Figure 5.5 Joint strength parameters for the rock units. Also shown are the Base friction angle (BFA) and residual friction angle (RFA) values for the various rock types.

The results of the direct shear tests on open and closed joints mentioned earlier showed much higher cohesion values than those estimated using the Barton-Bandis criterion. Based on these results, it was suggested that the shear strength along the foliation planes be represented by the strength parameters estimated for the joints in the shale units as shown in Figure 5.5, but increasing the cohesion by a factor of 4.

5.3.4 Rock Mass Elastic parameters

The modulus of elasticity of the rock mass (ERM) is based on the empirical relationship between ERM, Ei, D and GSI proposed by Hoek et al (2006). The characteristic modulus ratio (MR) for each rock unit was estimated from the average values of E and UCS defined with the laboratory testing results. The intact rock modulus E_i was calculated for every geotechnical interval in the borehole logs from the respective characteristic modulus ratio (MR) and the UCS value in that interval. The modulus ratio is the ratio of the Young's modulus to the UCS of intact rock. Typical MR values for each rock type were obtained from tables and using the UCS from the borehole logs, the value of E_i was calculated. The rock mass elastic parameters used for the design are in Table 5.4. The rock mass elastic modulus, ERM in Table 5.4, was calculated using the Hoek-Diederichs empirical relation (Hoek and Diederichs, 2006).

Table 5.4 Summary of elastic parameters

Code	MR	Ei (GPa)	ERM (GPa)	ν
CS	310	28	2.3	0.25
DM	431	96	12.7	0.25
DOL	325	76	7.8	0.25
KIM	273	10	1.0	0.25
LS	446	39	1.9	0.26
QS	350	61	5.3	0.25

5.4 Analysed Section

One section was used for the modelling, representing an overall scale slope, with a height of 581m and an overall slope angle of 38°. Figure 5.6 shows the final profile of the section.

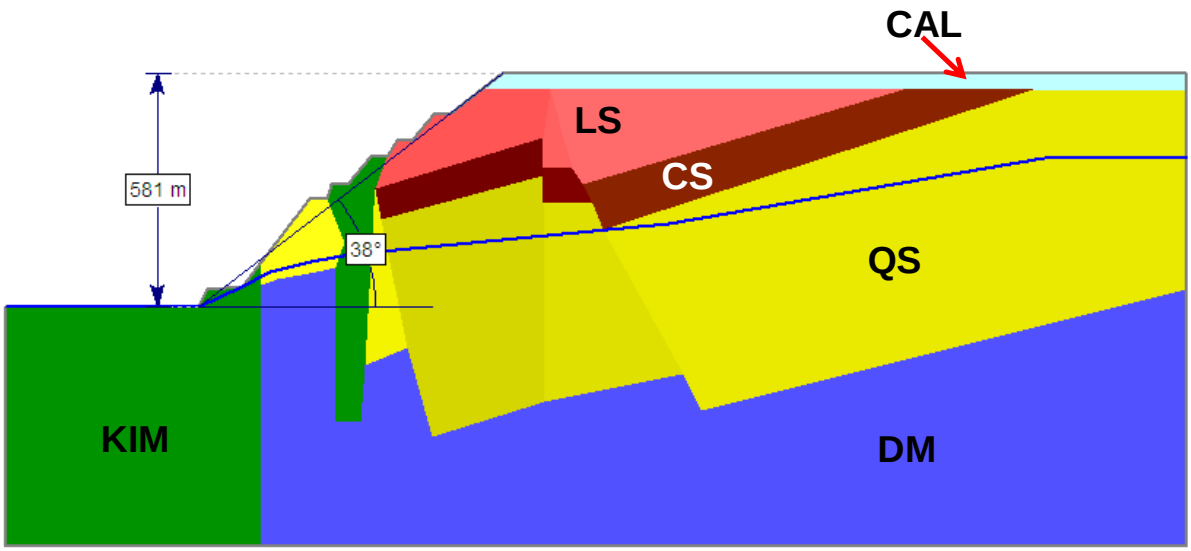

Figure 5.6 Section used for the stability analysis for Mine X showing the rock units, slope height, overall slope angle, and the water table (blue line).

A number of faults that strike sub parallel to the slope face appear in the cross section dividing the rock units into domains. Foliation planes appear in all the shale units (CS, LS, and QS). These foliation planes have different angles in the different domains as shown in Figure 5.7. Since these faults dip in a direction opposite to the dip direction of the slope face, planar sliding along the fault planes is not a kinematically feasible failure mechanism. Moreover there are no combinations of these faults that form valid wedges. Thus the faults are not expected to play a significant role in the stability of the slopes. Therefore, the faults were not included in the stability analyses in order to keep the analyses tractable. However

for the slopes that are on the opposite side of the pit, the faults do have an influence and a discrete element numerical modelling code like UDEC (Itasca Inc.) would be needed. The foliation angles (apparent dip) in the different domains along with the faults (black lines) are shown in Figure 5.7.

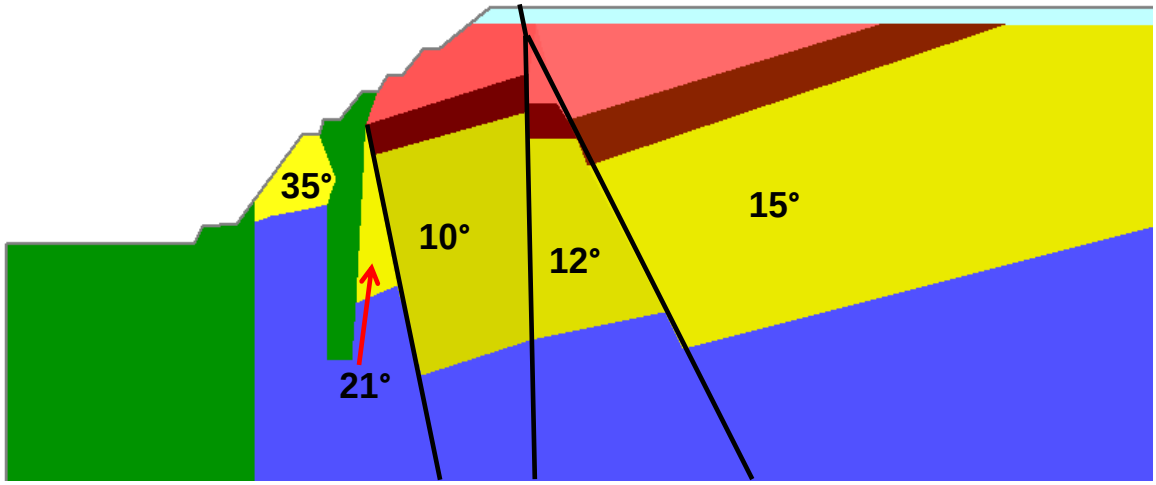

Figure 5.7 Slope showing the apparent dip of the foliation planes in each domain.

5.5 FOS, POF and Risk models

The program SLIDE was used to carry out the LE stability computations while FLAC was used for the numerical analyses. All POF values were computed using the Response Surface Methodology so as to ensure a fair comparison of the SLIDE and FLAC results. The POF values were then used with typical costs to determine the expected loss of profits due to an overall slope failure. The results of the expected loss of profits from the SLIDE models and those from the FLAC models were compared and graphed.

5.5.1 Variable input parameters

The derivation of the Response Surface Method suggests that the best results are obtained when the input variables are statistically independent. Since cohesion and friction angle are known to be correlated in some way, it was better to use the UCS and GSI as the variables in the analyses. The latter two variables can confidently be assumed to be independent. However, FLAC cannot implement FOS calculations (the SSR method) using the Hoek-Brown constitutive model, implying that the UCS and GSI had to be converted to the equivalent Mohr-Coulomb parameters. This means that for each combination of the UCS and GSI variables, a new set of C and Φ was calculated and then used in the stability model. From the analysis of the field data, the mi parameter showed very little variability

for all rock units and thus it was assumed to be a constant. Appendix B shows a summary of the strength parameters used for the deterministic FOS and probabilistic modelling. Both GSI and UCS were assumed to follow normal distributions.

5.5.2 SLIDE models

The SLIDE models were built using the Mohr-Coulomb strength criterion for the kimberlite, calcrete and dolomite rock units. In order to model the foliation planes in the shale units, the anisotropic strength function was used. The Anisotropic Function model allows the user to define discrete angular ranges of slice base inclination, each with its own cohesion and friction angle. Hence the foliation plane can be implicitly modelled, (Rocscience, 2008). Bishop and Janbu corrected methods of slices were used, with the lowest value between the two reported as the FOS.

The 'Block Search' search method was used for the case study instead of the 'Path Search' that was used for the analyses in Chapter 3. For slopes involving anisotropic rocks, the path search in most cases failed to locate the global minimum surface and the block search yielded a better result. The search windows were placed so as to include surfaces that run parallel to the foliation planes. Only one pair of slope limits was used; with one behind the crest and the other close to toe. This condition means that SLIDE was free to pick any surface that extends from any point on the lower half of the slope to any point on the upper half of the slope. 20 000 surfaces were analysed in the search for the global minimum.

5.5.3 FLAC models

The Mohr-Coulomb constitutive model was used for the kimberlite, calcrete and dolomite rock units. As for the foliated shale units, the ubiquitous joint constitutive model was used. In this model, which accounts for the presence of an orientation of weakness (weak plane) in a FLAC Mohr-Coulomb model, yield may occur in either the solid or along the weak plane, or both, depending on the stress state, the orientation of the weak plane and the material properties of the solid and weak plane, (Itasca, 2005). The FLAC models used the same strength parameters as the SLIDE models as well as the deformation parameters of Table 5.4. Since no stress measurements have been done on the mine, a k ratio of 1 was assumed for all models. Joint dilation angles were obtained from lab tests, but the dilation angle for the rock mass was assumed as zero as no tests had been done to determine

these. Table 5.5 summarises the dilation parameters used in the stability analyses with FLAC.

Table 5.5 Rock mass and foliation dilation angles

Unit	Dilation angle (°)	Foliation Dilation angle (°)
CS	0	12
LS	0	15
QS	0	22
KIM	0	NA
DM	0	NA
CAL	0	NA

The mining in the FLAC models was modelled in 5 stages, following the actual expected profile of the mine at 4 year intervals, so as to simulate the gradual relaxation of stresses due to mining. The 5 stages corresponded to mining depths of 175m, 275m, 425m, 500m, and 580m. The FLAC grid was set up including all the boundaries, and the stresses were set up to conform to the required k ratio. The first mining step was executed, after which the model was cycled to equilibrium. The next stage of excavation was then implemented and the model again cycled to equilibrium. This procedure was repeated for all mining steps. After the last mining step, the SSR was invoked and a FOS calculated. The setting up of stresses to conform to the required k ratio was achieved by means of FLAC's inbuilt programming language called FISH.

5.5.4 Consequence analysis

The impact of the slope failure on safety was not considered in this analysis. With regard to economic impact, only the probability of loss of profits was included in the analysis, and other consequences such as force majeure and damage to equipment were ignored. The total loss of profits was assumed to be made up of two components; the cost of cleaning up after a failure and the cost due to production delays. The cross-section being analysed contained the access ramp into the pit, and any overall slope failure would result in production delays. The event tree of Figure 3.12 and the corresponding probabilities in Table 3.8 were used for the evaluation of consequences. Cost figures were not provided by the mine so the hypothetical costs used for the risk analyses in Chapter 3, have again been used for illustrative purposes. As noted earlier, the specific costs used do not have a bearing on the relative comparison of the results from the LE analysis and from the

numerical analysis. Table 3.9 shows the assumed costs. The out of plane extent of the failure was derived by assuming that the failure height to width ratio is 3.

5.6 Results

The results from the analyses of the cross-section are presented in this section. The FOS results are given first followed by the POF results. The risk analysis results are then given before a summary of all the results is given.

5.6.1 FOS

The base case FOS for the SLIDE models was 1.10 whereas that from the FLAC models was 1.20. The FLAC model gives a higher FOS value, consistent with the results from Chapter 4. The predicted failure surfaces show a more marked difference, with FLAC predicting a much larger failure volume (Figure 5.8). The SLIDE failure surface extends from the ramp down to the toe. On the other hand, the FLAC failure surface starts from behind the crest down to the toe. The SLIDE failure height is 427m compared with 581m from the FLAC models, a difference of 154m! This agrees quite well with Itasca (2005)'s assertion that the limit equilibrium solution only identifies the onset of failure, whereas the numerical solution includes the effect of stress redistribution and progressive failure after movement has been initiated.

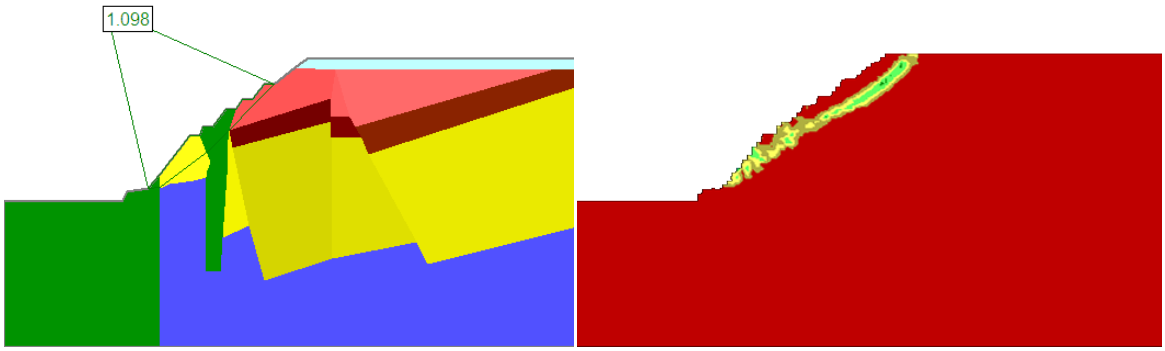

Figure 5.8 Predicted failure surfaces from the SLIDE (left) and FLAC model.

A FLAC plot of the plasticity indicators (Figure 5.9) shows that the failure of the slope is due to shearing of the intact rock except in the quartzitic shales where the slope fails along the foliation planes. The blue crosses show slip along ubiquitous joints, the red crosses indicate

yielding in shear or volumetric yielding, and the purple circles indicate yielding in tension. From the figure it is clear the area behind the crest will fail due to tensile strains, maybe with the formation of tension cracks. Figure 5.10 is a plot of the velocity vectors at failure.

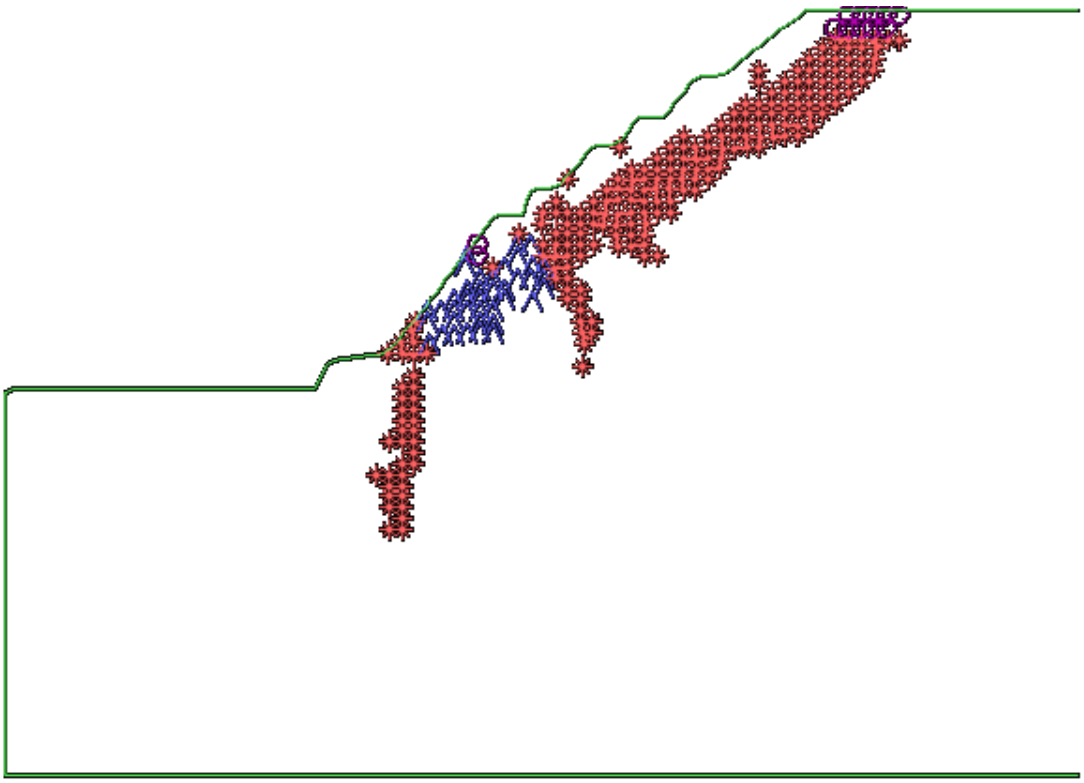

Figure 5.9 **FLAC plots of plasticity indicators showing the mode of failure of the slope.**

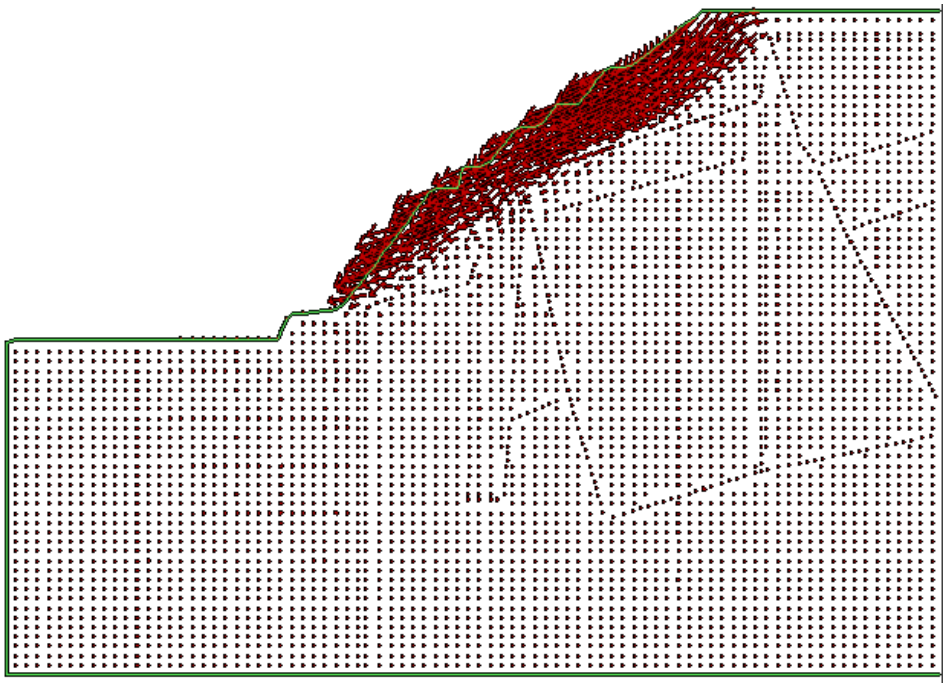

Figure 5.10 FLAC plots of velocity vectors at failure

5.6.2 Probability of failure

The POF from the SLIDE models was 16% as compared to 11% from the FLAC models. Expectedly, SLIDE gives a slightly more conservative indication of stability. Figure 5.11 shows the results of the Monte Carlo simulations in Crystal Ball for both the SLIDE and FLAC models. The base case FOS values are marked on the charts.

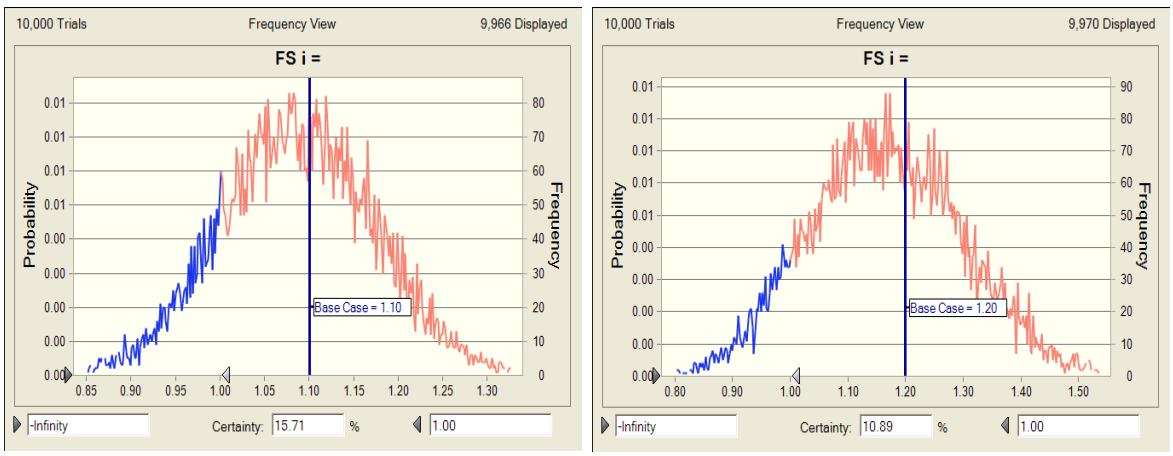

Figure 5.11 Results of Monte Carlo simulations in Crystal Ball for the: a) SLIDE (left) and b) FLAC models.

The corresponding sensitivity analysis results are in Figure 5.12. Both SLIDE and FLAC indicate that the rock mass strength of the quartzitic shale has a negligible contribution to the variance. This is because the failure surface is along the foliation planes in the QS unit, as indicated by the plasticity indicators of Figure 5.10. Therefore, it is the foliation strength that controls resistance to failure in that unit. However, there are two big differences in the sensitivity plots. Firstly the SLIDE models indicate that the UCS of the Kimberlite has the greatest contribution to variance (47%) while the FLAC models give the UCS and GSI of the Laminated Shale as the greatest contributors to variance (47% and 27%). This discrepancy comes from the fact that the failure surface in SLIDE passes through very little of the LS unit whereas in FLAC it passes through a substantial volume of LS rock. As a result the LS unit has a much bigger influence on stability in the FLAC models than in the SLIDE models. Another difference between the 'contribution to variance' plots is that the foliation strength of the QS has a much greater influence on the POF in the SLIDE models (22%) than in the FLAC models (3%). The reason for this difference is that the substantial portions of the failure surface that pass through the LS unit in the FLAC models means that a large proportion of the contribution to variance comes from the LS strength (74%). Consequently, all the remaining variables have much lower contributions in the FLAC models as compared to the SLIDE models. Secondly, the dilation angle of the foliation planes in the QS unit (22°) might have had an effect of increasing the resistance to sliding along the foliation in the QS.

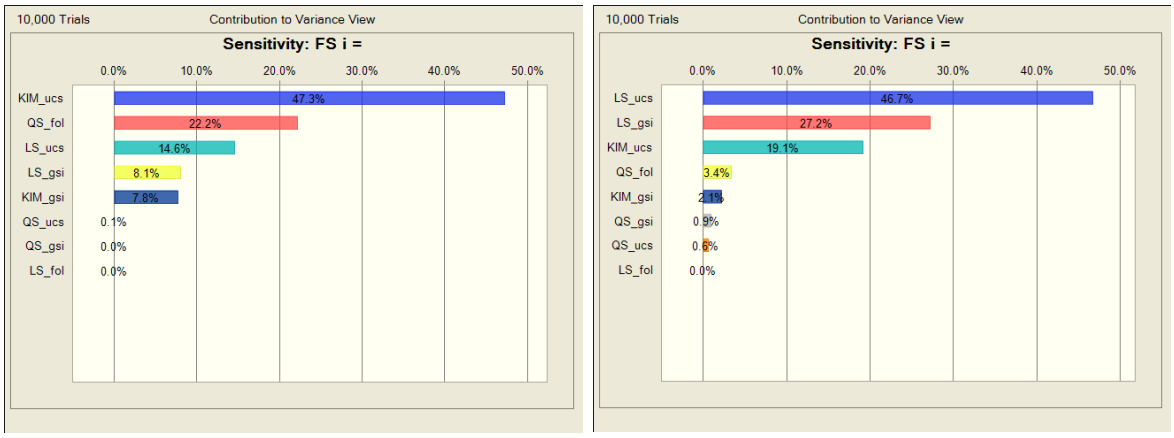

Figure 5.12 Contribution to variance of the different variables for the: a) SLIDE (left) and b) FLAC models.

5.6.3 Risk analysis

The results of the risk analysis are summarised in Table 5.6. The failure volume from the FLAC model was calculated using the approach explained in Chapter 3. These volumes were taken from the base case models where all input variables were at their mean values.

Table 5.6 Results of the risk analysis for SLIDE and FLAC models

Result	Units	SLIDE	FLAC
Failure volume	10^3m^3	36	86
POF	%	16	11
P (LOP)	%	10	7
Risk	**MZAR**	**28**	**63**

P(LOP) = Probability of loss of profits
MZAR = Million South African Rands

The risk quantity is simply the expected loss of profits due to the slope failure. As explained earlier, all other economic consequences of the slope failure have been ignored from the analysis. The results show that even though the probability of loss of profits is not very different between the two modelling approaches, the consequences of the failure are very different. The failure volume from the SLIDE model is more than 100% smaller than that from the FLAC model. As a result the expected loss of profits for the slope geometry is predicted as 28 million rand from the LE models, but when numerical analysis is used the expected loss of profits rises to 63 million rand, an increase of 123%! In this particular case, the SLIDE result is a more optimistic estimate than the FLAC result. Figure 5.13 shows this result graphically. The chart shows a plot of the POF and Risk for the two approaches to slope design, LE and numerical modelling. Even though the SLIDE models gave a conservative POF value, the overall assesed risk is less than that from the FLAC models due to SLIDE's underestimation of the the failure volumes.

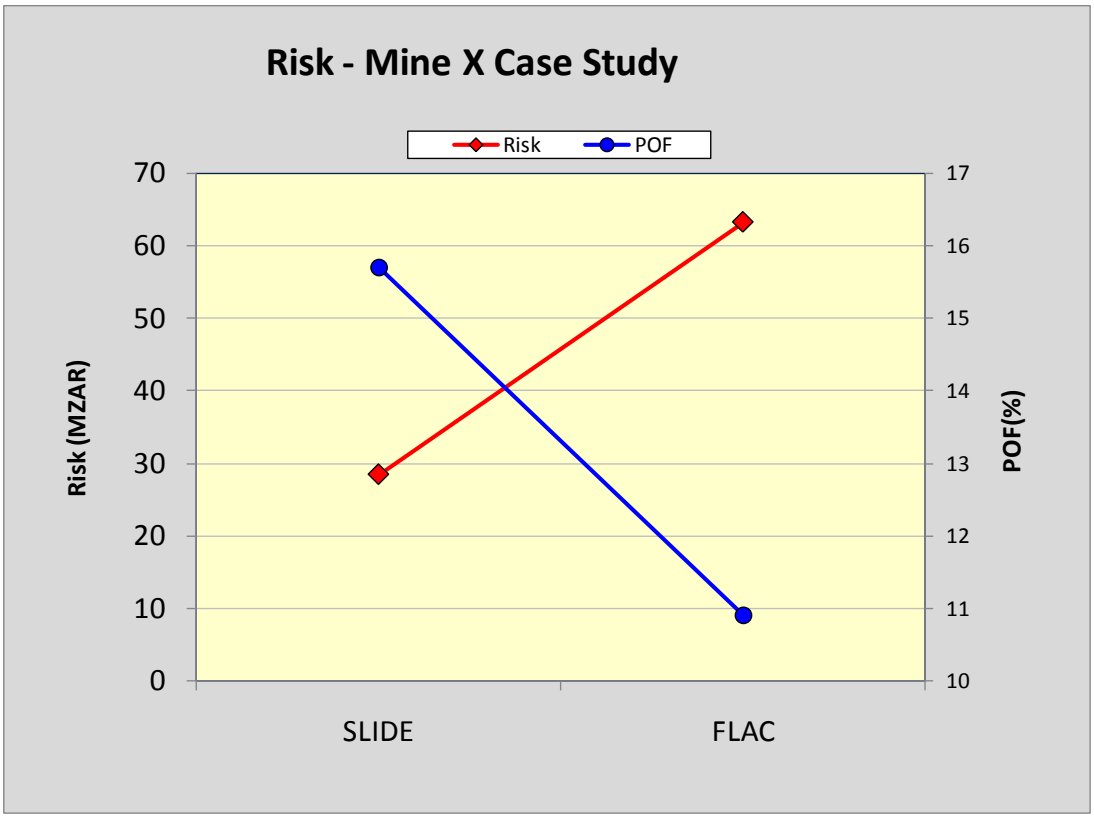

Figure 5.13 **Plot showing the POF and the assessed risk from the SLIDE and FLAC models. The blue curve is the POF and the red is the risk curve.**

5.6.4 Summary of results

The results from this case study of mine X agree quite well with the results from the hypothetical models of Chapters 3 and 4. FLAC gave a higher FOS and a lower POF for the slope. The apparent increase in stability was approximately 10% when a numerical analysis was carried out instead of an LE analysis. The sensitivity analysis results from the SLIDE and FLAC were markedly different due to the different failure surfaces predicted by the respective modelling tools. Moreover, the failure volumes from SLIDE were much lower than those from FLAC. This resulted in the overall expected loss of profits being much higher in the FLAC models than in the SLIDE.

The conclusion from the case study is that the use of numerical modelling instead of LE methods results in different assessments of the risk involved with an open pit mine slope design. This difference comes from the differences in the FOS, POF, and failure volumes computed by the LE and numerical models. As in this case study, even when the FOS and POF do not appear too different, the risk can still differ significantly due to the different failure volumes (consequences of a slope failure).

CHAPTER 6

6 CONCLUSIONS AND RECOMMENDATIONS

Currently most risk analysis on slopes is carried out with the use of Limit Equilibrium stability models. The work carried out in this dissertation involved comparing the results of carrying out a risk assessment for slopes using Limit Equilibrium stability models and using numerical models. The Response Surface Methodology (RSM) was used to calculate all probabilities of failure. A case study on a risk analysis for a diamond open pit mine was also included to verify the conclusions from the hypothetical models. Conclusions have been drawn from a comparison of the LE and numerical approaches to risk analysis.

The major conclusion from the research is that using numerical models, instead of LE models, in carrying out risk analyses results in significant differences in the assessed risk. In some cases the LE models give a lower estimate of the risk than numerical models while in other cases they give higher estimates of the risk. These differences in the assessed risk are mainly due to two reasons.

- LE methods are simplistic in their approach and ignore some very important complex mechanisms of rock mass failure. Parameters like the dilation angle and the horizontal to vertical stress ratio (k ratio), to name a few, are not included in an LE analysis, and yet they can have an effect on slope stability. The effect of these parameters tends to make the slope more stable than the result of an LE analysis. This means that, generally speaking, LE methods are conservative in terms of their stability (both FOS and POF) estimates. For some models the POF values from LE models were higher than those from numerical models by a factor of up to 2.
- The failure volumes (and hence the consequences of failure) predicted by LE models are almost always less than those from numerical models. Limit equilibrium solutions only identify the onset of failure, whereas numerical solutions include the effect of stress redistribution and progressive failure after movement has been

initiated. Thus the failure surfaces from numerical models extend further behind the crest than in LE models.

In light of the above reasons, the risk assessed using numerical analyses seems to be a more reliable estimate of the risk associated with a rock slope. Therefore, it is recommended that numerical modelling be incorporated into risk analyses instead of the simplistic LE models. An approximate approach that has been used involves calibrating an LE model using a numerical model and then carrying out the probabilistic and risk analysis using the calibrated LE model. This approach was also investigated in this work and it always resulted in risk levels that were less than those predicted by both the un-calibrated LE model and the numerical model. Therefore this approach should not be used for risk analysis as it results in perhaps dangerously optimistic estimates of the risk levels.

A practical way of directly incorporating numerical models into probabilistic/risk analyses is by using the response surface methodology (RSM). A comparison of the RSM with the traditional Monte Carlo (MC) simulation method revealed good agreement between the two methods, with the RSM requiring far fewer model runs that MC simulation. This research also revealed that the major contributors to variance in the FOS estimates (and hence, POF) are the strength parameters. Parameters like dilation angle and the k ratio contribute very little to the variance, and can be treated as deterministic inputs in the RSM probabilistic analysis without introducing any significant errors in the result. This significantly reduces the required number of runs using the numerical model.

The effect of assuming 2D plane strain on various pit geometries was also investigated by comparing the risk assessed using 2D numerical models (FLAC) with the result from 3D numerical models (FLAC3D). The conclusion from these comparisons was that using 3D models results in different levels of the assessed risk than when using 2D plane strain models. In some models the 3D gave higher assessments of the risk than the 2D models while in other models they gave lower risk results. The reasons for these differences were mainly:

- For a circular or elliptical pit (in plan), 2D plane strain analyses underestimate the stability (FOS and POF) of the slope. The difference between the 2D and 3D stability results increases as the concave radius of curvature decreases. When the radius of curvature was sufficiently large, more than twice the slope height, 2D plane strain analyses gave results very comparable to those from the 3D models. For an elliptical pit (in plan), 2D analyses can be valid along the "straight" portions of the pit, provided the cross section is taken at a distance sufficiently far from the curved ends of the pit.
- The failure surfaces predicted by 3D models are deeper than those from the 2D models. However, comparing the failure volumes from 3D and 2D models was complicated by the fact that the 2D models do not give 'volumes' but simply the surface area of the failing material. To simplify the comparison, the depth of the failure surface was used as an indication of the failure 'volume'. Using this simplified approach, the 3D models gave larger volumes than the 2D models.

It is therefore recommended that for circular pits with low values of the radius of curvature (less than twice the slope height), 3D analyses must be used in assessing the stability and risk. Similarly, for elliptical pits, if the section of interest is close to the curved ends of the pit then 3D analyses are recommended.

REFERENCES

Adhikary, D. P., Dyskin, A. V., Jewell, R. J. And Stewart, D. P., (1997), A study of the mechanism of flexural toppling failures of rock slopes. J. Rock Mech. Rock Engng, 30(2), 75–93.

Aryal, K.P., 2008, Differences between LE and FE Methods used in Slope Stability Evaluations, The 12th International Conference of International Association for Computer Methods and Advances in Geomechanics (IACMAG) 1-6 October, 2008 Goa, India

Atkinson C.L., 2000, The Role and Mitigation of Groundwater in Slope Stability, In Hustrulid W.A., McCarter M.K., and Van Zyl D.J.A., Slope Stability in Surface Mining, Society for Mining, metallurgy and exploration Inc.

Australian Geomechanics Society Sub-Committee on Landslide Risk Management (2000), Landslide risk management concepts and guidelines, Australian Geomechanics 35(1), 49–92 and 37(2), 1–44.

Baecher, G. B., and Christian, J. T. (2003b). Reliability and statistics in geotechnical engineering, Wiley, Chichester, U.K.

Baecher, G.B., and J.T. Christian. 2003. Reliability and statistics in geotechnical engineering. Wiley, Chichester, U.K.

Baker, J.W., and Cornell, C.A., 2003. Uncertainty Specification and Propagation for Loss Estimation Using FOSM Methods

Barton, N. 1976. The shear strength of rock and rock joints. Int. J. Rock Mech. Min. Sci. and Geomech. Abstr. 13, 1-24.

Barton, N. And V. Choubey. 1977. The Shear Strength of Rock Joints in Theory and Practice. Rock Mechanics, 10, pp 1-54

Barton, N.R. and Bandis, S.C. 1990, Review of predictive capabilites of JRC-JCS model in engineering practice. In Rock joints, proc. int. symp. on rock joints, Loen, Norway, (eds N. Barton and O. Stephansson), 603-610. Rotterdam: Balkema.

Bawden W.F., 2008, Risk Assessment in Strategic and Tactical Geomechanical Underground Mine Design, American Rock Mechanics Association, ARMA 08-305

Bishop, A. W. (1955), The use of the slip circle in the stability analysis of earth slopes. Geotechnique, 5, 7–17.

Bobet, A. (1999) Analytical solutions for toppling failure (Technical Note). Int. J. Rock Mech. Min. Sci., 36, 971–80.

Bosman J.D., Malan D.F. and Drescher K., 2000, Time dependent Tunnel Deformation at Hartebeestfontein Mine, Journal of the South African Institute of Mining and Metallurgy

Box G.E.P., and Wilson K.B., (1951), On the Experimental Attainment of Optimum Conditions (with discussion), Journal of the Royal Statistical Society Series B 13(1):1–45.

Byerlee, J. 1978. Friction of Rocks. Pure Appl. Geophys., 116, pp. 615-626.

Cala M. and Flisiak J. 2001, Slope stability analysis with FLAC and limit equilibrium methods. In Bilaux, Rachez, Detournay and Hart (eds.) FLAC and Numerical Modelling in Geomechanics: 111-114. A.A. Balkema Publishers.

Cala M., Flisiak J., and Tajdus, A., 2006, Slope stability analysis with FLAC in 2D and 3D. 4th International FLAC Symposium, Madrid, Spain

Carley K.M., Kamneva N.Y., Reminga J., 2004, Response Surface Methodology, CASOS technical report

Casamichelle, P., Maugeri, M. and Motta, E. 2004. New ap-proach for a three-dimensional analysis of slope stability. In Lacerda, Ehrlich, Fontoura and Sayao (eds.) Landslides: Evaluation and Stabilization: 1617-1623. Taylor and Francis Group, London.

Chen, Z., Wang, X. and Haberfield, C. 2001. A three-dimensional slope stability analysis using the upper bound theorem. Part I: theory and analysis. Int. J. Rock Mech. Mining Sci. 38: 369-78.

Chonggang Xua, Hong S. Heb, Yuanman Hua, Yu Changa, Xiuzhen Lia, Rencang Bua, 2004. Latin hypercube sampling and geostatistical modelling of spatial uncertainty in a spatially explicit forest landscape model simulation.

Christian, J.T and Baecher, G.B. 2002. The point estimate method with large numbers of variables, International Journal for Numerical and Analytical Methods in Geomechanics, 26: 1515-1529.

Christian J.T., 2004, Geotechnical Engineering Reliability: How Well Do We Know What We Are Doing, Thirty-Ninth Karl Terzaghi Lecturer, 2003, Nashville, Tenn., Journal of Geotechnical and Geoenvironmental Engineering © ASCE / October 2004

Contreras, L.F., R. LeSueur and J. Maran. 2006. A Case Study of Risk Evaluation at Cerejon Mine. In Proceedings of the International Symposium on Stability of Rock Slopes in Open

Pit Mining and Civil Engineering Situations, 3-6 April 2006, Cape Town, South Africa. SAIMM. Symposium Series S44, Johannesburg, South Africa.

Contreras L.F., 2009a, Personal communication, Johannesburg, South Africa

Contreras L.F., 2009b, Unpublished paper, SRK Consulting Engineers, Johannesburg, South Africa

Corkum A.G., and Martin C.D., 2004, Analysis of a rock slide stabilized with a toe-berm: a case study in British Columbia, Canada.

Cundall, P.A. (2002). "The replacement of limit equilibrium methods in design with numerical solutions for factor of safety." Powerpoint presentation, Itasca Consulting Group, Inc.

Cundall P.A., and Damjanac B., 2009, A Comprehensive 3D Model for Rock Slopes Based on Micromechanics, Slope Stability 2009, Santiago, Chile

Davies M.P., 1997, Potential Problem Analyses, A Practical Risk Assesment Technique for the Mining Industry, Mineral Economics Society of CIM

Dawson E.M. and Roth W.H, 1999. Slope stability analysis with FLAC, Detournay and Hart (eds.) FLAC and Numerical Modeling in Geomechanics: 3-9. Rotterdam: Balkema.

Dawson, E. M., Roth, W. H. and Drescher, A. (1999) Slope stability analysis by strength reduction, Géotechnique, 49(6), 835–840.

De Bruyn I.A., Mylvaganam J., Price J., Du Plooy K., Baczynski N.R., and Coulthard M.A., 2009, Numerical analyses for evaluation of pit wall stability and stresses resulting from proposed underground mining excavations beneath the Ok Tedi open pit, Papua New Guinea, Slope Stability 2009, Santiago, Chile

Desai, C. S., and J. T. Christian. 1977, Numerical Methods in Geomechanics. New York: McGraw-Hill.

Diederichs M.S. and Kaiser P.K., 1996, Rock Instability and Risk analyses in Open stope Mine design, Canadian Geotechnical Journal, 33 (3), 431-439

Diering J.A.C., and Stacey T.R., 1987, Three Dimensional Stress Analysis: A Practical Planning Tool for Mining Problems, Proceedings of the twentieth Interntional Symposium on the Application of Computers and Mathematics in the Mining Industries, Vol 1

Dight P.M., and Baczynski N.R.P., 2009, Rock Bridges and their Influence on Slope Stability, Slope Stability 2009, Santiago, Chile

Duncan, J. M. (1996) Landslides: Investigation and Mitigation, Transportation Research Board, Special Report 247, Washington, DC, Ch. 13, Soil Slope Stability Analysis, pp. 337–71.

Eberhardt E., 2003, Rock Slope Stability Analysis-Utilization of Advanced Numerical Techniques.

Eberhardt E., Stead D., Coggan J.S., and Willenberg H., 2003, Hybrid finite-/discrete element modelling of progressive failure in massive rock slopes, SAIMM

Eberhardt E., D. Stead and J.S. Coggan, 2004, "Numerical Analysis of Initiation and Progressive Failure in Natural Rock Slopes - the 1991 Randa Rockslide", Int. J. Rock Mech. Min. Sci., Vol. 41, 2004, 69-87.

Edelbro C., 2008, Prediction of failure and fallouts in access drifts at the Kiirunavaara mine using numerical analysis, Proceedings of the 5th International Conference and Exhibition on Mass Mining, Lulea, Sweden 9-11 June 2008

Edelbro C., and Sandstrom D., 2009, Interpretation of failure and fallouts based on numerical modelling of an underground mine stope, International Symposium on Rock Mechanics: Rock Characterisation, Modelling and Engineering Design Methods, SINOROCK2009, Hongkong, China

Elmo D., Moffitt K., D'Ambra S., and Stead D., 2009, Characterisation of brittle rock fracture mechanisms in rock slope failures, Slope Stability 2009, Santiago, Chile

Elmo D., M. Yan, D. Stead and S. Rogers, "The Importance of Intact Rock Bridges in the Stability of High Rock Slopes: Towards a Quantitative Investigation Using an Integrated Numerical Modelling - DFN Approach", Int. Symp. on Rock Slope Stability in Open Pit Mining and Civil Engineering, Perth, Australia, Australian Centre for Geomechanics, 2007.

Franz J., Y. Cai and B. Hebblewhite, 2007, "Numerical Modelling of Composite Large Scale Rock Slope Failure Mechanisms Dominated by Major Geological Structures", 11th ISRM Congress, Lisbon, Portugal, 2007, Vol. 1, 633-636

Firestone M., and Fenner-Crisp P., 1997, Guiding Principles for Monte Carlo Analysis, Technical Paper, EPA/630/R-97/001, March 1997

Galera M.J., Montero J., Perez C., Vega L., and Varona P., 2009, Coupled Hydromechanical Analysis of Cobre Las Cruses Open Pit, Slope Stability 2009, Santiago, Chile

Goodman, R. E. and Bray, J. (1976) Toppling of rock slopes. ASCE, Proc. Specialty Conf. on Rock Eng. for Foundations and Slopes, Boulder, CO, 2, 201–34.

Greco, V.R. (1996). "Efficient Monte Carlo Technique for Locating Critical Slip Surface." Journal of Geotechnical Engineering, Vol. 122, No. 7, July 1996.

Griffiths D.V. and Lane P.A, 1999, Slope stability analysis by finite elements. Geotechnique. 49(3): 387-403.

Guo M., Ge X., Li C., and Wang S., 2009, A new method for three-dimensional slope stability analysis: the vector sum analysis method, The 43rd US Rock Mechanics Symposium and 4th U.S.-Canada Rock Mechanics Symposium

Hack, R., 1996, Slope Stability Probability Classification, 2nd Edition, International Institute for Aerospace Survey and Earth Sciences (ITC)

Hajiabdolmajid V., Kaiser P.K., and Martin C.D., 2002, Modelling brittle failure of rock, International Journal of Rock Mechanics and Mining Sciences. **39** pp. 731–741

Hammah, R.E., Curran, J.H., Yacoub, T.E., and Corkum, B., 2004, Stability Analysis of Rock Slopes using the Finite Element Method. In Proceedings of the ISRM Regional Symposium EUROCK 2004 and the 53rd Geomechanics Colloquy, Salzburg, Austria.

Hammah, R.E. and Yacoub, T.E., 2009, Probabilistic Slope Analysis with the Finite Element Method, 43rd US Rock Mechanics Symposium and 4th U.S.-Canada Rock Mechanics Symposium, Asheville, ARMA 09-149

Han J., and Leshchinsky D., 2004, Limit Equilibrium and Continuum Mechanics-Based Numerical Methods for Analyzing Stability of MSE Walls, 17th ASCE Engineering Mechanics Conference, University of Delaware, EM2004

Harr M.E., 1987, Reliability-based design in civil engineering. New York: McGraw-Hill.

Health and Safety Executive, (2001) “Reducing risks, protecting people – HSE’s decision-making process”. HSE books. U.K. 2001.

Hoek Evert, 2006, Practical Rock Engineering, Course notes

Hoek E., and Bray J.W., 1974. Rock slope engineering, Institute of Mining and Metallurgy, London.

Hoek, E. and Bray, J. (1981) Rock Slope Engineering, 3rd edition, Institute of Mining and Metallurgy, London, UK.

Hoek, E., Wood D. and Shah S. 1992. A modified Hoek-Brown criterion for jointed rock masses. Proc. Rock Characterization, Symp. Int. Soc. Rock Mech.: Eurock '92, (ed. J.A. Hudson), 209-214. London, B rit. Geotech. Soc.

Hoek, E., Marinos, P. and Benissi, M. 1998. Applicability of the Geological Strength Index (GSI) classification for very weak and sheared rock masses. The case of the Athens Schist Formation. Bull. Engg. Geol. Env. 57(2), 151-160.

Hoek E., 2009, Fundamentals of Slope Design, Slope Stability 2009, Santiago, Chile

Hoek, E. and Brown, E.T. 1997. Practical Estimates of Rock Mass Strength, International Journal of Rock Mechanics and Mining Sciences, Vol 34, No 8, pages 1165-1186

Hoek, E., Carranza-Torres C., and Corkum B., (2002). Hoek Brown Failure Criterion – 2002 Edition, *Proc. NARMS-TAC Conference*, Toronto, 2002, 1, 267-273.

Hoek, E., and Diederichs M.S., 2006, Empirical estimation of rock mass modulus, International Journal of Rock Mechanics and the Mining Sciences 43

Hoek, E., Grabinsky, M.W. and Diederichs, M.S., (1993), Numerical modelling for underground excavations, Transactions of the Institution of Mining and Metallurgy - Section A 100: A22-A30.

Hoek E., Kaiser P.K., and Bawden W.F., 1995, Support of Underground Excavations in Hard Rock, A.A. Balkema, Rotterdam

Hoek E., Read J., Karzulovic A. and Chen Z.Y., 2000, Rock slopes in Civil and Mining Engineering, Proceedings of the International Conference on Geotechnical and Geological Engineering, GeoEng2000, 19-24 November, 2000, Melbourne.

Hong P., 1996, Point estimate moment-based reliability analysis, Civil Engineering and Environmental Systems, Volume 13, Issue 4, August 1996 , pages 281 - 294

Hong P., 1998, An efficient point estimate method for probabilistic analysis, Reliability Engineering and System Safety, Volume 59, Number 3, March 1998 , pp. 261-267(7)

HSE (Health and Safety Executive), 2001, "Reducing risks, protecting people – HSE's decision-making process", HSE books, U.K. 2001.

Hungr, O. 1987. An extension of Bishop's simplified method of slope stability analysis to three dimensions. Geotechnique 37(1): 113-117.

Hürlimann, M., Ledesma, A. and Marti, J. 2002. Geotechnical analysis of large volcanic landslides. The La Orotava events on Tenerife, Canary Islands. In Rybar, Stemberek and Wagner (eds) Landslides. pp. 571-577. Lisse: Swets and Zeitlinger.

Itasca Consulting Group Inc. (2002) FLAC3D (Fast Lagrangian Analysis of Continua in 3 Dimensions), Version 2.1, Minneapolis, MN.

Itasca Consulting Group, Inc. (2004). UDEC (Universal Distinct Element Code). Ver. 4.0. Minneapolis: Itasca Consulting Group, Inc.

Itasca Consulting Group, Inc. (2005). FLAC – Fast Lagrangian Analysis of Continua, Ver. 5.0 User's Guide. Minneapolis: Itasca.

Janbu, N., 1954, Application of composite slide circles for stability analysis. Proc. European Conference on Stability of Earth Slopes. Stockholm, 3, pp. 43–9.

Jeyapalan, J.K., and Jayawickrama, P.W., 1983, Influence Of Excavation Sequence On The Stresses In Open Pit Mine Slopes, The 24th U.S. Symposium on Rock Mechanics (USRMS), June 20 - 23, 1983 , College Station, TX

Jing L., 2003, A Review Of The Techniques, Advances And Outstanding Issues In Numerical Modeling For Rock Mechanics And Rock Engineering. International Journal of Rock Mechanics And Mining Sciences

Karzulovic, A. 2004. The importance of rock slope engineer-ing in open pit mining business optimization. In Lacerda, Ehrlich, Fontoura and Sayao (eds.) Landslides: Evaluation and Stabilization. pp. 443-456. London: Taylor and Francis.

Kinzelbach W. And Siegfried T., (2002). Conditional first-order second-moment method and its application to the quantification of uncertainty in groundwater modelling, Water Resources Research, Vol. 38, No. 4, 1035, 10.1029/2000WR000022.

Kirsten, H. A. D. (1982) Significance of the Probability of Failure in Slopes Engineering, The Civil Engineer in South Africa, Vol. 25, No. 1, pp 17-27

Konietzky, H., Lorenz, K. and Witter, W. 2004. Complex 3D landslide simulation. In Lacerda, Ehrlich, Fontoura and Sayao (eds.) Landslides: Evaluation and Stabilization. pp. 1053-1059. London: Taylor and Francis.

Laubscher D.H., 1990, A geomechanics classification system for the rating of rock mass in mine design, South African Institute of Mining and Metallurgy, vol 90, no. 10, Oct 1990, pp 257 - 273

Lilly, P.A, 2000, The minimum total cost approach to optimise pit slope design, Western Australia School of Mines.

Lorig L., 1999, Lessons Learned From Slope Stability Studies, in FLAC and Numerical Modeling in Geomechanics (Proceedings of the Conference, Minneapolis, September 1999), pp. 17-21. C. Detournay and R. Hart, Eds. Rotterdam: Balkema, 1999.

Lorig L., and Varona P., 2004, Numerical Analysis in Rock Slopes - Civil and Mining Engineering, Ch. 10. D.C. Wyllie and C.W. Mah, Compilers. London: Spon, 2004.

Low, B.K. (2003), Practical Probabilistic Slope Stability Analysis, Proceedings: Soil and Rock America 2003, 12th PanAmerican Conference on Soil Mechanics and Geotechnical Engineering and 39th U.S. Rock Mechanics Symposium, M.I.T., Cambridge, Massachusetts, June 22-26.

Low, B.K. and Phoon, K.K. (2002) “Practical First-Order Reliability Computations Using Spreadsheet”, In proceedings Probabilistics in Geotechnics: Technical and Economic Risk Estimation, Graz, Ausria, September 15-19, 2002, pages 39-46.

Low, B.K. and Tang, W.H. (1997a). “Efficient reliability evaluation using spreadsheets.” Journal of Engineering Mechanics, ASCE 123(7): 749-752

Madsen, H. O., Krenk, S., Lind, N. (1986): Methods of Structural Safety. Prentice Hall, Englewood Cliffs.

Malan D.F., Vogler U.W., and Drescher K., 1997, Time-dependent behaviour of hard rock in deep level gold mines, Journal of the South African Institute of Mining and Metallurgy, SA ISSN 0038–223X/3.00 + 0.00

Marinos, P., and Hoek, E. 2001 – Estimating the geotechnical properties of heterogeneous rock masses such as flysch. *Bulletin of the Engineering Geology and the Environment (IAEG)*, **60**, 85-92.

McKay, M.D., Beckman, R.J., and Conover,W.J., 1979. A comparison of three methods for selecting values of input variables in the analysis of output from a computer code. Technometrics 21, 239–245.

Milford, J.B., Russel, A.G., and MacRae, G.J., (1988). “Spatial Patterns in Photochemical Pollutant Response to NOX and ROG reductions,” Environmental Science and Technology

Mollon G., Dias D., and Soubra A., 2009, Probabilistic Analysis of Circular Tunnels in Homogeneous Soils Using Response Surface Methodology, Journal of Geotechnical and Geo-Environmental Engineering, Vol. 139, No 9, ASCE September 2009.

Morgan, M.G. and Henrion, M., (1990), “Uncertainty: a guide to dealing with uncertainty in quantitative risk and policy analysis”. Cambridge University Press.

Morgenstern, N. R. and Price, V. E. (1965), The analysis of the stability of general slide surfaces. Geotechnique. 15, 79–93.

Narendranathan S., 2009, Fundamentals of Probabilistic Slope Design and Its Use in Pit Optimization, 43rd US Rock Mechanics Symposium and 4th U.S.-Canada Rock Mechanics Symposium, Asheville, ARMA 09-008

Nonveiller, E., (1965), The stability analysis of slopes with a slide surface of general shape. Proc. 6th Int. Conf. Soil Mech. Foundation Engng. Montreal. 2, pp. 522.

Novak D., (2005) “Methods and Software for Reliability Analysis and Engineering Risk Assesment”, Centre for Integrated Design of Advanced Structures.

Palisade Corporation, 1994, Bestfit (Distribution Fitting For Windows) and @Risk (Risk Analysis for Spreadsheets), Palisade Corporation, Newfield, NY

Piteau, D. R. and Jennings, J. E. (1970) The effects of plan geometry on the stability of natural slopes in rock in the Kimberley area of South Africa. In: Proceedings of the 2nd Congress of the International Society of Rock Mechanics (Belgrade). Vol 3: Paper 7–4.

Priest S. D. and Brown E. T., 1983, Probabilistic stability analysis of variable rock slopes. Trans. Instn Min. Metall. 92, AI-AI2.

Rackwitz, R. (2001). “Reliability analysis—a review and some perspectives.” Structural Safety, 23, 365-395, Elsevier Science Ltd.

Read J.R.L., 2009, Data Uncertainty, Slope Stability 2009, Santiago, Chile

Read J.R.L., and Stacey P.F., 2009, Guidelines for Open Pit Slope Design, CSIRO Publishing, Melbourne, Australia, 2009.

Rocscience Inc., 2001, RocPlane version 2.0 User Manual

Rocscience Inc., 2008, SLIDE version 5.0 User Manual

Rocscience Inc., 2009, Phase2 version 7.0 User Manual

Rosenblueth E., 1975, E. Point estimation for probability moments, Proc. Nat. Acad. Sci. U.S.A. 1975, 72, 3812-3814

Rosenblueth E., 1981, Two-point estimates in probability. Appl. Math. Modelling 1981, 329-335

Ross-Brown, D. R. (1973) Slope Design in Open Cast Mines, PhD Thesis, London University, 250 pp.

Ryder J.A., and Jager A.J., 2002, A Textbook on Rock Mechanics for Tabular Hard Rock Mines, The Safety in Mines Research Advisory Committee (SIMRAC), Johannesburg, South Africa

Sageseta, C., Sánchez, J. M. and Cañizal, J. (2001) A general solution for the required anchor force in rock slopes with toppling failure. Int. J. Rock Mech. Min. Sci., 38, 421–35.

Sarma, S. K. (1979) Stability analysis of embankments and slopes. J. Geotech. Engng Div., ASCE, 105 (GT12) 1511–24.

Simmonds J., and Simpson P.J., 2006, Composite failure mechanisms in coal measures rock masses – myths and reality. International Symposium on Stability of Rock Slopes in Open Pit Mining and Civil Engineering behaviour SAIMM.

Sjoberg J., 1997, Estimating Rock Mass Strength Using the Hoek-Brown Failure Criterion and Rock Mass Classification – A Review and Application to the Aznalcollar Open Pit, Lulea University of Technology, Internal report

Sjoberg J., 1999, Analysis of large scale slopes, Doctoral Thesis, Lulea University of Technology

Spencer, E. (1967), A Method of Analysis of the Stability of Embankments Assuming Parallel Inter-Slice Forces, Geotechnique 17:11-26

SRK Project Report, 2006, The Stability of Rock Slopes in Large Open Pit Mines Design Manual, Report Prepared for CSIRO Research Project No. 2004-ha62

SRK Project Report, 2008, Slope design for diamond open pit mine (Name withheld for proprietary reasons).

Stacey T.R., 1981, A simple extension strain criterion for fracture of brittle rock, Int. J. Rock Mech. Min. Sci., vol. 18, 469-474

Stacey T.R., and Swart A.H, 2001, Best Practice Engineering Handbook for Other Mines, Safety in Mines Research Advisory Committee Final Report, OTH602

Stacey T.R., and Wesseloo J., 1998, In-situ Stresses in Mining Areas in South Africa, The Journal of The South African Institute of Mining and Metallurgy, November/December 1998

Stacey T.R, Yu Xianbin, Armstrong R., and Keyter G.J., 2003, New slope stability considerations for deep open pit mines, V. 103, pp373-389, The South African Institute of Mining and Metallurgy.

Stacey T.R., 2006, Design-a strategic issue, Strategic vs. Tactical Approaches in Mining Conference, Perth, Western Australia.

Stacey T.R., 2007, "Slope stability in high stress and hard rock conditions", Slope Stability 2007 – Proceedings International Symposium on Rock Slope Stability in Open Pit Mining and Civil Engineering, Potvin (ed), Australian Centre for Geomechanics, 12–14 September 2007, Perth, Australia, 2007, 187-200.

Starfield, A. M. and Cundall, P. A. (1988) Towards a methodology for rock mechanics modelling. Int. J. Rock Mechanics, Mining Sci. and Geomech. Abstr., 25(3), 99–106.

Steffen, O. K. H., Contreras, L. F., Terbrugge, P. J., Venter, J., 2008, "A Risk Evaluation Approach for Pit Slope Design". 42nd US Rock Mechanics Symposium and 2nd U.S.-Canada Rock Mechanics Symposium, held in San Francisco, June 29- July 2, 2008.

Steffen, O.K.H. (1997) "Planning of open pit mines on a risk basis". Journal of SAIMM, March / April 1997.

Steffen O. K. H., Terbrugge P. J., Wesseloo J., Venter J., 2006, A Risk Consequence Approach to Open Pit Slope Design, SAIMM International Symposium on Stability of Rock Slopes in Open Pit Mining and Civil Engineering,

Tapia, A., Contreras, L.F., Jefferies, M.G., and Steffen, O. (2007) Risk evaluation of slope failure at Chuquicamata Mine. In Proc. Int. Symp. Rock Slope Stability in Open Pit Mining and Civil Engineering,47̃7 485, Perth. Australian Centre for Geomechanics, ISBN 978 0 9756756 8 7.

Valdivia C., and Lorig L., 2000, Slope Stability at Escondida Mine, In Hustrulid W.A., McCarter M.K., and Van Zyl D.J.A., Slope Stability in Surface Mining, Society for Mining, metallurgy and exploration Inc.

Vaurio, J.K., (1982 September). Statistical Identification of effective Input Variables, Reactor Analysis and Safety division, ANL-82-57, Argone National Laboratory, Argone, Ill

Wesseloo J., and Dight P.M., 2009, Rock mass Damage in Hard Rock Open Pit Mines, Slope Stability 2009, Santiago, Chile

Wilson, R. and Crouch, E.A.C. (1987), Risk Assessment and Comparisons: An Introduction. Science, Vol. 236.

Whitman, R.V. (1983), The 7th Terzaghi lecture, Evaluating and calculated risk in geotechnical engineering. Journal of Geotechnical Engineering, Vol. 110, No.2, pp 145-188

Wyllie D.C., and Mah C.W., 2004, Rock slope engineering (Civil and Mining), 4th Edition, The Institute of Mining and Metallurgy, Milton Park, Abingdon, Oxon, OX14 4RN

Yuz-hen, Y., Liquan, X. and Bingyin, Z. 2005. Stability of earth-rockfill dams: Influence of geometry on the three-dimensional effect. Computer and Geotechnics (32): 326-339.

Zanbak, C., 1983, Design charts for rock slope susceptible to toppling. ASCE, J. Geotech. Engng, 109 (8), 1039–62.

Zettler A.H., Poisel R., Roth W., and Preh A. 1999. Slope stability analysis based on the shear reduction technique in 3D. In Detournay and Hart (eds.), FLAC and Numerical Modeling in Geomechanics: 11-16. Rotterdam: Balkema.

Zienkiewicz, O. C., Humpheson, C. and Lewis, R. W. (1975) Associated and non-associated visco-plasticity and plasticity in soil mechanics, Géotechnique, 25(4), 671–89.

Zhu H., and Zhou Z., 2009, Displacement analysis of the left abutment slope of the Jinping I dam, Slope Stability 2009, Santiago, Chile

APPENDIX A

Visual Basic for Applications code to convert Laubscher's indices Joint Condition rating (JCr) and Fracture Frequency rating (FFr), into a GSI value. The Excel formula takes FFr and JCr rating as inputs and gives the GSI as the output.

```
Function gsif(ffr, jcr)
    'GSI index from Laubsher(90) FF and JC ratings
    m1 = 0.011092
    b1 = 1.029822
    m2 = 0.987503
    b2 = 2.436058
        If ffr > 31 And jcr < 16 Then
            gsif = "N/A"
        Else
            If ffr < 3 And jcr > 24 Then
                gsif = "N/A"
            Else
            End If
        End If
    gsi = (m1 * jcr + b1) * ffr + (m2 * jcr + b2)
    gsif = gsi
        If gsif > 100 Then
            gsif = 100
        Else
            If gsif < 1 Then
                gsif = 1
            Else
            End If
        End If
End Function
```

Appendix B

Rock Mass and Foliation strength parameters used for the probabilistic analyses for the case study

Unit	Case	UCS (MPa)	GSI	mi	MR	Rock Mass		Foliation	
						c (kPa)	Φ (°)	c (kPa)	Φ (°)
CS	basecase	120.9	46.6	5	310	608	34	81	34
	UCS_"-"	75.8	46.6			476	31	66	31
	UCS_"+"	166.1	46.6			732	37	95	36
	GSI_"-"	120.9	42.5			511	32	81	34
	GSI_"+"	120.9	50.6			737	36	81	34
DM	basecase	217.5	54.2	13	431	1231	51	NA	NA
	UCS_"-"	173.0	54.2			1081	49	NA	NA
	UCS_"+"	262.1	54.2			1378	52	NA	NA
	GSI_"-"	217.5	49.3			996	49	NA	NA
	GSI_"+"	217.5	59.0			1575	53	NA	NA
DOL	basecase	239.2	48.7	9	325	1010	46	NA	NA
	UCS_"-"	173.1	48.7			844	44	NA	NA
	UCS_"+"	305.3	48.7			1171	48	NA	NA
	GSI_"-"	239.2	43.6			806	44	NA	NA
	GSI_"+"	239.2	53.8			1311	48	NA	NA
KIM	basecase	39.4	49.6	9	273	450	32	NA	NA
	UCS_"-"	19.6	49.6			344	27	NA	NA
	UCS_"+"	59.2	49.6			531	36	NA	NA
	GSI_"-"	39.4	46.5			412	31	NA	NA
	GSI_"+"	39.4	52.8			493	34	NA	NA
LS	basecase	62.4	39.4	5	446	340	24	80	34
	UCS_"-"	25.0	39.4			271	21	67	31
	UCS_"+"	99.8	39.4			401	27	94	36
	GSI_"-"	62.4	35.6			292	22	80	34
	GSI_"+"	62.4	43.2			398	26	80	34
QS	basecase	172.8	46.8	5	350	758	38	85	36
	UCS_"-"	130.9	46.8			644	36	72	34
	UCS_"+"	214.7	46.8			869	39	97	38
	GSI_"-"	172.8	41.3			588	35	84	36
	GSI_"+"	172.8	52.2			1013	40	84	36

NB: Both GSI and UCS were assumed to follow a normal distribution